UNIVERSITÀ DEGLI STUDI DI TRIESTE

Dipartimento Universitario Clinico di Scienze Mediche, Chirurgiche e della Salute

XXXIII CICLO DEL DOTTORATO DI RICERCA IN

SCIENZE DELLA RIPRODUZIONE E DELLO SVILUPPO

PO FRIULI VENEZIA GIULIA - FONDO SOCIALE EUROPEO 2014/2020

Identification and functional characterization of new candidate genes and variants associated with Hereditary Hearing Loss and Presbycusis

Settore scientifico-disciplinare: **MED03**

Ph.D Student

Sissy Bassani

Ph.D program Coordinator

Prof. Paolo Gasparini

Thesis Supervisor

Prof. Giorgia Girotto

Thesis Co-Supervisors

Prof. Alexandre Reymond

Prof. Mireille Rossel

ANNO ACCADEMICO 2019 / 2020

Alla mia famiglia che mi ha sempre supportato
per raggiungere i miei sogni.

Curiosity
is the most beautiful gift
we have in life

Contents

ABSTRACT

Hearing loss is the most common sensory disorder affecting over half a million people worldwide (WHO). In the work presented in this thesis we have considered two forms of deafness: Non-Syndromic Hereditary Hearing Loss and Age-Related Hearing Loss.

Non-Syndromic Hereditary Hearing Loss (NSHHL) is a sensorineural disorder with high genetic heterogeneity and over 115 genes already associated. Through whole-exome sequencing and data aggregation, we identified an Italian family with six affected individuals and two unrelated Dutch patients displaying NSHHL and carrying predicted-to-be deleterious missense variants in *USP48*. We uncovered a ninth French patient presenting unilateral cochlear nerve aplasia and presenting a *de-novo* splice variant in the same gene. *USP48* encodes for a de-ubiquitinating enzyme under evolutionary constraint.

The Pathogenicity of the missense variants is supported by 3-D protein modeling and *in-vitro* functional assays. Immunohistology experiments showed that USP48 is expressed in the developing human inner ear's specific structures.

Engineered zebrafish knocked-down models for the *USP48* orthologue presented with a delay in developing primary motoneurons, less developed and less organized statoacoustic neurons innervating the ears, decreased swimming velocity and circle swimming behavior indicative of vestibular dysfunction and hearing impairment.

Acoustic startle response assays revealed a significant decrease of the auditory response of *usp48* knocked-down zebrafish at 600 Hz and 800 Hz wavelengths. In conclusion, we describe a novel autosomal dominant NSHHL gene through a multipronged approach combining exome sequencing, animal modeling, immunohistology, and molecular assays.

Age-related hearing loss (ARHL) or presbycusis is the most common sensory disorder in aging individuals. In spite of an incidence of more than 30 % in individuals over 65 years, only a few susceptibility genes have been identified so far. The analysis of a set of 46 ARHL candidate genes in a cohort of 464 Italian ARHL patients allowed the identification of a series of ultra-rare likely pathogenic variants in *DCLK1*, *SLC28A3*, *CEP104*, and *PCDH20* genes. The potentially causative role of these variants has been tested through functional *in-silico* and *in-vitro* studies. While the expression of these genes in structures responsible for the auditory function has been evaluated through the Mouse or Zebrafish orthologs study.

These results provide novel insights in the genetic and molecular bases of this complex and heterogeneous common disorder.

1 INTRODUCTION

1.1 The Human Ear Structure

The human ear contains the organ of hearing, able to detect and analyze sound waves by transduction (or the conversion of sound waves into electrochemical impulses), and the organ of the equilibrium, for maintaining the sense of balance [1]. The ear presents three distinguishable parts: the outer, middle, and inner ear (**Figure 1.1**).

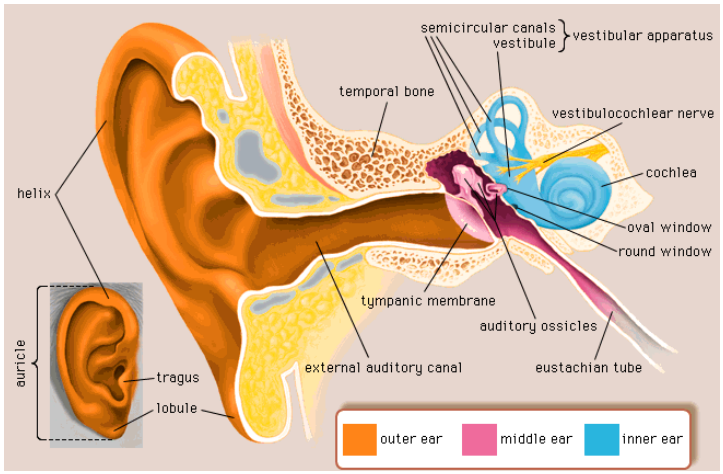

Figure 1.1. *Representative image of the auditory system.*
The mammalian ear consists of three distinct sections: the outer ear (auricle and external auditory meatus), the middle ear (tympanic membrane and auditory ossicles) and inner ear (vestibules, semicircular canal, cochlea) (adapted from “Encyclopaedia Britannica” https://www.britannica.com/science/middle-ear).

1.1.1 Outer ear

The external section of the ear consists of a visible portion called the auricle, or pinna, and a short external auditory canal that ends with the tympanic membrane, commonly called the eardrum[1]. The pinna is essential to collect sounds waves and canalize them through the auditory canal into the tympanic membrane (**Figure 1.1**). The sound waves reaching the tympani are in part reflected, while the absorbed ones cause the vibration of the tympanic membrane representing the first step of the sound transduction[2].

1.1.2 Middle ear

The cavity of the middle ear is a narrow air-filled space located between the eardrum and the oval membrane of the inner [3]. The middle ear contains: three tiny ossicles named malleus, incus and stapes, one auditory tube known as Eustachian tube and the round and oval windows (**Figure 1.1**). The three ossicles are able to convert the mechanical air vibrations into fluid-membrane pressure waves, amplifying and transmitting them through the oval window within the inner ear [2]. The Eustachian tube connects the middle ear cavity with the nasal cavity. This tube is closed at rest and opened during swallowing, permitting the equalization of the pressure between the middle and the inner ear[1]. The round and oval windows are essential to connect the middle ear with the inner ear.

1.1.3 Inner ear

The inner ear, settled in the temporal bone, is placed into a complex fluid-filled cavity called bony labyrinth cavity [3]. It consists of two functional units: 1) the Vestibular System, dwelling of vestibule and semi-circular canals, the sensory organs of postural equilibrium; 2) the snail-shell-like shape cochlea, the sensory organ of hearing (**Figure 1.2**). These structures are connected with the brain cortex thanks to specialized ends of the vestibulo-cochlear nerve (VIII cranial nerve).

When the sound waves reach the ear, the vibration of the tympanic membrane induces the mechanical oscillation of the small ossicles transmitting the signal into the inner ear through the oval membrane. In the cochlea the mechanical stimuli are transformed in electrical signals that, traveling along the eight cranial nerve, reach the auditory cortex allowing the auditory perception[1].

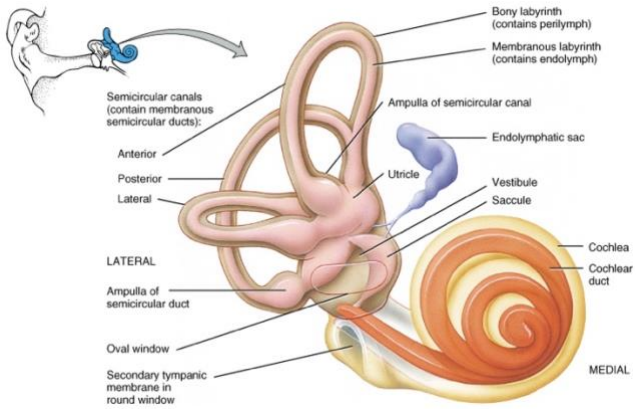

Figure 1.2. *Schematic image of the inner ear.*
It consists of two districts: the vestibular system (vestibule and semi-circular canals) and the cochlea (adapted from John Wiley & Sons, Inc).

1.1.4 Cochlea

The cochlea is a spiral-shaped cavity that in humans make 2 ½ turns around a hollow central pillar, the modiolus. When stretched out, from the base to the apex, it is approximately 30 mm in length. Two thin layers, the vestibular membrane known as Reissner's membrane and the basilar membrane project across the cochlea canal dividing it in three compartments. The Reissner's membrane separates the scala vestibuli, (upper chamber) with the scala media, whereas the basilar membrane divides the scala media with the scala tympani (lower chamber – **Figure 1.3**).

The scala vestibuli starts from the oval window up to the apex of the cochlea where it is connected with an opening, called the helicotrema, to the scala tympani which ends blindly below the round window. These two compartments are filled with perilymph, an extra-cellular liquid similar to the cerebro-spinal fluid rich in sodium (Na^+ 150 mM) and poor in potassium (K^+ 5 mM) and calcium (Ca^{2+} 1.2 mM) [1,3]. The smaller channel called scala media lands between the vestibular and tympanic scalae. This triangular-shaped duct closes blindly at both ends, below the round window and at the apex of the cochlea. It is filled with a watery liquid named endolymph, unique among the extracellular fluids, which is poor in sodium (Na^+ 1 mM) and rich in potassium (K^+ 140 mM). This ion composition characterizes the fluid with an electric potential around 80-90 mV, more positive than perilymph[4]. On the basilar membrane is located the Kolliker's organ presented only during the development of the auditory function and the organ of Corti, the sensory organ for hearing, essential for the auditory transduction.

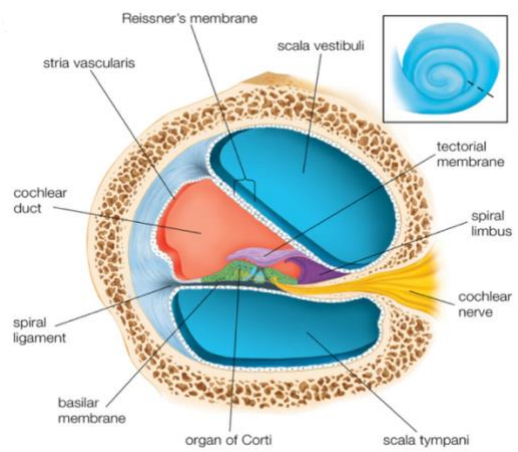

Figure 1.3. *Schematic image of a cross section through one of the turns of the cochlea.*
The cochlea is divided in three fluid-filled sections: scala vestibuli and scala tympani, which contain perilymph, and scala media filled with endolymph (adapted from "Encyclopaedia Britannica" https://www.britannica.com/science/middle-ear).

1.1.5 Kölliker's organ

The Kölliker's organ has been firstly described in 1863 by the Swiss anatomist and physiologist Albert von Kölliker[5,6]. The Kölliker's organ is a transient structure and undergoes a large remodeling in the embryonic or early postnatal stages.

The differentiated organ is composed by tightly packed columnar epithelial cells present in the developing auditory sensory organ in a wide variety of mammals such as humans[7].

It is one of the first visible epithelial structures in the developing cochlea and it is the source of the sensory cells[7].

Once the sensory cells differentiate and become sensitive to external sound it is eventually transformed into the inner sulcus region of organ of Corti[7].

Although Kölliker's organ have been described over a century ago, its function is still largely unknown[7].

1.1.6 Organ of Corti

The organ of Corti (or basilar papilla) took the name of the Italian anatomist Alfonso Corti (Kolliker's student) who first described it in 1851 in the "Zeitschrift für wissenschaftliche Zoologie"[6,8]. It consists of a complex neuro-epithelium formed by mechanosensory cells enclosed by their supporting cells.

The specialized sensory cells, orderly distributed along the cochlea, are separated by two rows of pillar cells that ensure the major support of this structure.

The sensory cells can be divided in two groups: one single row of big pear-shaped Inner Hair Cells (IHC), supported by inner phalangeal cells; and three rows of smaller cylindric Outer Hair Cells (OHC), supported by inner supporting cells of Deiters (**Figure 1.4**).

A reticular lamina extends from Deiters' cells upward the Organ of Corti covering the top of the hair cells, whose body is suspended in fluid. Beyond the hair and Deiter's cells, there are three other epithelial units named cells of Boettcher, Claudius and Hensesn that are probably involved in maintaining the correct ion composition of the endolymph[1] (**Figure 1.4**).

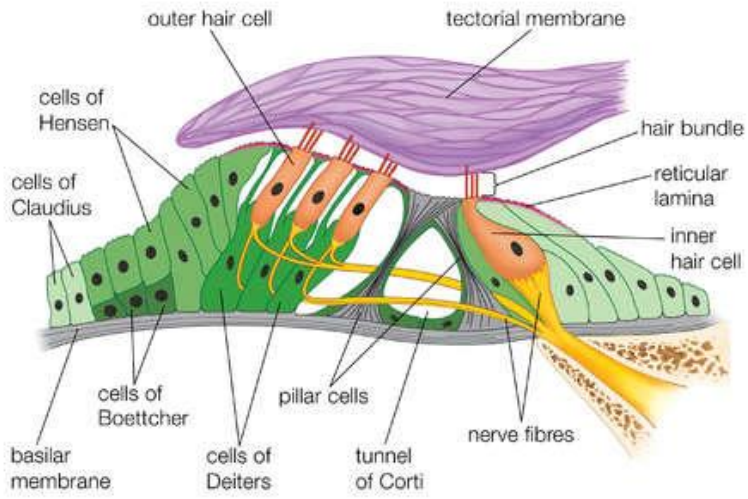

Figure 1.4. *Schematic view of organ of Corti.*

The organ of Corti consists of a complex neuroepithelium formed by: mechanosensory cells named inner (IHC) and outer hair cells (OHR) showed in orange, enclosed by several supporting cells. The hair are specific actin-rich structures that protrude from the top of mechanosensory cells and take contact with the tectorial membrane (adapted from "Encyclopaedia Britannica" https://www.britannica.com/science/organ-of-Corti).

The sensory hair cells are characterized by a cytoskeleton of actin filaments arranged in a staircase pattern and rows of stereocilia, around 3-5 µm in length, on their top.
The IHCs present 40 to 60 stereocilia in two or more irregular rows, whereas the OHCs show around 100 stereocilia in a W pattern (**Figure 1.5**).
The longest cilia, that is named axonemal kinocilium in the non-matured hair cells, takes contact with the tectorial membrane, an extracellular gelatinous structure that extend in parallel to the basal membrane and stores Ca^{2+} ions[1,3].

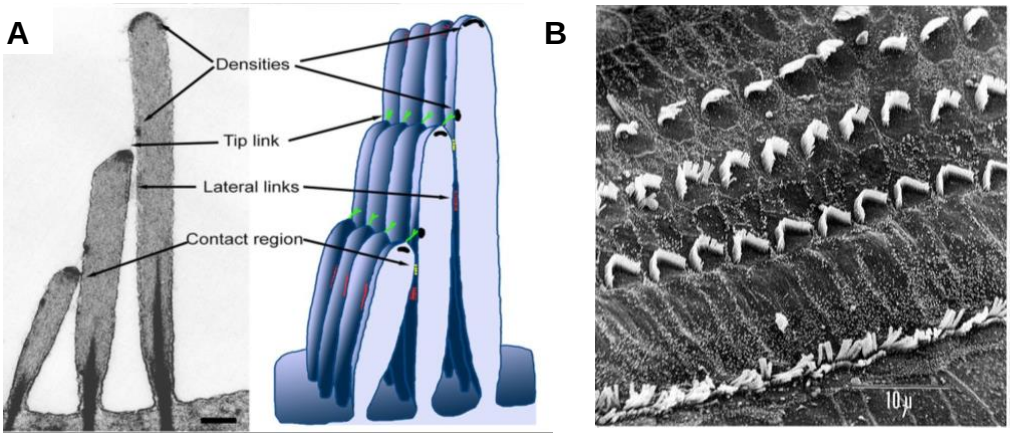

Figure1.5. *Overview of Stereocilia organization.*
(A) Scanning electron microscopy of stereocilia protruding from the top of the hair cells, in which several cross links are visible (left) and the schematic illustration of the corrisponding cross links (right) [9]; **(B)** Scanning electron microscopy image of the top view of three rows of outer hair cells and a single row of inner hair cells (adapted from “Encyclopaedia Britannica” https://www.britannica.com/science/organ-of-Corti).

The organ of Corti is innervated by the Spiral Ganglion (SG) characterized by a group of bipolar neurons based in the modiolus. These neurons project their axons to the cochlear nerve, branch of vestibulo-cochlear nerve (VIII Cranial Nerve), and their dendrites create synaptic contact with the base of IHC and OHC[1,3].

1.1.7 The Physiology of Hearing

In presence of an auditory stimulus, the sound waves flow inside the outer ear and along the auditory canal causing the vibration of the tympanic membrane. It induces the oscillation of the three ossicles in the middle ear: the first bone attached to the tympanic membrane is the malleus, whose movement is transmitted to the incus that cause the vibration of the third bone, the stapes. The mechanical vibration of the stapes footplate at the oval window induces pression changes within the inner ear. This transmission allowed the amplification and the conversion of the mechanical signal into fluid-membrane pressure waves. The fluid vibration set up pressure waves in the perilymph of scala vestibuli that propagates through the helicotrema into the scala tympani and dissipate when hit the round window[1].

The vibration of the round window allowed the transmission of the motion to the endolymph, inside the cochlea duct, that induces the oscillation of the basilar membrane. The basilar membrane presents a tonotopic organization: it is stiffest and narrowest at the base (near the stapes) and becomes less stiff and larger at the apex of the cochlea. Interestingly, high-frequency waves cause maximal movement at the base whereas low-frequency waves also activate the apical parts of the basilar membrane, forming a frequency-tuned delay line[1,3].The oscillation of the basilar membrane causes the waving of Organ of Corti against the tectorial membrane. It results in the movement of the stereocilia back and forth beneath the tectorial membrane. The hair bundle displacement towards the tallest cilia induces the stretching of the tip links, mainly formed by cadherin 23 (CDH23) and protocadherin 15 (PCDH15), allowing the opening of mechano-transduction (MET) channels at the apical end of the cilia[10,11](**Figure 1.6**).

The opening of MET channels allows the flow of K^+ ions into the hair cells resulting in the reduction of concentration gradient. It leads to the cell depolarization that turns in the opening of voltage gated Ca^{2+} channels (MGCs). The resultant increase of Ca^{2+} concentration causes the release of neurotransmitters glutamate from the basal pole of the hair cells to the auditory nerve endings[10] (**Figure 1.6**).

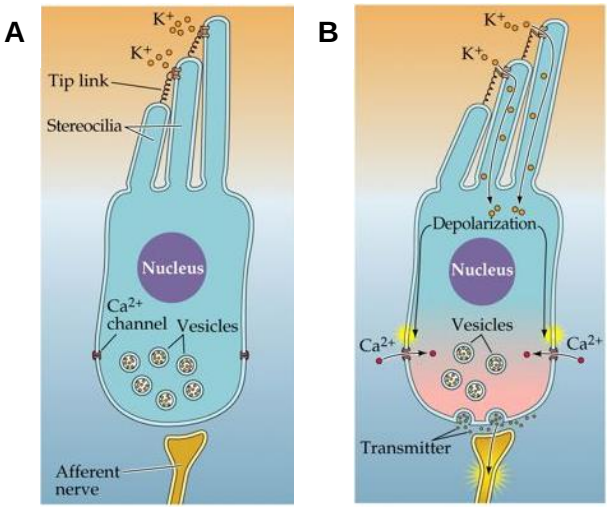

Figure 1.6. *Transduction mechanism in hair cells of cochlea.*
(A) When the stereocilia are bent, K^+ ions flow into the cells causing their depolarization; **(B)** the Ca^{2+} voltage-gate opens stimulating the release of neurotransmitters in the synaptic space to transfer the signal to post-synaptic neurons (http://www.cns.nyu.edu/~david/courses/perception/lecturenotes/ear/ear.html).

When the glutamate binds to the post-synaptic neurons that form ribbon synapses with IHCs, it favors the transient influx of positive ions which depolarizes the afferent membrane. The post-synaptic potentials excite the voltage-depended Na^+ channels triggering the action potentials. These potentials propagate along the afferent myelinated process relay the electrical signals to the neurons of spiral ganglion (SG). These SG neurons transmit the signals to the auditory brain centers, through the VIII cranial nerve[10]. The OHCs behave as sounds amplifiers responsible for sharpening the response at specific frequency and are innervated by efferent dendrites[12].

In response to a step deflection of the bundle, the current develops in sub-millisecond and then declines despite a sustained stimulus.
The activation of MET channels induces also the opening of somatic K^+ channels favoring the K^+ efflux and thus re-polarization of the cells. It occurs because the perilymph that surrounds the basal end of the cells is low in K^+ relative to hair cells cytosol. The re-polarization is also supported by Ca^{2+}-depended K^+ channels, that open when inner Ca^{2+} concentration increase, promoting the K^+ efflux[12].

1.2 Hearing

There are different physiologic tests to determine the status of the auditory system of a person. In particular, the pure-tone audiometry (air and bone conduction) allows to determine the lowest intensity (measured in decibel) at which an individual "hears" a pure tone, as a function of frequency[13]. The output of a pure-tone audiometry can be presented with an audiogram figure (**Figure 1.7**). In humans, normal hearing is characterized by hearing ability thresholds of ≤ 25 dB in both ears (**Figure 1.7**).

The hearing loss is defined by World Health Organization (WHO) as a speech-frequency pure tone average > 25 dB at 500, 1000, 2000, and 4000 Hz in the better hearing ear[14]. In particular, disabling deafness is described as loss of auditory ability > 40 dB in adults and > 30 dB in children, in the better hearing ear" (see who.int/news-room/fact-sheets/detail/deafness-and-hearing-loss). Deafness can be classified in different degrees from mild (26 dB - 40 dB), moderate (41 dB - 55 dB), moderately severe (56 dB - 70 dB), severe (71 dB - 90 dB) up to profound hearing loss (≥ 91 dB)[15] (**Figure 1.7**).

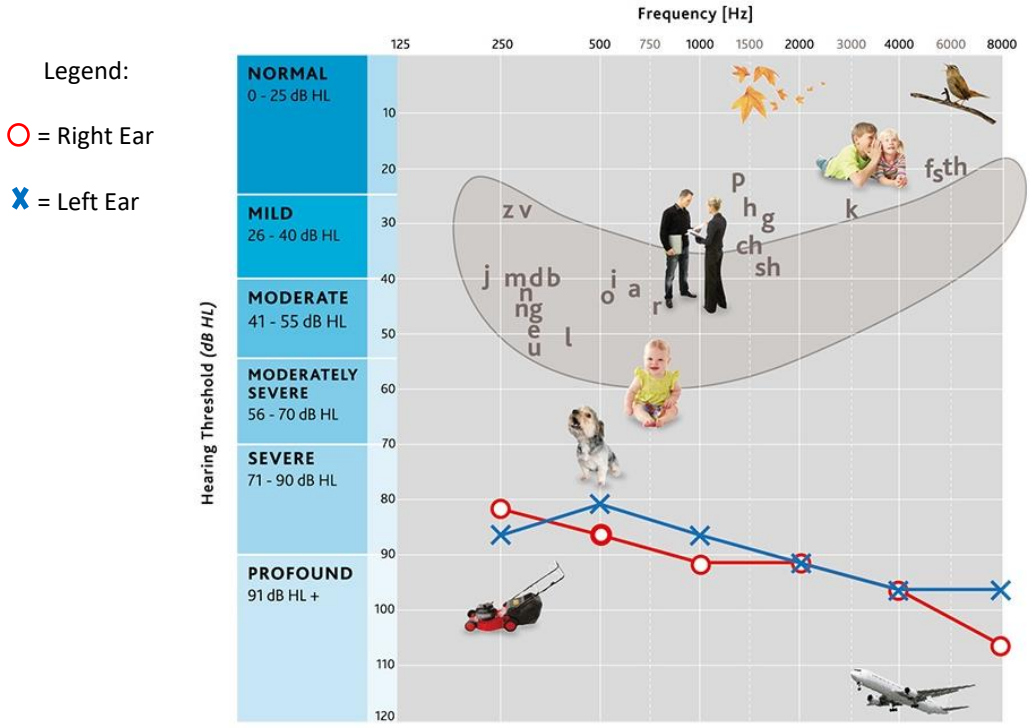

Figure 1.7. *Schematic example of an audiogram.*

The red and blue lines, right and left ear respectively, represent the auditory ability of a person at 250, 500, 1000, 2000, 4000 and 8000 Hz. In the graph are pictured the frequency at which is possible to hear specific sounds i.e., dog barking at 500 Hz or human communication 250-6000 Hz. The frequencies are reported in the *y*-axis, intensity and degree of deafness in dB in *x*-axis (Hearing Health Foundation, 2020).

1.2.1 Hearing Loss overview

Hearing Loss is the most common sensory disorder affecting around 6 % of the world population (https://www.who.int/health-topics/hearing-loss#tab=tab_1). It is typically described by its clinical features, i.e., etiology, onset and severity (**Table 1.1**).

Classification	***Description***
Type	Conductive: abnormalities of external or middle ear
	Sensorineural: malfunction of inner ear structures
	Mixed: combination of conductive and sensorineural
	Central: dysfunction or damage of VIII cranial nerve, auditory brain stem or cerebral cortex
Etiology	Genetic
	Acquired
Onset	Pre-lingual: presents before speech development (all congenital (present at birth) hearing loss forms are pre-lingua)
	Post-lingual: shows up after speech development
Presentation	Syndromic: associated with other clinical defects
	Non-syndromic
Laterality	Unilateral
	Bilateral
Stability	Progressive
	Non-progressive
	Fluctuating
Severity (dB)	Mild: 26-40 dB
	Moderate: 41-55 dB
	Moderately Sever: 56-70 dB
	Sever: 71-90 dB
	Profound: > 90 dB
Frequencies affected	Low < 500 Hz
	Middle 501-2000 Hz
	High > 2000 Hz

Table 1.1. *Example of clinical characteristics to describe Hearing Loss* [13,16].

Due to the high existing heterogeneity, there are many ways to categorize Hearing Loss (HL). As example, I report below an etiologically based classification established in 2019[16]:

- Genetic Hearing Loss that refers to a genetically inherited etiology and might be presented at birth (i.e. congenital) or developed at any time during life[16].
  The genetic hearing loss can be subcategorized into:
  a) Mendelian inheritance (congenital), that in turn can be divided in syndromic or non-syndromic based on the presence or absence of co-inherited anatomical anomalies. These two conditions can be further classified by the inheritance pattern: autosomal dominant, autosomal recessive, mitochondrial and X-linked[17];
  b) Complex inheritance is associated to multiple intrinsic (e.g., genetic predisposition) and extrinsic (e.g., lifestyle) factors. The most known forms of multifactorial hearing loss are: age-related HL, aminoglycosides-induced HL and otoclerosis[16].
- Non-Genetic Hearing Loss includes different broad categories such as infectious, head trauma and noise-induced HL[16].

In this thesis I will only focus on two forms of deafness: Non-Syndromic Hereditary Hearing Loss (NSHHL) and Age-related Hearing Loss (ARHL), for which I present a brief description.

Non-Syndromic Hereditary Hearing Loss

Approximately half of hearing loss cases have a genetic background (**Figure 1.7**)[15]. Among them the ~70 % presents a non-syndromic etiology[16]. Non-Syndromic Hereditary Hearing Loss (**NSHHL**) can be classified based on its inheritance pattern: the majority of the cases ~75 % – 80 % is autosomal recessive while the autosomal dominant represents ~20 %, the X-linked < 2 %, and the mitochondrial < 1 %[17].

Autosomal Recessive

This form of HL tends to present with a prelingual onset and is usually severe to profound at all frequencies[18]. According to literature, 71 genes have been so far associated[19] (https://hereditaryhearingloss.org/recessive-genes), with around three-fourths of the diagnosis attributable to ten genes[16,20].

The most frequently hearing loss player, *GJB2,* encodes for connexin 26, a gap junction protein and a critical component in maintaining the correct K^+ ion concentration between the endolymph and perilymph fluids. Mutations in this gene account for up to 22 % of patients with autosomal recessive NSHHL. In particular, 35delG deletion is the most common mutation in the European and European-American population[16,18]. The other three most frequently implicated genes are:

STRC that encodes for an extracellular structural protein named stereocilin expressed in the stereocilia of OHCs[21]. It is important for the proper positioning and cohesion of the stereociliar tips. Mutation in *STRC* accounts for 16 %[16,19] of the cases and are most commonly associated with mild-to-moderate phenotypes[13];

SLC26A4 encodes for an iodide and chloride anion transporter known as pendrin. It has been shown to exchange anions across the plasma membrane in several tissues[22]. Mutations in *SLC26A4* are present in 7 %[16,19] of the cases and are often associated with enlarged vestibular aqueducts[22]. Alterations of this gene may also cause syndromic HL, in the form of Pendred syndrome[18];

TECTA encodes the alpha-tectorin protein, a component of the tectorial membrane overlying the OHCs[18] and *TECTA*$^{-/-}$ mouse models exhibit deformation of this membrane[23]. Mutations in this gene regroup 5 %[16,19] of all cases and result in a peculiar middle-frequency (U-shaped) HL[18]. The specific mechanism by which these mutations cause middle-frequency HL is still unknown[23]. *TECTA* is also often involved in Autosomal Dominant inheritance of NSHHL. The involvement of some genes, such *TECTA*, in both recessive and dominant form of HL could be explained either by the existence of different mutations within the same gene that contribute to the phenotype or alternatively, by the presence of two tightly linked genes in the interval which are responsible for the different forms of deafness[24,25]. There are several examples of dominant and recessive form of human disease caused by mutations in the same gene. For example, dominant and recessive forms of myotonia have been shown to be caused by different variants in the skeletal muscle chloride channel[26] or again dominant missense mutations and a recessive non-sense mutation have been identified in the rhodopsin gene in cases of retinitis pigmentosa[27].

Other genes frequently mutated in NSHHL are *OTOF, CHD23, CHD15, MYO15A* and *TMC1*[18].

Autosomal Dominant (AD)

It is usually characterized by a post-lingual onset, progressive course and middle degree of HL[17,18], but few pre-lingual cases have also been reported. According to Hereditary Hearing Loss Homepage, to date 46 AD genes have been described (https://hereditaryhearingloss.org/dominant-genes). Some common causative genes are: *KCNQ4*, a voltage-gated K^+ channel that plays essential roles in regulating hair cell membrane potential and in maintaining ion homeostasis. Mutation in this gene are associated with progressive HL at all frequencies[28];

WFS1 encodes for Wolframin protein localized in the endoplasmic reticulum, and plays an important role in protein processing, membrane trafficking, and regulation of Ca^{2+} homeostasis[29]. Mutations in *WFS1* are associated with a very peculiar low frequencies hearing loss below 2 kHz [13,18]. This gene is also associated with Wolfram syndrome1. Some genes, such as *COCH*, may cause adult-onset autosomal dominant NSHHL[18].

X-Linked

X-Linked HL counts a low number of cases. Among, the five causative genes that have been identified (https://hereditaryhearingloss.org/xlinked-genes), the most frequent mutations occur in the transcription factor *POU3F4*[16]. These mutations result in a distinct malformation characterized by stapes fixation with cochlear hypoplasia and bulbous internal auditory canals[17]. These alteration are usually associated with mixed HL[17,18].

Mitochondrial

It tends to present as progressive sensorineural HL, begins at 5 to 50 years and the degree of deafness is variable[18]. One common form of Non-syndromic mitochondrial deafness is due to A1555G mutation in the mitochondrial 12S ribosomal ribonucleic acid (rRNA) gene[30]. It can result in severe HL from exposure to normal therapeutic levels of amino-glycosides antibiotics. However, mitochondrial disorders are usually multisystemic and thus syndromic[18].

Despite over 115 genes have already been associated with NSHHL to date[31], the current genetic tests fail to provide a diagnosis in most of the cases[32], suggesting that many novel genes still need to be characterized.

1.2.2 Presbycusis

Age-related Hearing Loss (ARHL), also known as presbycusis, is a multifactorial and complex degenerative disease. It is considered one of the most prevalent chronic conditions and is already the most common sensory disease in the elderly, affecting 321 million people worldwide[16].

Hearing ability physiologically decreases with age becoming pathological most often in the third decade[33] causing difficulties in communication associated with cognitive decline, social isolation and depression[33]. ARHL is characterized by progressive bilateral sensorineural hearing loss, that usually affects high frequencies at first.

Data published in 2020 showed that ARHL affects around 40 % of adults over 50 years old, rising to ~71 % of people over 70 years[34], and its prevalence is expected to grow even further with the progressive ageing of world population[35].

Being it a multifactorial disease, both environmental and genetic causes contribute to ARHL. The environmental factors that contribute to its development can be summarized into several categories: cochlear aging (biological age), gender, ethnicity, environment (e.g., noise exposure), lifestyle (e.g., smoking, drinking) and medical comorbidities (e.g., stroke, diabetes, hypertension and tobacco use)[14,16].

Although several risk factors have been identified, little is still known about genetics behind ARHL[36]. Its heritability is estimated in the range of 30-55 %, but to date only a low number of genes have been confidently associated to ARHL[37–40].

This suggests that there is still a strong need of new research to understand the genetic predisposition and molecular bases underlying this form of deafness.

1.3 Identification of new deafness genes

1.3.1 Next-Generation Sequencing

The identification of deafness genetic causes provides important information for the diagnosis and the treatment of this disease.

In the past decades, linkage analysis has been the most widely used and powerful strategy. In this method a genome-wide set of few hundred or thousand markers spaced millions of bases apart is typed in families with multiple affected relatives[41]. However, it requires large cohorts of homogeneous and informative families, is time consuming and a large number of cases remain genetically unexplained[41]. These limitations were recently overcome by the advent of next-generation sequencing (NGS) technologies that offer unprecedent powerful tools to identify rare variants and discover new genes[18,41]. NGS platforms allow genotype-to-phenotype association to identify the molecular basis of deafness, including targeted-genes sequencing, whole exome sequencing (WES) and whole genome sequencing (WGS)[41].

In this chapter, I briefly introduce the two methods we used for this project TRS and WES.

Target Re-Sequencing (TRS) offers the advantage of sequencing panels of genes in parallel with low cost and higher time-efficiency, becoming a fundamental tool for the HL diagnosis[42]. This method presents also several drawbacks: (i) the causative gene might be present from the panel obliging to use subsequently another pan-genome or pan-exome approach, (ii) it might sometimes induce us to falsely consider that we have identified the causative variant (e.g. identification of a variant of unknown significance in a good candidate gene); on a technical point of view it is prone to (iii) uneven coverage of the target regions due to unequal PCR efficiency across the amplicons and to (iv) allelic dropout, and (v) inability to detect large deletion and insertion events[43]. While powerful this method does not allow by definition to identify the genetic bases of the phenotype in all the cases. Furthermore, many novel deafness genes still need to be characterized[32].

In this light, the exome sequencing has become an efficient strategy for identifying novel causative genes and mutations involved in heritable disease[42].

Approximately 85 % of these mutations are located in the protein coding region, although it constitutes only around 1 % of the entire human genome[44], suggesting that WES represents a good compromise between the comprehensiveness and time-cost to analyze NSHHL patients[45]. Although, exome sequencing has allowed the identification of more than 20 new NSHHL genes in the last decade (https://hereditaryhearingloss.org/), it

presents some limitations, for example when causative variants are located intra-genically or inter-genically away from exons.

However, the combination of TRS and WES could lead to the identification of causative mutations of NSHHL owing comprehensive view of a large number of genes, time-costs reduction, high accuracy and more convincing database[41,42].

Concerning this thesis, the application of these two technologies allowed the identification of a new candidate gene associated with NSHHL that will be presented in the results chapter.

1.3.2 GWAS

The identification of genetic risk factors involved in Age Related Hearing Loss (AGHL) is difficult as its genetic complexity is probably high.

Complex traits are believed to result from variants within multiple genes and their interaction with behavioral and environmental factors[46].The contribution of rare mendelian variants is not clear yet as they can have rather a predisposing or protective effect.

Multifactorial diseases can present an oligogenic inheritance, that can occur when one gene is sufficient to cause a trait, however its expression or penetrance is influenced by another gene. This condition represents an intermediate between monogenic and polygenic inheritance[47].

These traits can also present a highly polygenic nature, when thousands of alleles across the genome contribute to heritable variance[48].

Most of the genetic variants mapped for complex traits tend to be non-coding and probably act by altering the control of gene expression, RNA stability, protein production, post-translational modification or altering the amino-acid sequence of the protein[46].

ARHL seems to be a polygenic trait but any major common genetic variants have been identified yet[49].

For these reasons, large-scale studies that compare the genetic background of ARHL patients with healthy controls are fundamental to clarify the genetics underlying this disease. The genome-wide association studies (GWAS) is an experimental design created to detect statistical association between a multifactorial trait (or disease) of interest and variants (mainly SNPs) along the genome[50]. These studies lead to the identification of many novel genetic variants associated to multifactorial diseases, such as ARHL[35,51,52].

To date just few association-studies have been performed[37,38,53–55] due to highly cost and the limitation of the study to a selected list of candidate markers or regions, they represent the best approach to understand the genetic bases of ARHL.

In this project, we have analyzed a set of 46 ARHL candidate genes form (i) previous GWAS data (ii) literature updates and (iii) animal models, in a large cohort of ARHL Italian patients. The most interesting variants emerged for this study will be presented in the results chapter.

1.4 Zebrafish as animal model for deafness studies

Native from Southeast Asia, Zebrafish, *Danio rerio*, are small tropical freshwater fish[56] and since 1930s they started to generate interest for biomedical research [57].
There are several advantages of using this species in biomedicine: genetic similarity with humans, external fertilization, high transparency of embryos, rapid development, and easy to manipulate[58]. For example, nearly 70 % of zebrafish genes have orthologues in the human genome[59], even if in many cases these are present in two copies as the genome of teleosts was recently duplicated[60].
For these reasons, in the last decade Zebrafish has become a suitable model to investigate the development and molecular genetics of the vertebrate inner ear[61–63].

Physiological studies suggest that Zebrafish have a complex sense of hearing, sharing many features with other vertebrates, including humans[64]. In particular, their sensory hair cells are homologous to those found in mammals[65], making them a good model to investigate the hearing function.

Zebrafish have developed two sensory organs that use mechanosensory hair cells:

1. the inner ear (similar to mammalian ear) is essential to detect sound waves, motion and gravity. In the inner ear there are different structures:
   three semi-circular canals and the utricle essential for the vestibular functions, the saccula, the main organ for hearing, and the lagena that represents an indeterminate mixed organ with hearing and vestibular functions[51] (**Figure 1.8**).
   The mechanosensory cells involved in hearing function are innerved by statoacoustic neurons part of the sensory ganglion (SG) that connects the inner ear with the brain[66];

2. the lateral line, a fish-/amphibian-specific organ, necessary to detect the water flow over the surface of the body[59,67]. This structure is also called neuromast and consists of clusters of sensory and supporting cells along the side of the body[59].

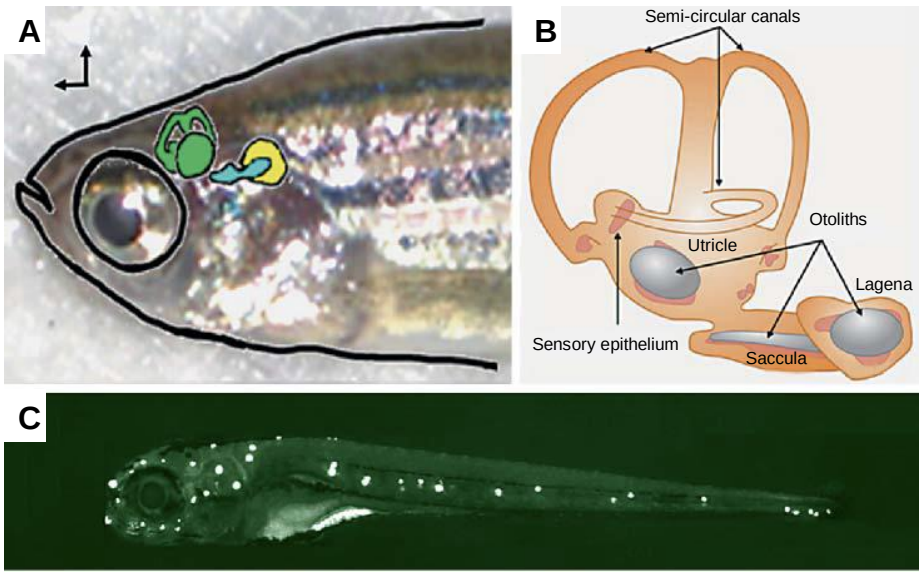

Figure 1.8. *The inner ear and the lateral line of Zebrafish.*
(A) Image of an adult zebrafish head oriented in a lateral view, with inner ear structure illustrated. The utricle and semi-circular canals are highlighted in green, the saccula in blue, and the lagena in yellow; **(B)** Schematic representation of adult zebrafish inner ear structure; **(C)** Fluorescent image of a zebrafish larva in a lateral view (head on the left). Each white dot in the head and along the body represents a cluster of hair cells centered in a neuromast (hair cells are stained using the fluorescent dye Yopro-1 - adapted image - Varshney GK et al., 2016).

Within the first five days, the Zebrafish embryos develop rapidly these specialized mechanosensory structures. In this way, it is possible to direct observe potential defects in the sensory epithelium of the inner ear, as their larvae are optically transparent for the first few days of development[59,67].
From five days post fertilization (dpf), they are perfectly able to detect sound waves[68], allowing researchers to test their auditory ability through the acoustic startle response test[64]. From a genetic point of view, more than 50 genes are known to impact the auditory inner ear and the vestibular system of zebrafish[64], and many of these genes are conserved and associated with the inner ear development and function in other vertebrates, including humans[69,70]. These features combined with their rapid development, ease of maintenance and accessibility to the inner ear, make Zebrafish an attractive and suitable model to investigate hearing loss.

2 AIM OF THE THESIS

Deafness is the most common sensory disorder worldwide (WHO).
Its molecular diagnosis is fundamental to better understand the biological mechanisms behind, provide prognostic information and personalized risk assessments of the patient.
This project aims to identify and characterize new genetic causes associated with two sub-set of deafness forms: Non-Syndromic Hereditary Hearing Loss (NSHHL) and Age-Related Hearing Loss (ARHL).
Considering the high heterogeneity of these two forms of deafness, different approaches have been adopted.
In particular, patients affected by NSHHL have been firstly screened for mutations in most common deafness genes exploiting TRS and subsequently analyzed through WES.
The combination of these two technologies permits a comprehensive view on the genome-coding sequence allowing the identification of novel potential candidate genes and variants involved in NSHHL.
On the other hand, considering that AGHL is a miscellaneous and multifactorial disorder, a list of genes identified through GWA studies and animal models have been analyzed in several inbred and outbred Italian cohort of individuals. The goal is to figure out the contribution and predisposition of new genetic variants to this form of deafness.

In conclusion, this project aims to provide fundamental discoveries to fathom the molecular bases of deafness displaying new possible targets involved in NSHHL and AGHL.
Furthermore, it could become useful for the development of new genetic therapeutic approaches that could improve the life quality of millions of people affected by deafness.

3 RESULTS

The results of the thesis will be divided in two main chapters based on the two different form of deafness studied: the first is focused on the NSHHL, while the second on the analysis of the ARHL.

3.1 Chapter 1

In this first chapter I will present the study of an Italian Family affected by NSHHL in which we identified *USP48* as a new candidate gene associated.

A summary of the contributions to this project and the awards received will anticipate the results that are presented with the respective article, submitted to Genetics in Medicine (ACMG) in October 2020, with the title: “Variants in the USP48 ubiquitin hydrolase are associated with Autosomal Dominant Non-Syndromic Hereditary Hearing Loss”.

After a short abstract, the article displays a brief introduction that precede the description of the material and methods. The main results are reported in the central section and are represented with few main figures, followed by the final discussion of the paper.

The article will end with the supplemental figures.

3.1.1 Summary of the contribution

As first author of this paper, I was in charge of the writing, literature mining and figures assembly, under the supervision of Alexandre Reymond.
I have designed the experimental study starting from the filtering analysis of WES data, the selection of candidate genes and further patients' identification through data aggregation.
I have performed *in-vitro* expression analysis and functional assay and I have designed, engineered and performed the phenotype evaluation of Knock-down Zebrafish models.
The analysis of auditory system of Zebrafish models have been performed in collaboration with Mireille Rossel. The 3-D protein modelling has been carried out in collaboration with Nicolas Guex, while the protein expression evaluation on human embryos inner ear have been done in collaboration with Edward van Beelen and Heiko Locher.
For this project, I have coordinated data sharing between six researcher groups and clinicians involved. Furthermore, I have received a fellowship from FREG found for Research and Education in Genetics at the University of Lausanne to pursue the study of this project at University of Montpellier.
I have personally presented this work at (I) European Society of Human Genetics (ESHG) Virtual meeting in 2020 with an oral presentation, and at (II) American Society of Human Genetics (ASHG) Virtual meeting in 2020 with a poster that has been selected as a "Reviewers' Choice" award, scored by reviewers in the top 10% of all poster abstracts.

The results are presented in three main figures (named **Figure 1-3**), and seven supplement figures (**Figures S1-7**).

3.1.2 Article

Variants in the *USP48* ubiquitin hydrolase are associated with Autosomal Dominant Non-Syndromic Hereditary Hearing Loss

Sissy Bassani[1,2], Edward van Beelen[3], Mireille Rossel[4], Norine Voisin[1], Anna Morgan[2,5], Yoan Arribat[6], Nicolas Chatron[1,7], Jacqueline Chrast[1], Massimiliano Cocca[5], Benjamin Delprat[4], Flavio Faletra[5], Giuliana Giannuzzi[1,*], Nicolas Guex[9], Roxane Machavoine[10], Sylvain Pradervand[1], Jeroen J. Smits[11], Jiddeke M. van de Kamp[12], Alban Ziegler[9], Francesca Amati[6], Sandrine Marlin[10], Hannie Kremer[11], Heiko Locher[3], Tangui Maurice[4], Paolo Gasparini[2,5], Giorgia Girotto[2,5], Alexandre Reymond[1].

[1]Center for Integrative Genomics, University of Lausanne, Lausanne, Switzerland
[2]Department of Medicine, Surgery and Health Sciences, University of Trieste, Trieste, Italy
[3]Department of Otorhinolaryngology, Leiden University Medical Center, Leiden, The Netherlands
[4]MMDN, Univ Montpellier, EPHE, INSERM, Montpellier, France
[5]Institute for Maternal and Child Health, IRCCS, Burlo Garofolo, Trieste, Italy
[6]Department of Biomedical Sciences, University of Lausanne, Lausanne, Switzerland
[7]Service de Génétique, Hospices Civils de Lyon, Lyon, France
[9]Bioinformatics Competence Center, University of Lausanne, Lausanne, Switzerland
[10]Centre de référence Surdités Génétiques, Hôpital Necker, Institut Imagine, Paris, France
[11]Department of Otorhinolaryngology and Department of Human Genetics, Donders Institute for Brain, Cognition and Behaviour, Radboud University Medical Center, Nijmegen, The Netherlands
[12]Department of Clinical Genetics, Amsterdam UMC, Vrije Universiteit Amsterdam, Amsterdam, The Netherlands

*present address: Institute of Biomedical Technologies, Italian National Research Council (CNR), Segrate, Milan, Italy

Correspondence should be addressed to:
Alexandre Reymond, alexandre.reymond@unil.ch

Running title: *USP48* and hearing loss

Keywords: hearing loss, zebrafish, ubiquitin hydrolase, Kolliker's organ, exome sequencing

Abstract

Non-Syndromic Hereditary Hearing Loss (NSHHL) is a genetically heterogeneous sensory disorder. Through exome sequencing and data aggregation, we identified a family with six affected individuals and three unrelated NSHHL individuals with predicted-to-be deleterious variants in *USP48*. *USP48* encodes a ubiquitin carboxyl-terminal hydrolase under evolutionary constraint. Pathogenicity of the missense variants is supported by three-dimensional representation and *in vitro* assays of the encoded protein. For example, the familial missense variant affects a loop that controls binding to ubiquitin thus leading to incapacity of the mutated protein to hydrolyze tetra-ubiquitin.

Consistent with a contribution of *USP48* to auditory function, immunohistology showed that the encoded protein is expressed in the developing human inner ear, specifically in the spiral ganglion neurons, the outer sulcus, the interdental cells of the spiral limbus, the stria vascularis, the Reissner's membrane, and in particular in the transient Kolliker's organ that is essential for auditory development.

Engineered zebrafish knocked-down for the *USP48* paralog presented with a delayed development of primary motoneurons, less developed statoacoustic neurons innervating the ears, decreased swimming velocity and circling swimming behavior indicative of vestibular dysfunction and hearing impairment. Corroboratingly, acoustic startle response assays revealed a significant decrease of auditory response of zebrafish lacking *usp48* at 600Hz and 800 Hz wavelengths.

In conclusion, we describe a novel autosomal dominant NSHHL entity through a multipronged approach combining exome sequencing, animal modeling, immunohistology and molecular assays.

Introduction

Hearing loss is the most common sensory disorder affecting an estimated 6 % of the population (WHO - https://www.who.int/health-topics/hearing-loss#tab=tab_1). Deafness is often the result of malfunction of inner ear structures such as the cochlea and the auditory nerve[72]. Notwithstanding that over 120 genes have already been associated with Non-Syndromic Hereditary Hearing Loss (NSHHL)[29], the current genetic tests fail to provide a diagnosis in almost half of the cases[30]. This suggests that many novel deafness genes need to be characterized. In this study we combined exome sequencing (ES), data aggregation from multiple laboratories, animal modeling and molecular assays to associate *USP48* (MIM**:** 617445) variants with an autosomal dominant NSHHL (ADNSHHL).

Material and Methods

Ethical Approval

Each participant signed consent forms for clinical studies. In Italy, the research approval was obtained from the Institutional Review Board of IRCCS Burlo Garofolo, Trieste. The study of the Dutch subjects was approved by the medical ethics committee of the Radboudumc (registration number: NL33648.091.10). The research was conducted according to the ethical standards defined by the Helsinki Declaration.

Use of human fetal specimens was in accordance with the Dutch legislation (Fetal Tissue Act, 2001) and the WMA Declaration of Helsinki guidelines. Approval was obtained from the Medical Research Ethics Committee of Leiden University Medical Center (protocol registration number B18.044). Written informed consent of the donor was obtained following the Guidelines on the Provision of Fetal Tissue set by the Dutch Ministry of Health, Welfare and Sport (revised version, 2018).

Clinical description

Italian family: All NSHHL living affected individuals of the Italian family underwent a clinical ENT examination. Hearing function was assessed by pure-tone audiometry, tympanogram, and oto-acoustic emissions. Other clinical tests were carried out to exclude syndromic forms. Briefly, the proband (IV:2; **Figure 1A**) presented with moderate to severe bilateral sensorineural hearing loss at all frequencies. She was diagnosed at 8 years of age and is using hearing aids since. Her mother (III:2) presented with mild to moderate hearing loss at middle frequencies, whereas her maternal uncle (III:1) showed profound bilateral sensorineural hearing loss. Hearing loss requiring prosthesis was diagnosed in the maternal

grandmother (II:2) at 50 years of age. Her brother (II:3) is affected by moderate hearing loss at all frequencies. His deafness was recognized at birth and worsened in adulthood.

Dutch proband 1: While the referring physician indicated autosomal dominant inheritance of NSHHL for this proband, we were unable to gather more detailed information on the phenotype given that the data were anonymized before analysis.
Dutch proband 2: This proband reported progressive hearing loss starting at 24 years of age without additional syndromic features. At 40 years of age her audiogram, displayed moderate to severe sensorineural hearing loss for all frequencies with asymmetry between both ears. A computed tomography of the bilateral temporal bones did not show abnormalities. Her mother complained of hearing loss since the age of 27 years that progressed to profound hearing loss. A maternal uncle was similarly reported to be hearing impaired. Whereas such a pedigree suggests autosomal dominant inheritance of hearing impairment, as the mother and maternal uncle did not consent samples, we were not able to confirm transmission.
French proband: She is the third child of unrelated parents of French origin without any familial medical history (Guyana and French metropolis). She was born at term (38+3 GW) from a twin pregnancy with normal weight (2830 g), length (46 cm) and head circumference (33 cm). She had good psychomotor development, sitting at six months, walking at 16 months. Isolated right profound sensorineural hearing impairment was diagnosed at 12 months, while left hearing was still normal during the clinical genetic consultation at 6 years old. Suggestive of a right cochlear nerve aplasia or hypoplasia, MRI of cerebral and internal auditory canals could not visualize the right cochlear nerve.

Genetic Analyses

Italian family: DNA was extracted from peripheral blood using a QIAsymphony instrument (Qiagen) and quantified with a Nanodrop ND-1000 spectrophotometer (NanoDrop Technologies). The family was sequentially assessed for causative variants in *GJB2* (MIM**:** 121011), *GJB6* (MIM**:** 604418), *MTRNR1* (MIM**:** 561000) and a panel of 96 deafness genes by targeted resequencing[92] with negative results. The affected subjects IV:2, III:1, III:2 and II:3, as well as the unaffected members IV:1 and III:3 of the family (**Figure 1A**) were thus subjected to ES using the Ion ProtonTM platform according to the manufacturer's protocols (Life Technologies). Briefly, 1 µg of genomic DNA was used to construct DNA libraries using the Ion AmpliSeqTM Exome Kit. The overall mean-depth base coverage was 102-fold, while

on average 89 % of the targeted region was covered at least 20-fold. Read mapping and variant calling were performed using Ion TorrentSuite v4.0 software (Life-Technologies). Variants were filtered using Varapp according to quality of the calling, their frequency in control populations (≤ 1% in 1000genome and Genome Aggregation Database (GnomAD) v2.1.1) and their predictive impact on the function of the protein (high and medium impact in PolyPhen-2 and SIFT databases, GERP score ≥ 3.00 and CADD (scaled) ≥ 10.00) as described [93] and an autosomal dominant inheritance scenario. Sanger sequencing was used to confirm segregation.

Dutch probands: Exome capture, sequencing and variant filtering was performed as previously described[94].

French proband: DNA was extracted from leucocytes from the proband and her parents. An array-CGH (400kb resolution) was normal. Exome capture was performed with the Sure Select Human All Exon kit (Agilent Technologies). Agilent Sure Select Human All Exon (58 Mb, V6) libraries were prepared from 3 µg of genomic DNA sheared with an Ultrasonicator (Covaris) as recommended by the manufacturer. Barcoded exome libraries were pooled and sequenced with a HiSeq2500 system (Illumina), generating paired-end reads. After demultiplexing, sequences were mapped on the human genome reference (NCBI build 37, hg19 version) with BWA. Variant calling was carried out with the Genome Analysis Toolkit (GATK), SAMtools, and Picard tools. Single-nucleotide variants were called with GATK Unified Genotyper, whereas indel calls were made with the GATK IndelGenotyper_v2. All variants with a read coverage ≤2× and a Phred-scaled quality ≤20 were filtered out. The overall mean-depth base coverage of the trio was between 142 and 217-fold, while more than 99% of the targeted region was covered at least 15-fold. Variant-filtering strategies especially familial segregation led to the identification of only one candidate variant: a *de novo* affecting a splice donor site in *USP48.*

Ubiquitin hydrolase activity assay

The plasmids pcDNA3 expressing hUSP48 wild-type (FLAG-USP48^{WT}; ENST00000308271.14) and a catalytically dead enzyme (FLAG-USP48^{C98S}) were donated by Dr. G. Mosialos, Aristotle University of Thessaloniki[95]. The *USP48* mutations identified in the French and Dutch probands were engineered using the QuikChange II XL Site-Directed Mutagenesis Kit (Agilent Technologies) following the manufacturer's instructions. The

FLAG-USP48$^{1-1019}$ encoding a truncated protein was engineered by site-directed mutagenesis of the Gln1019 CAA codon into an ochre TAA stop codon. Sanger sequencing confirmed each variant. HEK293T cells were transfected with FuGene (FuGene Hd Transfection, #E2312, Promega). Cells were cultured at 37°C under 2 to 4 % CO2 in DMEM supplemented with 10 % FBS and 1 % Pen/Strep. Cells were lysed 24 or 48 hours after the transient transfection in RIPA buffer (#20-188, Millipore) supplemented with proteases inhibitors (Halt Protease & Phosphatase inhibitor cocktail, #78440, Thermo Scientific). The protein lysate concentration was determined by BCA Assay (Pierce, BCA Protein Assay Kit #23227, Thermo Scientific). Equal amounts of proteins were resolved on 4-15 % SDS-PAGE mini-gels and transferred to nitrocellulose membranes (GE Healthcare, Life Science) to assess FLAG-USP48 expression. Immunoblots were blocked in 5 % milk powder in TBST (50 mM Tris-HCl, pH 7.4, 200 mM NaCl, and 0.1 % Tween 20) for 1 h at room temperature (RT). Membranes were incubated overnight at +4°C with primary anti-bodies: anti-Flag 1:20000 (#F3165, anti-Mouse, Sigma) and anti-α-actin 1:2500 (anti-Rabbit, Sigma) diluted in TBST. Secondary antibodies: anti-Mouse-HRP (#W402B, Promega) and anti-Rabbit-HRP (#sc-2030, Santa Cruz Biotechnology) were diluted, 1:2500 and 1:5000 respectively, in TBST and incubated for 1h at RT. Reactive bands were detected with ECL detection kit (Immobilon Western Kit, Millipore). Ubiquitin hydrolase activity assay were performed as described[95]. Briefly, wild-type or mutated FLAG-tagged USP48 proteins were immunoprecipitated from cell lysates without protease inhibitors 48 h post-transfection. Immunoprecipitated proteins were incubated with 0.8/1 μg of tetraubiquitin molecules (63-linked polyubiquitin chain, Boston Biochem). Reactions were separated by SDS-PAGE followed by Coomassie staining.

Protein model

A USP7 (MIM: 602519) model was built using Swiss-PdbViewer (spdbv)[96] as described[97]. The chain C of pdb entry 4YOC[98] was superposed onto pdb entry 5J7T using the iterative magic fit function of spdbv. Residues Phe787 and onward of 5J7T were deleted and replaced by residues Phe787 - Gly1078 of 4YOC chain C, which was renamed to chain A. The structure of USP9X (MIM: 300072; pdb entry 5WCH)[99] was then superposed onto the model of USP7; the backbone of pdb entry 5WCH chain A residues Arg1896-Cys1908 and Ala1948-Arg1955 were superposed onto the corresponding residues of the USP7 model (residues Lys476-Cys488 and Ala513-Arg520). Finally, the USP48 sequence (Swiss-Prot entry Q86UV5) was aligned onto the USP7 template.

Human inner ear expression

Human fetal inner ears were collected after elective termination of pregnancy by vacuum aspiration. Fetal age (in weeks, W), defined as the duration since fertilization, was determined by obstetric ultrasonography prior to termination. Tissue was obtained at the following developmental stages: W12 (n = 3), W14 (n = 3), W15 (n= 2), W16 (n = 2), W17 (n = 1). Inner ears were fixed in 4% paraformaldehyde, decalcified and embedded in paraffin as previously described[100]. Sections (5 µm) were cut using a HM 355 S rotary microtome (Thermo Fisher Diagnostics). Sections were deparaffinized in xylene and rehydrated, followed by standard immunohistochemistry procedure[100]. Sections were incubated overnight at +4°C with a monoclonal mouse anti-USP48 antibody (1:10, #H00084196-M01, Abnova). Next, sections were incubated with a secondary AF594 donkey anti-mouse antibody (1:500, #A-21203, Thermo Fisher Scientific) for 1h at RT. Nuclei were stained with DAPI. Negative controls were carried out by matching isotype controls and omitting primary antibodies. Positive controls were carried out by staining sections of known positive human tissue samples. At least three separate immunostaining experiments for each fetal stage were performed.

Zebrafish model

Zebrafish (*Danio rerio*, Oregon AB) were maintained at 28.5 °C and on a 14:10 h light/dark cycle and staged by hours (h) or days (d) post fertilization (pf). Eggs were obtained by random mating between sexually mature individuals. All procedures complied with both the European Convention for the Protection of Animals used for Experimental and Scientific Purposes and the National Institutes of Health guide for the care and use of Laboratory animals. Housing and experiments were approved by the local authorities, i.e. the Vaud cantonal authority (authorization VD-H21) and INSERM, Montpellier University. We generated founder F0 mutant zebrafish depleted for *usp48* by CRISPR/Cas9 genome editing. Three distinct guide (g)RNAs targeting coding sequence in *usp48* exon 4 (g*usp48*-4 5'-AGATGCTCGCAAATCGTCCGTGG-3'), exon 9 (g*usp48*-9 5'-AGCGCGGTGTTGATTCATCG-3') and exon 10 (g*usp48*-10 5'-GACAGAAGAGATTAACCAGA-3') were designed using the CHOPCHOP tool[101]. Briefly gRNAs were transcribed *in vitro* using the GenArt gRNA synthesis kit (#A29377, ThermoFisher) according to the manufacturer's instructions. A total of 1 nl of a cocktail containing 100 ng/µl of each gRNA was injected with 200 ng/µl of Cas9 protein (PNA Bio),

as treatment, or with the same amount (µl) of water, as control, was injected into one-cell stage embryos. KCl (200 mM) was added to increase the efficiency of the method and Phenol-Red (4x) to visualize the injection. Toxicity of the three guides was compared at 48 hpf while their efficacy was assessed after 72 hpf analyzing fish locomotion. To determine targeting efficiency in founder (F0) mutants, we extracted genomic DNA from 2 dpf embryos and PCR amplified the region flanking the gRNA target site. PCR products were denatured, reannealed slowly and separated on a 20% TBE 1.0-mm precast polyacrylamide gel (Thermo Fisher Scientific), which was then incubated in ethidium bromide and imaged on a ChemiDoc system (Bio-Rad, Hercules, CA) to visualize hetero- and homoduplexes.

Locomotion assays

A first qualitative analysis was performed exploiting the touch-response test on 72 hpf larvae, by a slight touch stimulation. The motion of each single larva was examined and scored as « normal swimming », « motionless », « looping swimming » or « pinwheel swimming ». Representative tracking video was obtained with a camera. A second quantitative test was performed analyzing 5 dpf zebrafish spontaneous motility using the Zebrabox® recording system (Viewpoint, Lissieu, France). Locomotion was recorded for each individual larva on a 96-well plate for 10/15 minutes and presented as slow (3-6 mm/s) and high velocities (>6 mm/s)[102].

Acoustic Startle Response (ASR)

5 dpf zebrafish larvae were transferred to a 96-well plate in 300 µl of water per well and then placed in a ZebraBox® (ViewPoint) inside a soundproof box. After 30 minutes of adaptation, larvae were exposed to three intermittent noise stimulations, 1 second per stimulus. Several frequencies were assessed at 90 dB: 400 Hz, 600 Hz, 800 Hz, 1000 Hz and a broad-band noise, a.k.a. white noise, consisting of all frequencies together. The experiments were performed in light condition. The noise was computer-generated and played through two commercial aerial loudspeakers placed in the chamber. The sound intensity within the box was measured with a noise detector. The variation in ASR were quantified to assess hearing ability. The activity of larvae was automatically and objectively measured before and after sound stimuli and then analyzed. Zebrafish activity was quantified using the quantization mode of ZebraLab® software (Viewpoint)[103]. The results were pooled into 1-s time bins to assess ASR.

Visual Motor Response (VMR)

5 dpf zebrafish larvae were transferred to a 96-well plate and then placed inside a ZebraBox® (ViewPoint) equipped with infrared illumination for imaging in the dark itself positioned in a soundproof box. In the box, white light can be controlled accurately. The light-dark protocol consisted of 30 minutes of adaptation in the dark followed by two alternating periods of light (100 % of light intensity) and dark of 10 min each one. Zebrafish activity was quantified using the ZebraLab® software (Viewpoint)[103]. Data were pooled into 1 min time bins to assess the VMR.

Statistics

Differences between experimental groups were determined by the GraphPad Prism software (version 8.0). Student's *t*-tests (two-tailed) were performed to analyze behavioral changes in response to noise and light stimulation. The minimum criterion for significance was $p < 0.05$.

Immunohistochemistry of Zebrafish embryos

Zebrafish were treated with 75 µM PTU from 24 hpf to prevent pigmentation. Zebrafish analyzed at 28 hpf were dechorionated before fixation. At appropriate developmental stages, they were anesthetized with 0.0168% tricaine (MS-222, E1052, Sigma-Aldrich) and fixed in 4% PFA for 1 h at RT, permeabilized first in 1X phosphate saline buffer (PBS), 0.5% Triton X-100, for 90 min and subsequently in 1X PBS, 1%Triton X-100, for 2 h on a shaker. Embryos were incubated in blocking buffer (1% BSA in 1X PBS) for 1 h at RT and incubated in primary antibodies overnight at 4°C on a shaker. Primary antibodies were from following sources: mouse anti-synaptotagmin 2 (Znp-1, 1:100, DSHB), mouse anti-islet 1 and 2 (39.4D5, 1:100, DSHB), anti-α-bungarotoxin Alexa Fluor™ 555 conjugate (B35451, 1:50, Invitrogen). Following washes with 1X PBS, the embryos were incubated in secondary antibodies overnight at 4°C. For immunofluorescence: Alexa Fluor™ 488 conjugated secondary antibody (1:500) and Phalloidin (1:2000) were used. Nuclei were stained with DAPI (1:8000) for 10 min at RT. Imaging was performed using confocal microscope LSM880 airyscan (Carl Zeiss). Quantification of motoneurons projection lengths was obtained with ImageJ software.

Otoliths, Hair Cells and Statoacoustic neuron structures in Zebrafish Larvae

Zebrafish larvae were analyzed at different timepoints to compare the phenotype and the morphology of specialized structures among treated, controls and wild-type fish. Eggs were obtained by random mating between sexually mature individuals (AB line). Some were fixed with PFA 4% in 1X PBS to assess the distance and dimension of otoliths at 5 dpf, and the morphological phenotype during development from 1 to 5 dpf. Eggs imaging was performed using an optical microscope. Fish length was measured from the head side of the swim bladder to the end of the tail from 3 dpf onwards. Fish length corresponded to the entire animal length from head to tail at 1 and 2 dpf. Other eggs were anesthetized with 0.0168% tricaine (MS-222, E1052, Sigma-Aldrich), bathed in 2 µM of YO-PRO-1 for 30 min, followed by three washes with 1X PBS, to assess the functionality of the hair cells at 3 and 5 dpf. Imaging was performed using a fluorescent macroscope (Olympus). A third group of eggs obtained by mating Brn3c:mGFP females in which hair cells of the inner ear and the lateral line neuromasts are specifically labelled in green[104] and NBT-dsRED males in which the neuronal system is labelled in red (neural-specific beta tubulin promoter driving expression of dsRed red fluorescent protein[105] were anesthetized with 0.0168 % tricaine and analyzed at 3, 4 and 5 dpf to assess the structure of the hair cells and statoacoustic neurons expressed in the ear. Imaging was performed using confocal microscope LSM880 airyscan (Carl Zeiss).

Results

Within our collection of NSHHL Italian families, we identified by ES a four generation family with six affected individuals in which the pathology segregated with the chr1: g.22056281G>A, NM_032236:c.1216G>A p.(Gly406Arg) *USP48* missense variant (GRCh37/hg19) (**Figure 1A**). While it is predicted to be deleterious by multiple prediction tools (PolyPhen-2: possibly damaging, score = 1; SIFT: deleterious, CADD = 29.1, GERP = 5.44), this variant is present in GnomAD v2.1.1 with a frequency of $6.7x10^{-5}$ (17 allele out of 251,304 with no homozygotes). Consistent with the presence of this variant in supposedly healthy individuals, we observed an incomplete penetrance of the disease within our family, with one hearing individual (III:4) carrying the variant (**Figure 1A**). This is consistent with the notion that many of the developmental disorder genes awaiting discovery are likely to be less penetrant than the currently known genes (Joanna Kaplanis et al., 2020). Note also that while GnomAD “has made every effort to exclude individuals with severe pediatric diseases, they do not rule out the possibility that some of their participants do actually suffer from a disease of interest”. No other rare variant segregated with the disease.

Our search for more cases led to the identification of two unrelated Dutch NSHHL affected individuals with predicted-to-be deleterious missense variants in *USP48* absent from GnomAD. These are chr1:g.22032676-77CA>TT c.2216CA>TT p.(Thr739Leu) (CADD=23.3) in proband 1 and chr1:g.22028059 c.2659A>G p.(Ser887Gly) (CADD = 22.2) (GRCh37/hg19) in proband 2. We uncovered a ninth affected individual in France presenting with unilateral hearing loss and cochlear nerve aplasia and a *de novo* splice variant in the same gene chr1:g.22013690T>C c.3058+2T>C. This variant abolishes the donor site according to MaxEntScan and NNSplice. These predictors also suggest that the next GT will not be used because of a unfavorable preceding TTT stretch, which will result in the addition of ten new residues before a TGA opal stop codon p.(Val1020Glyext*9). While we cannot exclude that the later association is spurious before identification of other similarly affected individuals, we think that it is important to document this case.

The pathogenicity of the Italian variant is supported by the three-dimensional representation of the encoded peptide. The mutated residue is located within a flexible loop that flanks over the catalytic site of the hydrolase and could play a role in substrate specificity. (**Figure 1B**). Of note the Met415 residue, often found somatically mutated in Cushing's disease, i.e. adenomas of the pituitary[74,75], is only a few residues after the end of the loop bearing Gly406, in a stretch of residues [AY**M**LVY] conserved in USP48 orthologs and in a region positioned close to ubiquitin (< 8 Å) and within 12 Å of active site residues Cys98 and His353 (**Figure 1B**). Whereas we were unable to model the portion of the protein comprising Ser887 due to only weak homologies to crystalized templates, Thr739 is situated in a conserved T-D-[VE]-L-Y stretch found in 185 Swiss-Prot sequences. A search for templates using HHPRED[76] identified a DUSP (domain present in USPs) fold (pdb entry 3LMN; DOI 10.2210/pdb3LMN/pdb). NetPhos 3.1[77] predicts that Thr739 could be phosphorylated by CKII or an unspecified kinase (score of 0.508 and 0.755, respectively), whereas Src could be phosphorylating the neighboring Tyr743 (0.505). These kinases have been identified in a screen for enzymes involved in ototoxic damage to the murine organ of Corti[78]. Mutation of this threonine residue could affect phosphorylation status and protein-protein interaction as it is exposed on the surface of the DUSP domain (**Figure S1**).

USP48 encodes a ubiquitin carboxyl-terminal hydrolase under evolutionary constraint with five observed loss of function variants (LoF, i.e. truncation variant) versus 65 expected (ratio o/e = 0.08 [0.04-0.16]; pLI = 1) and 256 observed missense variants versus 548 expected (o/e = 0.47 [0.42-0.52]; Z = 4.37) in GnomAD. Whereas some of the genes associated with

autosomal dominant NSHHL (ADNSHHL) are not constrained especially the prevalent ones (e.g., *GJB2* o/e = 2.62 and *GJB6* o/e = 1.07), the observation that 30 out of 46 (65%) presents with o/e LoF below 50 % favors the hypothesis of some evolutionary pressure on dominant non-syndromic deafness genes (o/e median = 0.37; **Figure 1C**).

We then assessed *in vitro* the effect of the *USP48* variants on the activity of the encoded ubiquitin carboxyl-terminal hydrolase. The peptides FLAG-USP48^{WT} (wild-type), FLAG-USP48^{C98S}, encoding a catalytically dead enzyme, FLAG-USP48^{G406R}, FLAG-USP48^{T739L}, FLAG-USP48^{S887G} and FLAG-USP48$^{1-1019}$ that encodes only the first 1019 amino-terminal residues of the protein and mimics the French variant, were expressed in HEK293T cells. The capacity of the corresponding anti-FLAG immunoprecipitated extracts to hydrolyze ubiquitin was tested upon incubation with tetra-ubiquitin. We observed that like the catalytically dead enzyme and contrary to the wild-type molecule, the truncated USP48 hydrolase and the ones containing the ADNSHHL missense variants were unable to cleave tetra-ubiquitin into tri-, di- and mono-ubiquitin (**Figure 1D**).

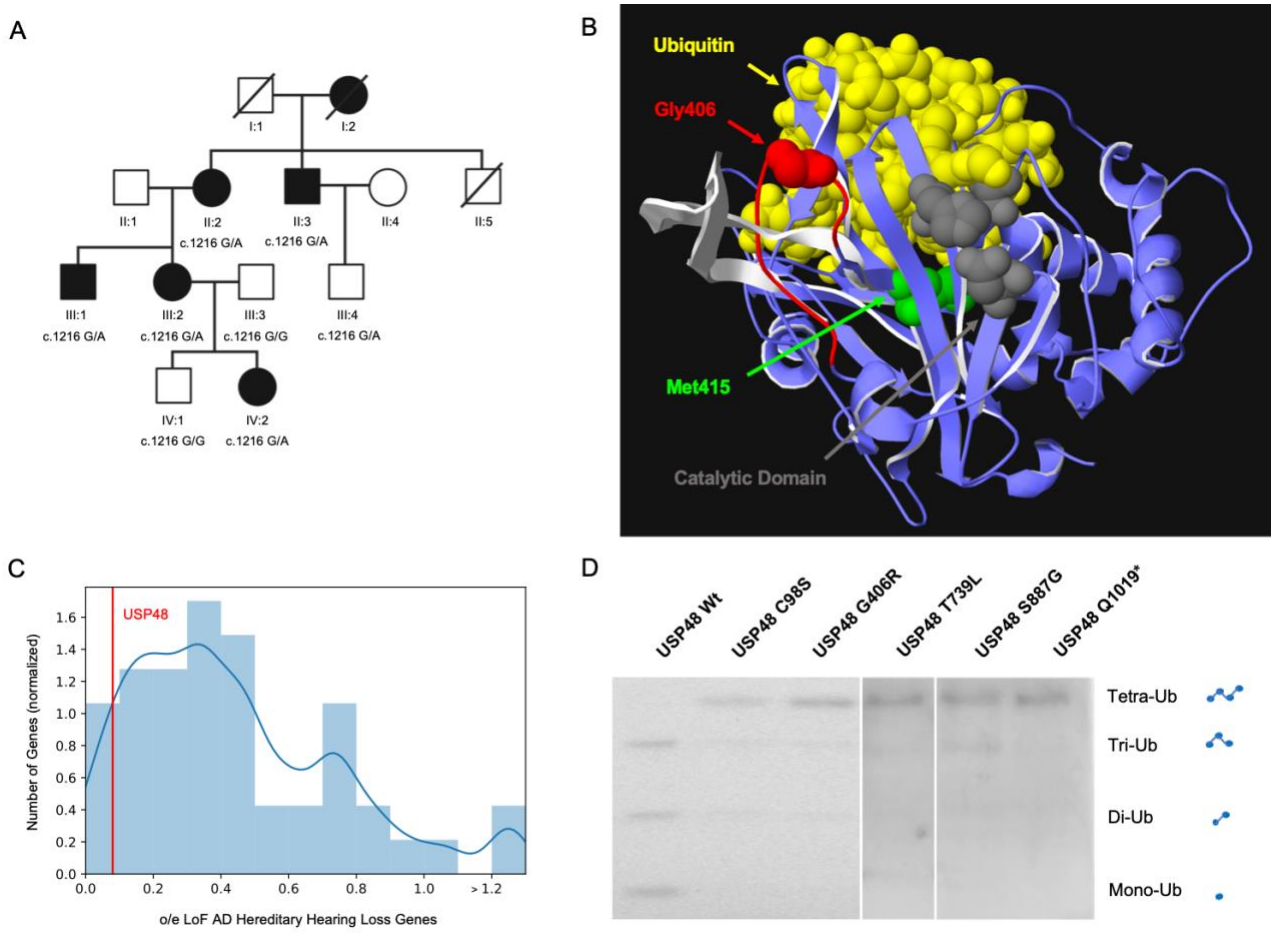

Figure 1. *Pedigree, 3-D modeling and in vitro functional analysis.*

A) Pedigree of the Italian family carrying the mutation (c.1216G/A) in *USP48*. Filled symbols represent affected individuals. **B)** USP48 tridimensional protein modeling based on the paralogous USP7 template (blue ribbon). In the model are highlighted the Ubiquitin molecule (yellow), Gly406 mutated in the Italian family (red space-filled residue) within the unstructured loop of residues Tyr498-Asn512 (red ribbon), the equivalent USP9X region bearing residues Phe1921-Asn1947, which form an antiparallel beta-sheet (white ribbon), Met415 mutated in Cushing's disease (green space-filled), three USP48 residues Cys98, His353, Asn370 of the catalytic triad corresponding to USP7 residues Cys223, His464 and Asp481 (gray space-filled). **C)** Distribution of evolutionary constraint of ADNSHHL genes based on ratio of observed over expected LoF variants in GnomAD v2.1.1 (n=46 genes, bin width=0.1). The density distribution and the data normalization have been performed through the Kernel density estimation function (KDE). About two-third of the ADNSHHL genes appear to be under evolutionary pressure. The o/e ratio of *USP48* is indicated with a red line. **D)** Ability of the USP48 alleles (FLAG-USP48 Wt, FLAG-USP48^{G98S} catalytically dead, FLAG-USP48^{G406R}, FLAG-USP48^{T739L}, FLAG-USP48^{S887G} and FLAG-USP48$^{1-1019}$) to hydrolyze tetra-ubiquitin molecules in tri- di- and mono-ubiquitin molecules.

Consistent with a contribution of *USP48* to auditory function, immunohistology showed that the USP48 protein is present in fetal human inner ear specimens. In inners ears of W12 and W14 old human fetuses, we found antigens recognized by anti-USP48 antibodies in the cytoplasm of supporting cells within the Kolliker's organ, the earliest epithelial structure present in the developing auditory sensory organ[7], in interdental cells, in cells of the outer sulcus, in the Reissner's membrane and in fibrocytes of the spiral ligament (**Figure 2A**). Transient expression was observed in intermediate cells of the stria vascularis at W14 (**Figure 2A**), but not at W12 (**Figure S2A**). Spiral ganglion neurons and the surrounding mesenchyme also expressed USP48 (**Figure 2B**). In addition, USP48 is present in the vestibular system, in particular in supporting cells of the saccular macula and ampulla, the periotic mesenchyme, the neuronal cell bodies of the Scarpa's ganglion and the epithelial cells of the semicircular canals of W15 embryos (**Figure 2C, Figure S2B-C**). No expression was seen in the inner or outer hair cells of the cochlea and in the hair cells of the vestibular system at these developmental stages.

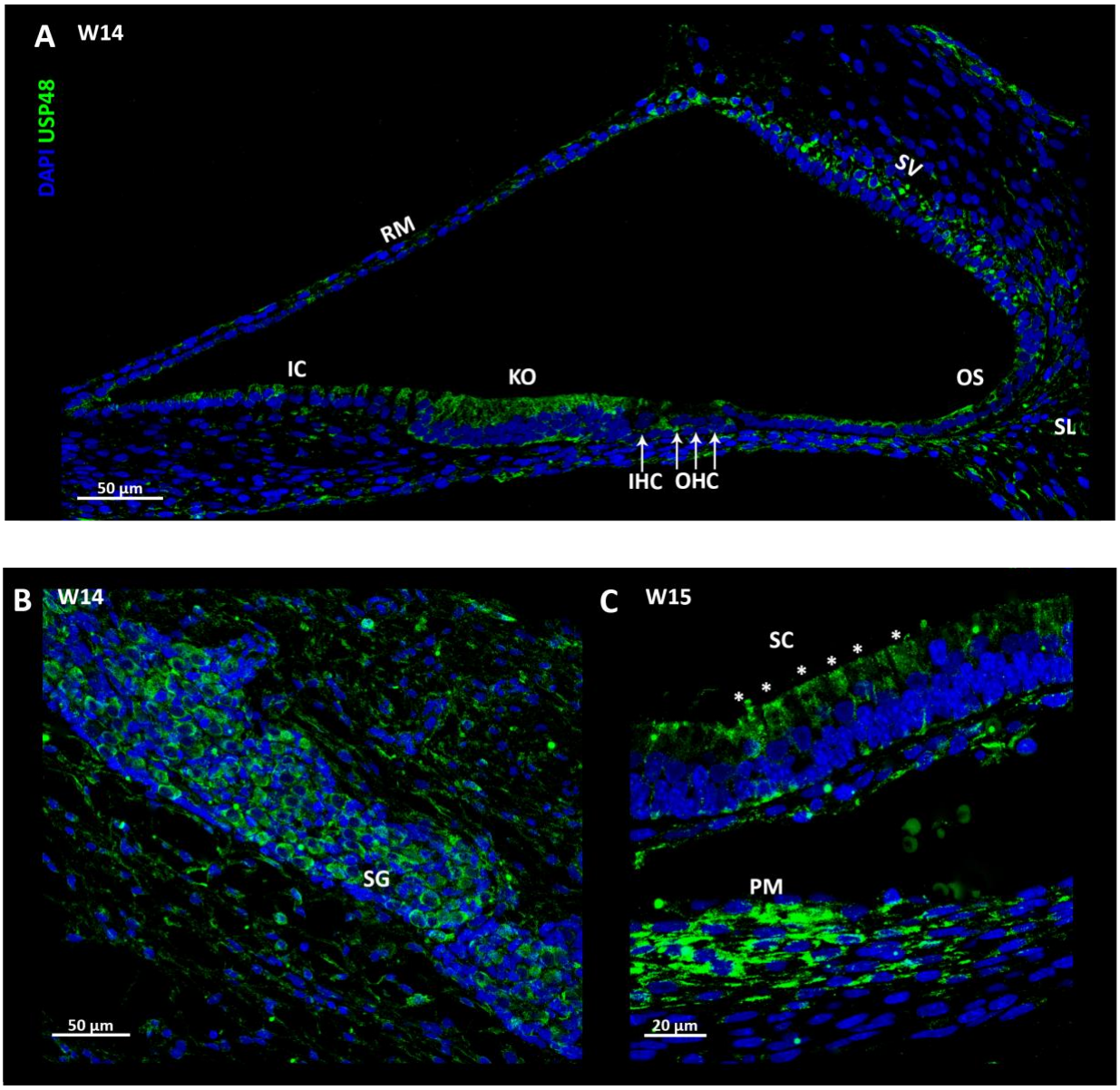

Figure 2. *USP48 expression in the human fetal inner ear.*

Human embryonic ear immunostaining showing DNA (DAPI) in blue and the USP48 protein in green. USP48 is expressed in several structures: **(A)** at W14, in Kolliker's Organ (KO), the Outer Sulcus (OS), the fibrocytes of the Spiral Ligament (SL), the interdental cells of the spiral limbus (IC), the intermediate cells of the Stria Vascularis (SV) and in Reissner's Membrane (RM), but not in the Inner Hair Cells (IHC) or Outer Hair Cells (OHC); **(B)** at W14, in the neurons and supporting mesenchyme of the Spiral Ganglion (SG); **(C)** at W15 in the Periotic Mesenchyme (PM) and the Supporting Cells (SC) of the saccule macula of the vestibular system (pinpointed by asterisks).

To gain insight into the function of *USP48*, we ablated the orthologous *usp48* in zebrafish by CRISPR/Cas9 genome editing[64]. We engineered F0 larvae using three different small guide RNAs targeting exons 4 (g*usp48*-4), 9 and 10 of *usp48* and assessed their locomotion and touch response. At 3 dpf we observed that an increased fraction of crispant animals swam in circle in response to a tactile stimulus compared to wild-type and mock-treated fish (**Figure 3A**). Similarly, 5 dpf mutant larval batches showed a reduction in both global velocity and net speed (**Figure S3**).

The g*usp48* targeting exon 4 appeared as the most efficient guide with notable effects on global velocity (g*usp48*- 4+Cas (treated) 1.0 versus g*usp48*-4 (mock-treated controls) 1.4 mm/s; p = 0.04), net speed (5.4 versus 6.1 mm/s; p = 0.01) and tactile response assays (78 % versus 12 % miss-responding) (**Figure 3A, Figure S3**).

We assessed the presence of microdeletion and showed that g*usp48*-4 induced genetic editing in 75 % of injected embryos (founders, F0). As the swimming in circle behavior was suggested to be an indicator of vestibular dysfunction [79], we then tested the auditory startled responses of *usp48* mutant larvae at 5 dpf. Consistent with hearing impairment they presented with a significantly decreased response to white noise (p = 0.05; **Figure 3B**). Upon stratifying by frequency, we found that *usp48* knocked-down fish larvae presented with a significantly decreased reaction when compared to wild-type and mock treated fish towards 600 Hz (p = 0.03) and 800 Hz (p = 0.0017) pulses but not to the shorter 400 Hz (p = 0.18) and longer 1000 Hz (p = 0.16) frequencies (**Figure 3B**). This impaired response to acoustic cues was not complemented by changes in the response to light as we observed no differences in the visual motor response of *usp48* knocked-down, wild-type and mock treated fish larvae during light-dark transitions (**Figure S4**). To possibly uncover the origin of this hearing impairment, we first analyzed the development of sensory hair cells of *usp48* knocked-down zebrafish. We investigated both AB-line zebrafish dyed with YO-PRO-1 that selectively labels neuromast hair cells and Brn3c:mGFP/NBT:dsRED zebrafish whose hair cells of the inner ear and lateral line neuromasts are labeled green while neurons are stained in red. The superficial sensory hair cells of *usp48* knocked-down fish showed a normal mechano-transduction function and the neuromasts presented a regular superficial distribution along the anterior (head) and posterior (trunk and tail) lateral-line systems (**Figure S5**).

We then assessed the development of the neuronal system and discovered that the vestibulo-acoustic neurons innervating the ear bases were less developed in 5 dpf *usp48* knocked-down than in mock-treated and wild-type fish. These fish presented with less

organized and significantly less statoacoustic neurons when compared with mock-treated fish (36.0 ± 6.4 versus 52.3 ± 8 neurons, p = 0.01) and wild-type fish (51.5 ± 2.1, p = 0.02) (**Figure 3C-D**). In addition, *usp48* crispants showed a significant delay in the development of primary motoneurons at 28 hpf that got exacerbated at 48 hpf (**Figure S6**).

During early development the size of 1 dpf *usp48* knocked-down embryos was smaller when compared to that of mock-treated and wild-type animals (p = 0.02) (**Figure S7**). The subsequent development of the swim-bladder, a double-chambered organ located in the coelom used to maintain buoyancy that may also function as an acoustic resonator appeared slower in treated fish (data not shown) suggesting a general delay in the development of *usp48* knock-downs.

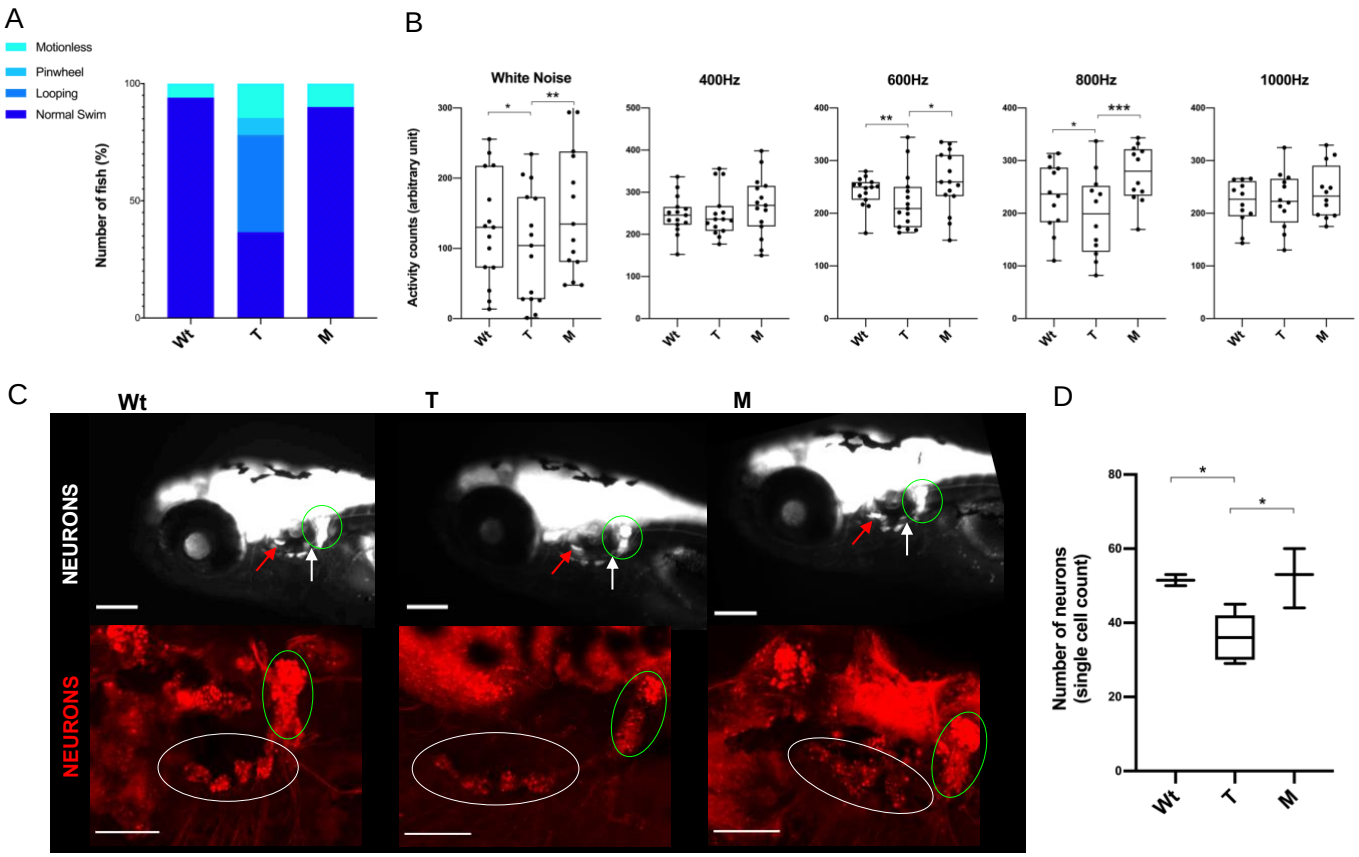

Figure 3. *usp48 knocked-down zebrafish model.*

(A) Touch Test Response of 3 dpf wild-type (Wt; n=71), *usp48* knocked-down (g*usp48*-4+Cas9; treated:T; n=41) and control zebrafish (g*usp48*-4*;* mock:M; n=32). **(B)** Acoustic Startle Response of 5 dpf wild-type (Wt; n>40), *usp48* knocked-down (g*usp48*-4+Cas9; treated:T; n>40) and controls zebrafish (g*usp48*-4*;* mock:M; n>40) towards white noise (broad-band noise), 400 Hz, 600 Hz, 800 Hz and 1000 Hz lengths. **(C)** Maximum projections of confocal images regarding specific neuronal structures in 5 dpf Wt, T and M fish: the statoacoustic neurons (red arrows), Xth ganglia (white arrows) and the posterior lateral line ganglia (PLLG, green ellipses) are indicated in the top panels; the statoacoustic neurons and PPLG are pinpointed with white and green ellipses, respectively in the bottom panels. **(D)** Number of statoacoustic neurons in 5 dfp Wt (n=2), T (n=5) and M (n=3) fish. P-value legend: * ≤ 0.02.

Discussion

We describe four families with ADNSHHL. The affected individuals of the first three families presented with bilateral hearing loss and carried predicted-to-be deleterious missense variants in the ubiquitin carboxyl-terminal hydrolase *USP48*, while the affected individual of the fourth family exhibited unilateral cochlear aplasia-associated hearing loss and a *de novo* splicing variant in the same gene. Whereas all assessed variants were unable to hydrolyze tetraubiquitin favoring a haploinsufficiency model, further cases are warranted to demonstrate if a single of multiple pathological processes are involved. Members of the ubiquitin-specific proteases family have been previously associated with hearing loss. The catalytically inactive tight junction-associated *Usp35* was shown to be essential for the survival of auditory hair cells and normal hearing in mice[80], while variants in the dog *USP31* were associated with adult-onset deafness in border collies[81]. Histological findings further support the involvement of ubiquitin in hearing as ubiquitin-positive granules were identified in the neuropil of cochlear nuclei of aging dogs[82]. Intriguingly, both USP31 and USP48 regulate the nuclear factor-κB[83], whose deficiency was associated with auditory nerve degeneration and increased noise-induced hearing loss[84]. We correspondingly observed expression of USP48 in the human spiral ganglion and Scarpa's neurons, as well as a general developmental delay of the neuronal system of *usp48* knocked-down zebrafish. These crispants presented with significantly less statoacoustic neurons and a decreased acoustic startle response suggesting that the *USP48*-encoded ubiquitin carboxyl-terminal hydrolase is important to auditory function. USP48 also controls the E3 ubiquitin-protein ligase Mdm2[85] (MIM: 164785), which ubiquitinates and antagonizes p53 (MIM: 191170). USP48 role in controlling DNA repair is further highlighted by its function as a histone H2A deubiquitinase that counteracts BRCA1 E3 ubiquitin-ligase activity[86] (breast cancer 1; MIM: 113705) and by the reduced chromosomal instability of Fanconi anemia cells upon knock-down of USP48[87,88]. USP48 was also shown to regulate the stability of TRAF2 (tumor necrosis factor receptor-associated factor 2; MIM: 601895) thus controlling E-cadherin-mediated adherent junctions. Such junctions are important for cochlear development and growth of auditory neurons[89]. The expression level of E-cadherin is determinant for hair cell differentiation; its level inversely correlates to the capacity of supporting cells to differentiate into sensory hair cells[90]. Data suggest that in the absence of sound, developing cochlear and primary auditory neurons undergo experience-independent activity. Two hypotheses were suggested for this activity: the inner supporting cells of the Kolliker's organ, an organ only present during the critical period of auditory development, release ATP hence

recapitulating auditory neuron activity or alternatively inner hair cells (IHCs) generate this spontaneous activity without ATP activation[7,91]. Nevertheless, it was proposed that “developmental abnormalities of the Kölliker’s organ may lead to congenital hearing loss as mutations in ion channels important for its activity (e.g. *GJB2, GJB6*) are associated with deafness”[7]. Whereas E-cadherin is present in outer hair cells, it is not expressed in IHCs or in the part of the Kolliker's organ in contact with them. We similarly observe expression of USP48 in the Kolliker’s organ, but not in the developing IHCs.

In conclusion we have identified a new ADNSHHL candidate gene. Our results support adding *USP48* to the list of genes associated with hearing function and to future HHL diagnostic panels. They also emphasize the importance of the temporary Kolliker’s organ in auditory development.

Acknowledgments

We thank the affected individuals and their families for their participation in this study. We are grateful to Jacques S. Beckmann for comments. We are indebted to the zebrafish facility and the cell imaging facility of the University of Lausanne and the Montpellier ZebraSens behavioral phenotyping platform (MMDN) in particular to N. Cubedo and J. Sarniguet for help. The Dutch DOOFNL Consortium consisting of M.F. van Dooren, S.G. Kant, H.H.W. de Gier, E.H. Hoefsloot, M.P. van der Schroeff , L.J.C. Rotteveel, F.G. Ropers, J.C.C. Widdershoven, J.R. Hof, E.K. Vanhoutte, I. Feenstra, H. Kremer, C.P. Lanting, R.J.E. Pennings, H.G. Yntema, R.H. Free and J.S. Klein Wassink-Ruiter, R.J. Stokroos, A.L. Smit, M.J. van den Boogaard, F.A. Ebbens, S.M. Maas, A. Plomp, T.P.M. Goderie, P. Merkus and J. van de Kamp, contributed to the clinical evaluation and medical genetic testing of a cohort of ~800 genetically unsolved index cases with hearing loss, evaluated for *USP48* variants. SB is recipient of scholarships from the European Social Fund, University of Trieste, Italy and the Fund for Research and Education in Genetics, University of Lausanne, Switzerland. This work was supported by grants from the Swiss National Science Foundation (31003A_182632 to AR and 320030_170062 to FA) and Horizon2020 Twinning project ePerMed (692145) to AR and from the Heinsius-Houbolt foundation to HK. The funders had no role in study design, data collection and analysis, decision to publish, or preparation of the manuscript.

Web Resources

ChopChop design tool: http://chopchop.cbu.uib.no

GnomAD: https://gnomad.broadinstitute.org/

MaxEntScan: http://hollywood.mit.edu/burgelab/maxent/Xmaxentscan_scoreseq.html

NNSplice: https://www.fruitfly.org/seq_tools/splice.html

OMIM (Online Mendelian Inheritance in Man): http://www.omim.org

WHO Deafness and hearing loss: https://www.who.int/health-topics/hearing-loss#tab=tab_1

Conflict of interest

We declare no conflict of interest

References

1. Kremer H. Hereditary hearing loss; about the known and the unknown. *Hear Res*. 2019;376:58-68. doi:10.1016/j.heares.2019.01.003
2. Azaiez H, Booth KT, Ephraim SS, et al. Genomic Landscape and Mutational Signatures of Deafness-Associated Genes. *Am J Hum Genet*. 2018;103(4):484-497. doi:10.1016/j.ajhg.2018.08.006
3. Morgan A, Koboldt DC, Barrie ES, et al. Mutations in PLS1, encoding fimbrin, cause autosomal dominant nonsyndromic hearing loss. *Hum Mutat*. 2019;40(12):2286-2295. doi:10.1002/humu.23891
4. Vozzi D, Morgan A, Vuckovic D, et al. Hereditary hearing loss : a 96 gene targeted sequencing protocol reveals novel alleles in a series of Italian and Qatari patients. *Gene*. 2014;542(2):209-216. doi:10.1016/j.gene.2014.03.033
5. Gueneau L, Fish RJ, Shamseldin HE, et al. KIAA1109 Variants Are Associated with a Severe Disorder of Brain Development and Arthrogryposis. *Am J Hum Genet*. 2018;102(1):116-132. doi:10.1016/j.ajhg.2017.12.002
6. Smits JJ, Oostrik J, Beynon AJ, et al. De novo and inherited loss-of-function variants of ATP2B2 are associated with rapidly progressive hearing impairment. *Hum Genet*. 2019;138(1):61-72. doi:10.1007/s00439-018-1965-1
7. Tzimas C, Michailidou G, Arsenakis M, Kieff E, Mosialos G, Hatzivassiliou EG. Human ubiquitin specific protease 31 is a deubiquitinating enzyme implicated in activation of nuclear factor-κB. *Cell Signal*. 2006;18(1):83-92. doi:10.1016/j.cellsig.2005.03.017
8. Guex N, Peitsch MC. SWISS-MODEL and the Swiss-PdbViewer: An environment for comparative protein modeling. *Electrophoresis*. 1997;18(15):2714-2723. doi:10.1002/elps.1150181505
9. Rougé L, Bainbridge TW, Kwok M, et al. Molecular Understanding of USP7 Substrate Recognition and C-Terminal Activation. *Structure*. 2016;24(8):1335-1345. doi:10.1016/j.str.2016.05.020
10. Cheng J, Yang H, Fang J, et al. Molecular mechanism for USP7-mediated DNMT1 stabilization by acetylation. *Nat Commun*. 2015;6(May):1-11. doi:10.1038/ncomms8023
11. Paudel P, Zhang Q, Leung C, et al. Crystal structure and activity-based labeling reveal the mechanisms for linkage-specific substrate recognition by deubiquitinase USP9X. *Proc Natl Acad Sci U S A*. 2019;116(15):7288-7297. doi:10.1073/pnas.1815027116
12. Locher H, Frijns JHM, van Iperen L, de Groot JCMJ, Huisman MA, Chuva de Sousa Lopes SM. Neurosensory development and cell fate determination in the human cochlea. *Neural Dev*. 2013;8(1). doi:10.1186/1749-8104-8-20
13. Labun K, Montague TG, Gagnon JA, Thyme SB, Valen E. CHOPCHOP v2: a web tool for the next generation of CRISPR genome engineering. *Nucleic Acids Res*. 2016;44(W1):W272-W276. doi:10.1093/nar/gkw398
14. Arribat Y, Mysiak KS, Lescouzères L, et al. Sonic Hedgehog repression underlies gigaxonin mutation-induced motor deficits in giant axonal neuropathy. *J Clin Invest*.

2019;129(12):5312-5326. doi:10.1172/JCI129788
15. Liu X, Lin J, Zhang Y, Guo N, Li Q. Sound shock response in larval zebrafish: A convenient and high-throughput assessment of auditory function. *Neurotoxicol Teratol*. 2018;66(August 2017):1-7. doi:10.1016/j.ntt.2018.01.003
16. Di Donato V, Auer TO, Duroure K, Del Bene F. Characterization of the Calcium Binding Protein Family in Zebrafish. *PLoS One*. 2013;8(1):1-13. doi:10.1371/journal.pone.0053299
17. Peri F, Nüsslein-Volhard C. Live Imaging of Neuronal Degradation by Microglia Reveals a Role for v0-ATPase a1 in Phagosomal Fusion In Vivo. *Cell*. 2008;133(5):916-927. doi:10.1016/j.cell.2008.04.037
18. Joanna Kaplanis1*, Kaitlin E. Samocha1*, Laurens Wiel2, 3*, Zhancheng Zhang4* KJA, 5 Ruth Y. Eberhardt1, Giuseppe Gallone1, Stefan H. Lelieveld2, Hilary C. Martin1 JF, 6 McRae1, Patrick J. Short1, Rebecca I. Torene4, Elke de Boer5, Petr Danecek1 EJ, et al. Integrating healthcare and research genetic data empowers the discovery of 28 novel developmental disorders. *bioRxiv*. 2020:1-20.
19. Fedele M, Maria G, Fusco A. The Genetics of Pituitary Adenomas. *Contemp Asp Endocrinol*. 2011;(Table 3):1-19. doi:10.5772/16639
20. Chen J, Jian X, Deng S, et al. Identification of recurrent USP48 and BRAF mutations in Cushing's disease. *Nat Commun*. 2018;9(1):1-9. doi:10.1038/s41467-018-05275-5
21. Zimmermann L, Stephens A, Nam SZ, et al. A Completely Reimplemented MPI Bioinformatics Toolkit with a New HHpred Server at its Core. *J Mol Biol*. 2018;430(15):2237-2243. doi:10.1016/j.jmb.2017.12.007
22. Blom N, Sicheritz-Pontén T, Gupta R, Gammeltoft S, Brunak S. Prediction of post-translational glycosylation and phosphorylation of proteins from the amino acid sequence. *Proteomics*. 2004;4(6):1633-1649. doi:10.1002/pmic.200300771
23. Ryals M, Pak K, Jalota R, Kurabi A, Ryan AF. A kinase inhibitor library screen identifies novel enzymes involved in ototoxic damage to the murine organ of Corti. *PLoS One*. 2017;12(10):1-21. doi:10.1371/journal.pone.0186001
24. Dayaratne MWN, Vlajkovic SM, Lipski J, Thorne PR. Kölliker's organ and the development of spontaneous activity in the auditory system: Implications for hearing dysfunction. *Biomed Res Int*. 2014;2014. doi:10.1155/2014/367939
25. Vona B, Doll J, Hofrichter MAH, Haaf T, Varshney GK. Small fish, big prospects: using zebrafish to unravel the mechanisms of hereditary hearing loss. *Hear Res*. 2020;(xxxx):107906. doi:10.1016/j.heares.2020.107906
26. Kindt KS, Sheets L. Transmission disrupted: Modeling auditory synaptopathy in zebrafish. *Front Cell Dev Biol*. 2018;6(SEP):1-17. doi:10.3389/fcell.2018.00114
27. Kazmierczak M, Harris SL, Kazmierczak P, et al. Progressive hearing loss in mice carrying a mutation in Usp53. *J Neurosci*. 2015;35(47):15582-15598. doi:10.1523/JNEUROSCI.1965-15.2015
28. Yokoyama JS, Lam ET, Ruhe AL, et al. Variation in Genes Related to Cochlear Biology Is Strongly Associated with Adult-Onset Deafness in Border Collies. *PLoS Genet*. 2012;8(9). doi:10.1371/journal.pgen.1002898
29. Shimada A, Ebisu M, Morita T, Takeuchi T, Umemura T. Age-Related Changes in the Cochlea and Cochlear Nuclei of Dogs. *J Vet Med Sci*. 1998;60(1):41-48.

doi:10.1292/jvms.60.41
30. Ghanem A, Schweitzer K, Naumann M. Catalytic domain of deubiquitinylase USP48 directs interaction with Rel homology domain of nuclear factor kappaB transcription factor RelA. *Mol Biol Rep*. 2019;46(1):1369-1375. doi:10.1007/s11033-019-04587-z
31. Lang H, Schulte BA, Zhou D, Smythe N, Spicer SS, Schmiedt RA. Nuclear factor κB deficiency is associated with auditory nerve degeneration and increased noise-induced hearing loss. *J Neurosci*. 2006;26(13):3541-3550. doi:10.1523/JNEUROSCI.2488-05.2006
32. Cetkovská K, Šustová H, Uldrijan S. Ubiquitin-specific peptidase 48 regulates Mdm2 protein levels independent of its deubiquitinase activity. *Sci Rep*. 2017;7(October 2016):1-9. doi:10.1038/srep43180
33. Uckelmann M, Densham RM, Baas R, et al. USP48 restrains resection by site-specific cleavage of the BRCA1 ubiquitin mark from H2A. *Nat Commun*. 2018;9(1). doi:10.1038/s41467-017-02653-3
34. Implications P. USP48 May Be Potential Therapeutic Target in Fanconi Anemia: Inactivation of USP48 reduced chromosomal instability of Fanconi anemia defective cells and highlights a role for this enzyme in controlling DNA repair. *Am J Med Genet A*. 2018;176(9):1794-1795. doi:10.1002/ajmg.a.40522
35. Velimezi G, Robinson-Garcia L, Muñoz-Martínez F, et al. Map of synthetic rescue interactions for the Fanconi anemia DNA repair pathway identifies USP48. *Nat Commun*. 2018;9(1). doi:10.1038/s41467-018-04649-z
36. Wang B, Hu B, Yang S. Cell junction proteins within the cochlea: A review of recent research. *J Otol*. 2015;10(4):131-135. doi:10.1016/j.joto.2016.01.003
37. Collado MS, Thiede BR, Baker W, Askew C, Igbani LM, Corwin JT. The postnatal accumulation of junctional e-cadherin is inversely correlated with the capacity for supporting cells to convert directly into sensory hair cells in mammalian balance organs. *J Neurosci*. 2011;31(33):11855-11866. doi:10.1523/JNEUROSCI.2525-11.2011
38. Wang HC, Bergles DE. Spontaneous activity in the developing auditory system. *Cell Tissue Res*. 2015;361(1):65-75. doi:10.1007/s00441-014-2007-5

Supplemental Figures:

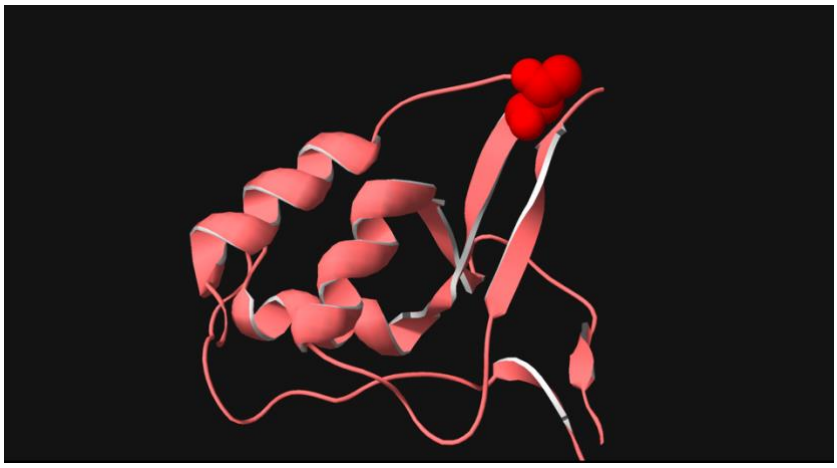

Figure S1. *USP48 3-D modeling.*
USP48 tridimensional protein modeling of the DUSP domain (salmon ribbon) highlighting the solvent exposed position of Thr739 (red space-filled) that is mutated in Dutch proband 1.

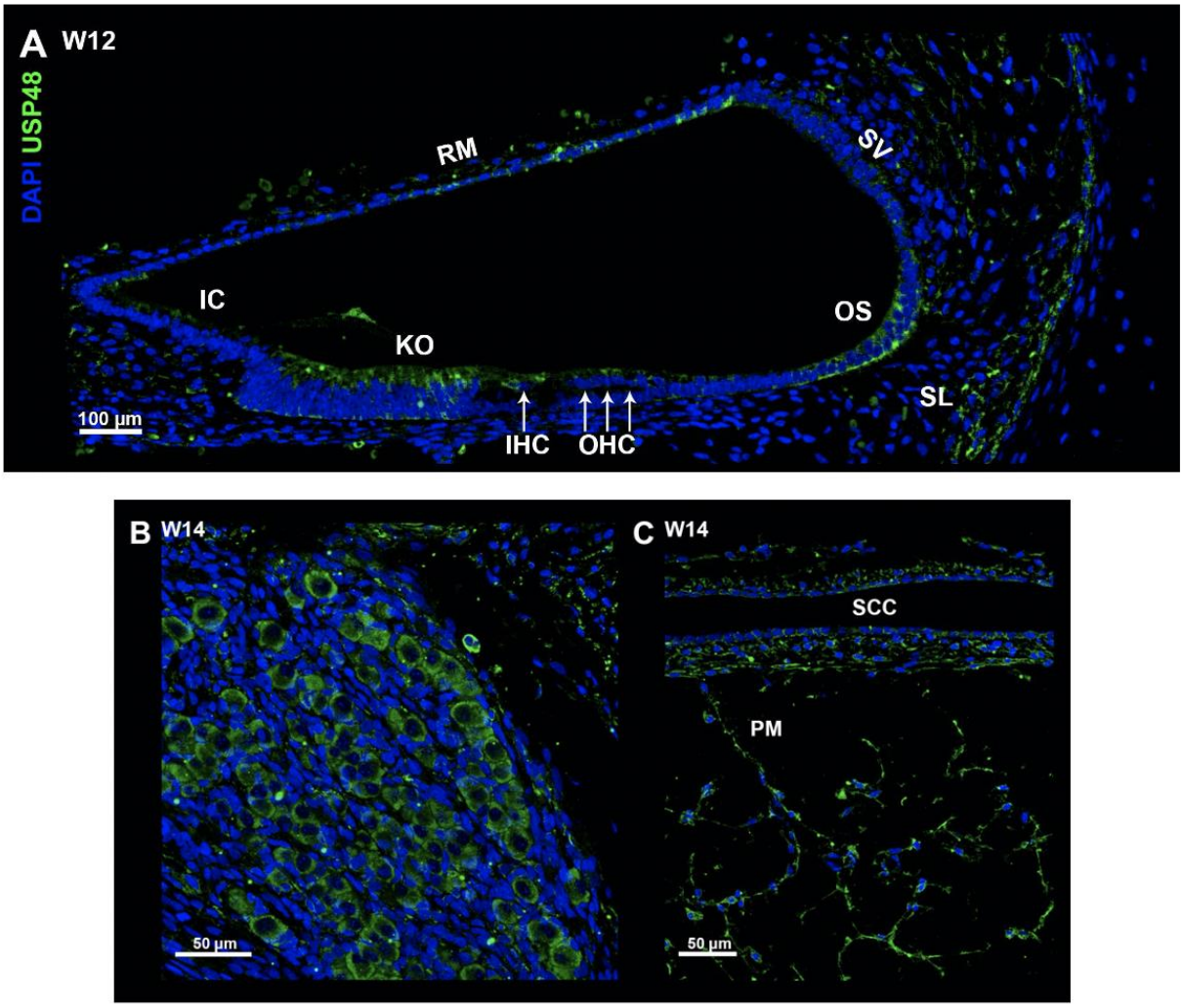

Figure S2. *USP48 expression in the human fetal inner ear.*

Human embryonic ear immunostaining showing DNA (DAPI) in blue and the USP48 protein in green. USP48 is expressed in several structures: **(A)** at W12, in Kolliker's Organ (KO), the Outer Sulcus (OS), the Spiral Ligament (SL) and in Reissner's Membrane (RM), but not in Inner (IHC) or Outer Hair Cells (OHC), interdental cells (IC) or intermediate cells of the stria vascularis (SV); **(B)** at W14, in neurons of Scarpa's Ganglion; **(C)** at W14, in the epithelial cells of the semicircular canals (SCC) and the periotic mesenchyme (PM) of the vestibular system.

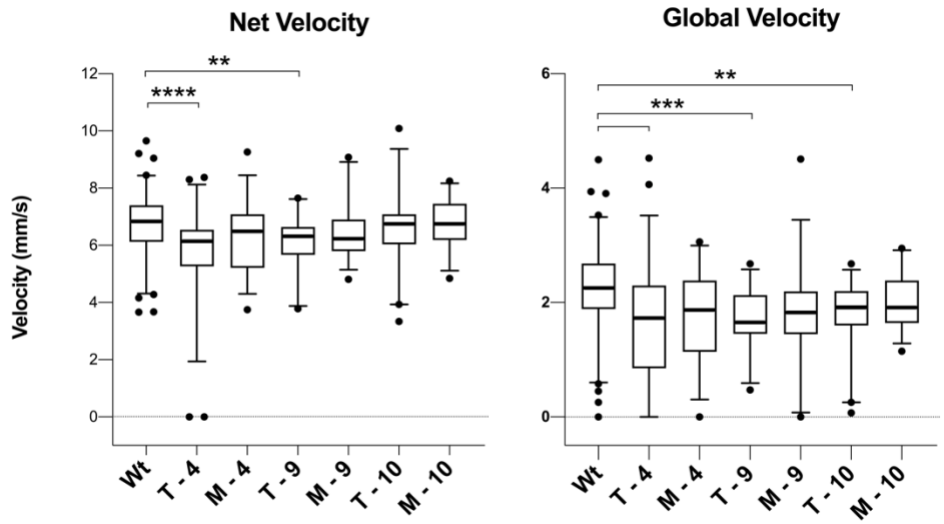

Figure S3. *usp48* knocked-down zebrafish model velocity.

Global and net velocity of 5 dpf wild-type (Wt; n=82), *usp48* knocked-downs (treated:T) and controls zebrafish (mock-treated:M). Three different guides RNA targeting exon 4, 9 and 10 with (T-4 n=52, T-9 n=33 and T-10 n=39, respectively) or without Cas9 (M-4 n=34, M-9 n=33 and M-10 n=28, respectively) were used. P-value legend net velocity (** = 0.005; **** < 0.0001); global velocity (*** < 0.0006; ** = 0.002).

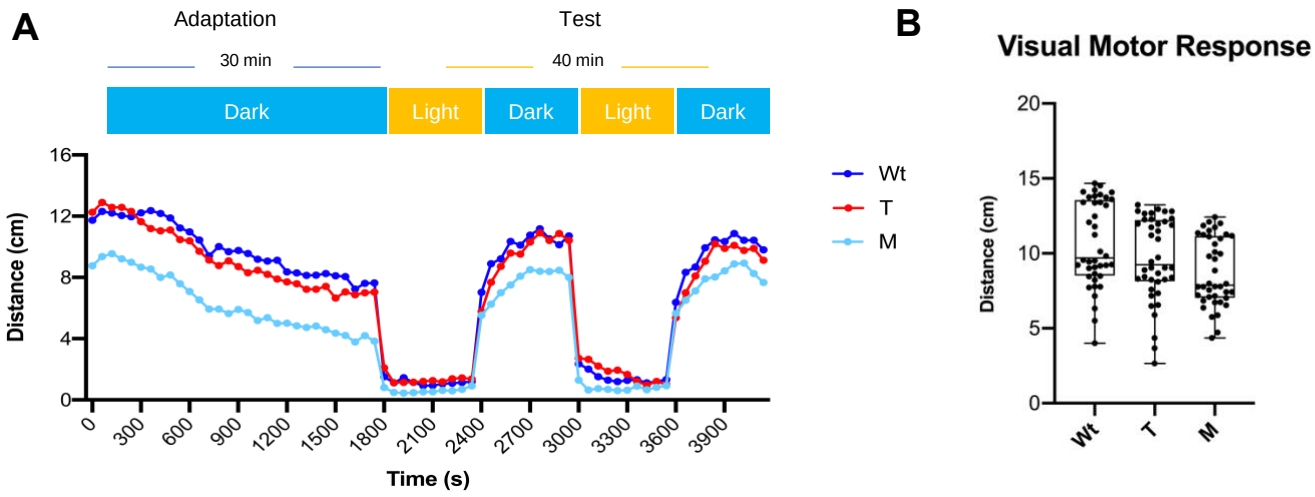

Figure S4. *usp48* knocked-down zebrafish model visual motor response (VMR).

The visual ability of 5 dpf wild-type (Wt; n=40), *usp48* knocked-down (g*usp48*-4+Cas9; treated:T; n=40) and controls Zebrafish (g*usp48*-4*;* mock:M; n=40) was assessed by measuring the distance travelled during light-dark transitions. **(A)** The light-dark protocol consisted of 30 minutes of adaptation followed by two alternating periods of light and dark every 10 min (600 seconds) as depicted on top. The graph shows the mean distance travelled by fish of the three groups. **(B)** Boxplots of fish reactivity during the two VMR tests considering the mean activity during the dark periods normalized with the mean activity during the light periods.

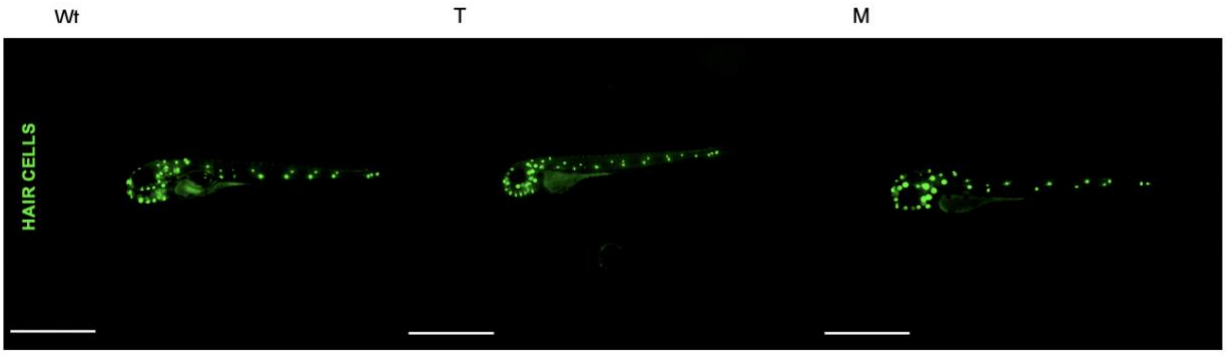

Figure S5. *Neuromasts of usp48 knocked-down zebrafish model.*

Distribution of neuromasts in wild-type (Wt; n>10), *usp48* knocked-down (g*usp48*-4+Cas9; treated:T; n>10) and controls Zebrafish (g*usp48*-4*;* mock:M; n>10) along the anterior (head) and posterior (trunk and tail) lateral-line systems. The YO-PRO-1 drug allowed assessing the receptive activity of hairs of the sensory hair cells.

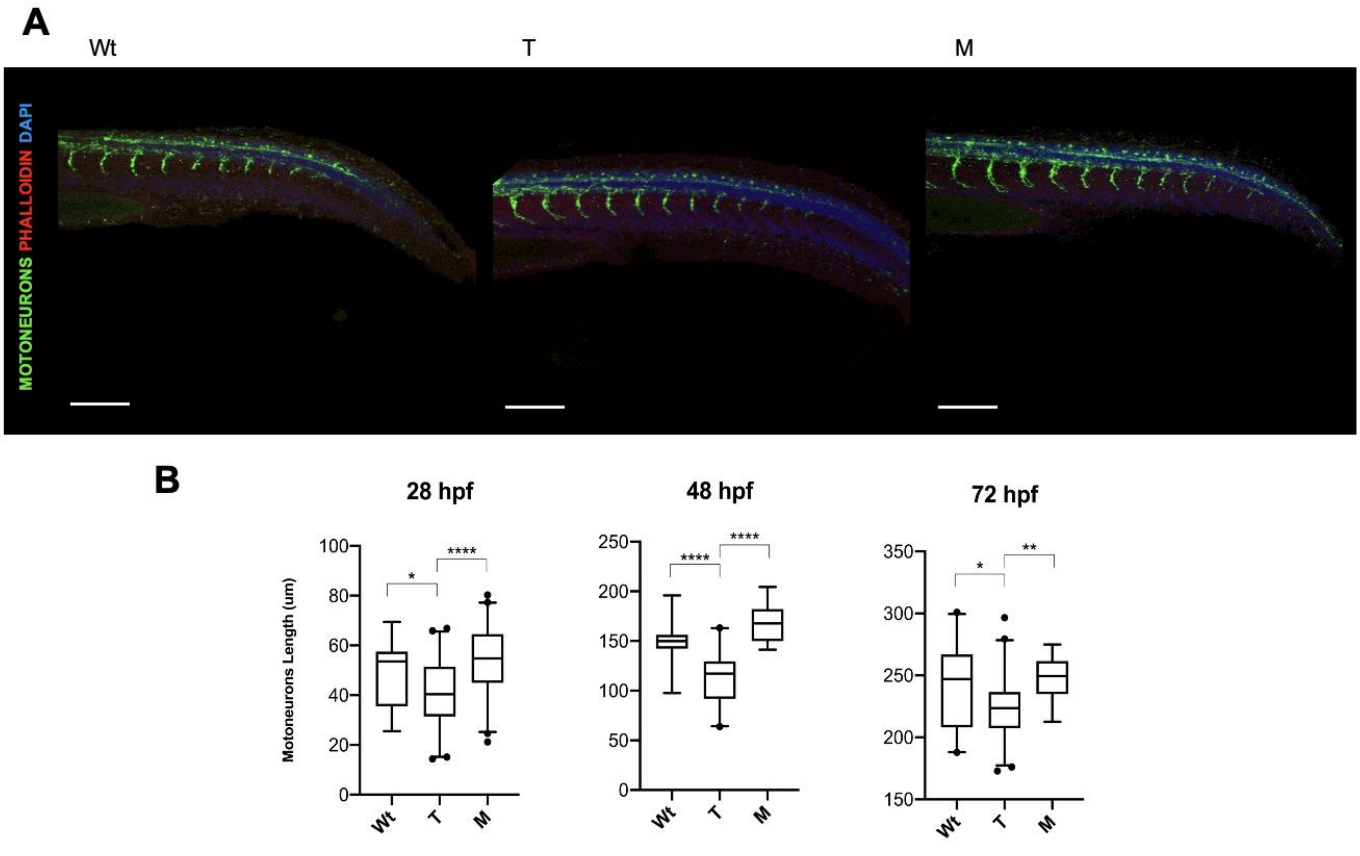

Figure S6. *Development of primary motoneurons of usp48 knocked-down zebrafish model.*
(A) Primary motoneurons (green), DNA (DAPI-stained, blue) and F-actin (red) of 28 hpf wild-type (Wt), *usp48* knocked-down (treated:T) and controls zebrafish (mock:M). **(B)** Boxplots of primary motoneurons length of 28, 48 and 72hpf of wild-type (Wt; 28hpf n=4; 48hpf n=4; 72hpf n=4), *usp48* knocked-down (g*usp48*-4+Cas9; treated:T; 28hpf n=9; 48hpf n=4; 72hpf n=9) and controls zebrafish (g*usp48*-4*;* mock:M; 28hpf n=8; 48hpf n=2; 72hpf n=3). P-value legend: * = 0.01; ** = 0.002; **** < 0.0001.

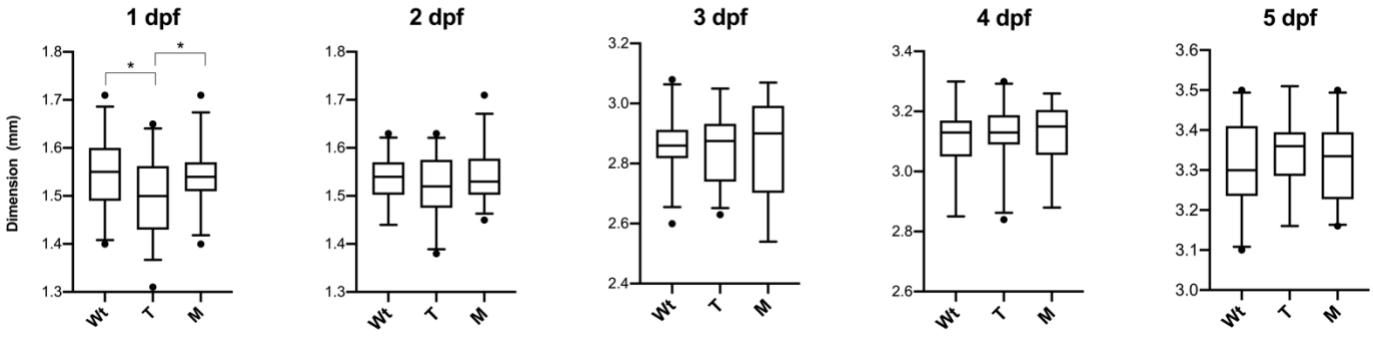

Figure S7. *Morphology of usp48 knocked-down zebrafish model.*
Fish size during the first five days after fertilization of wild-type (Wt; 1dpf n=27 ; 2dpf n=36; 3dpf n=30; 4dpf n=19; 5dpf n=21), *usp48* knocked-down (g*usp48*-4+Cas9; treated:T; 1dpf n=38 ; 2dpf n=37; 3dpf n=30; 4dpf n=22; 5dpf n=17) and controls zebrafish (g*usp48*-4*;* mock:M; 1dpf n=37; 2dpf n=33; 3dpf n=18; 4dpf n=17; 5dpf n=23). P-value legend: * < 0.02.

3.2 Chapter 2

In this second chapter I present the analysis of a large cohort of Italian patients affected by ARHL in which we identified new variants and genes that could contribute to the development of this form of deafness.

A summary of the contributions to this project and the awards received will anticipate the results that are presented with the article, published in Gene journal in June 2020, with the title: “New age-related hearing loss candidate genes in humans: an ongoing challenge” (doi: doi.org/10.1016/j.gene.2020.144561).

The article presents a short abstract followed by the introduction. The results are showed in the central section, represented with few main figures, that precede the material and methods description. The article will end with the final discussion.

Supplemental figures available on-line.

3.2.1 Summary of the contribution

My contribution to this work concerned in part the evaluation of gene expressions analyzed by qRT-PCR in several mouse tissues, and in particular the *in-vitro* expression studies and protein translation analysis. I have contributed as well to the manuscript writing together with Mariateresa Di Stazio and Morgan Anna under the supervision of Giorgia Girotto and Paolo Gasparini. Zebrafish models have been engineered in collaboration with ZeClinics company.

In 2019 I have been awarded with a fellowship by A.I.R.H. (Italian Association for Handicap Care and Prevention Research) with the charity Foundation Kathleen Foreman Casali in recognition of Best Projects to cure disabling disease.

The results are presented in three main figures (named **Fig. 1-3**), one table included in the text and one supplementary table (named **Table 1**). The supplement figures (**Fig. S1-2**) and tables (**Table S1-2**) are available on-line.

3.2.2 Article

Gene 742 (2020) 144561

Contents lists available at ScienceDirect

Gene

journal homepage: www.elsevier.com/locate/gene

Research paper

New age-related hearing loss candidate genes in humans: an ongoing challenge

M. Di Stazio[a,*,1], A. Morgan[a,b,1], M. Brumat[b], S. Bassani[b], D. Dell'Orco[c], V. Marino[c], P. Garagnani[d,e,f], C. Giuliani[g,h], P. Gasparini[a,b], G. Girotto[a,b]

[a] Institute for Maternal and Child Health – IRCCS, Burlo Garofolo, Trieste, Italy
[b] Department of Medicine, Surgery and Health Sciences, University of Trieste, Trieste, Italy
[c] Department of Neurosciences, Biomedicine and Movement Sciences, Section of Biological Chemistry, University of Verona, Verona, Italy
[d] Department of Experimental, Diagnostic and Specialty Medicine (DIMES), University of Bologna, Italy
[e] Interdepartimental Centre L. Galvani (CIG), University of Bologna, Italy
[f] Clinical Chemistry, Department of Laboratory Medicine, Karolinska Institutet at Huddinge University Hospital, Stockholm, Sweden
[g] Laboratory of Molecular Anthropology & Centre for Genome Biology, Department of Biological, Geological and Environmental Sciences (BiGeA), University of Bologna, Italy
[h] School of Anthropology and Museum Ethnography, University of Oxford, United Kingdom

ARTICLE INFO

Keywords:
Age-related hearing loss gene discovery
In vitro studies
Protein modelling
Gene expression

ABSTRACT

Age-related hearing loss (ARHL) is the most frequent sensory disorder in the elderly, affecting approximately one-third of people aged more than 65 years. Despite a large number of people affected, ARHL is still an area of unmet clinical needs, and only a few ARHL susceptibility genes have been detected so far.

In order to further investigate the genetics of ARHL, we analyzed a series of 46 ARHL candidate genes, selected according to previous Genome Wide Association Studies (GWAS) data, literature updates and animal models, in a large cohort of 464 Italian ARHL patients. We have filtered the variants according to a) pathogenicity prediction, b) allele frequency in public databases, c) allele frequency in an internal cohort of 113 healthy matched controls, and 81 healthy semi-supercentenarians. After data analysis, all the variants of interest have been tested by functional "*in silico*" or "*in vitro*" experiments (i.e., molecular dynamics simulations and protein translation analysis) to assess their pathogenic role, and the expression of the mutated genes have been checked in mouse or zebrafish inner ear.

This multi-step approach led to the characterization of a series of ultra-rare likely pathogenic variants in *DCLK1*, *SLC28A3*, *CEP104*, and *PCDH20* genes, contributing to describe the first association of these genes with ARHL in humans.

These results provide essential insights on the understanding of the molecular bases of such a complex, heterogeneous and frequent disorder, unveiling new possible targets for the future development of innovative therapeutic and preventive approaches that could improve the quality of life of the millions of people affected worldwide.

1. Introduction

Hearing is an extremely complex trait whose performance results from the interaction of a large number of players (e.g., the many cells types characterizing the human inner ear, the numerous genes and environmental factors impacting on hearing function and loss, etc.) that altogether explain the hearing threshold variability among individuals. People's hearing is known to worsen with age, causing a condition called Age-Related Hearing Loss (ARHL). ARHL is the most frequent sensory disorder in the elderly, affecting approximately ~11,2% of people in the 50–59 age group, 24,7% of those in the 60–69 age group and about 63% in subjects over 70 years, and it is inevitably associated to communication difficulties, to anxiety, social isolation, late-onset depression, reduced physical, cognitive function, and dementia (Tu and Friedman, 2018; Salvi et al., 2018; Bainbridge and Wallhagen, 2014). Despite a large number of people affected, ARHL is still an area of

Abbreviations: ARHL, Age-related hearing loss; GWAS, Genome Wide Association Studies; SNVs, Single nucleotide variants

* Corresponding author.
E-mail address: mariateresa.distazio@burlo.trieste.it (M. Di Stazio).

[1] These authors equally contributed to the work.

https://doi.org/10.1016/j.gene.2020.144561
Received 20 December 2019; Accepted 8 March 2020
Available online 12 March 2020
0378-1119/

unmet clinical needs since, hearing aids, the most common treatment for these patients, are considered to have limited effectiveness.

ARHL is a multifactorial disorder that results from the cumulative effect of aging, genetics, and long-term exposure to environmental agents on the auditory system. While the involvement of several environmental factors (i.e. noise, smoking, alcohol, stress, metabolic and systemic diseases such as diabetes, hypertension, etc.) has been partially elucidated, the identification of the genetic risk factors is still at its very early stage and only a few genes have been clearly associated to the disease (Keithley, 2019; Van Laer et al., 2010). The discovery and validation of the genetic risk factors of ARHL are hampered by the fact that it is not yet clear whether rare Mendelian gene variants cause it with large-scale effects or multiple variants, each contributing to the disease. Moreover, in the hypothesis of a burden of multiple variants, some of them would have a predisposing effect, while others would have a protective one. In this light, large-scale studies that compare the genetic background of ARHL cases with controls are fundamental to elucidate the genetics underlying this disorder.

In the present study, we analyzed at the genomic level a series of 46 ARHL candidate genes, carefully selected according to previous results of (a) Genome Wide Association Studies (GWAS) data (b) literature updates and (c) animal models, in a large cohort of 464 Italian ARHL patients (Morgan et al., 2018).

We validated the most interesting variants by excluding their presence in an internal database of 113 healthy matched controls and in a collection of data of 81 semi-supercentenarians (i.e., people aged ≥104 years old), but also using expression studies in the animal inner ear and functional "*in vitro*" experiments. The final results provide essential insights in the understanding of the molecular bases of such a complex, heterogeneous and frequent disorder, unveiling new possible targets for the future development of innovative therapeutic approaches that could ultimately improve the quality of life of millions of people affected.

2. Results

We recruited a total of 464 ARHL unrelated Italian patients coming from several inbred and outbred communities (i.e., Sardinia (N = 150), Friuli Venezia Giulia-FVG (N = 142), Carlantino (N = 79) and Milan (N = 93) cohorts), showing bilateral mild to severe high-frequencies hearing loss with no other pathological signs or symptoms, and screened with a Targeted Re-Sequencing (TRS) panel of 46 ARHL candidate genes. A mean of 33.5 megabases (Mb) of raw sequence data was available for each subject. The coverage, on 95% of the targeted region, was at least 20-folds, with a 270-fold mean-depth total coverage. On average 333 single nucleotide variants (SNVs) and small insertions/deletions (INDELs) were called for each patient. After applying the filtering pipeline described in the "Materials and Methods" section, a series of interesting variants were detected in 7 out of 464 patients in the following genes: *DCLK1*, *SLC28A3, CEP104*, *PCDH20*, *SLC44A2*, *STRN* and *SIK3* previously associated with a normal hearing function (Girotto et al., 2014; Vuckovic et al., 2015; Satish Tammana et al., 2013; Nair et al., 2016; Moqrich et al., 1998; Wolber et al., 2014).

The phenotypes of all the patients carrying a likely pathogenic variant are described in Table S1.

As regards ***DCLK1*** (NM_004734), which encodes a protein that binds microtubules and regulates microtubule polymerization (Mohammadi et al., 2018; 'The evolving doublecortin (DCX) superfamily. - PubMed - NCBI', n.d.) (Doublecortin Like Kinase 1 protein), a novel and likely pathogenic heterozygous missense variant, c.1243G>C, p.(E415Q), was identified in a patient of the FVG cohort (Table 1). For ***SLC28A3*** (NM_022127), that encodes a nucleoside transporter which regulates multiple cellular processes, including neurotransmission, vascular tone, adenosine concentration (Errasti-Murugarren et al., 2009) (the Solute Carrier Family 28 Member 3), a nonsense ultra-rare variant, c.166C>T, p.(Q56X), was detected at the

Table 1
List of the variants identified in the ARHL patients.

Gene	Variant	Individual	Gender	Age	Hearing loss	Genotype	Polyphen2_HDIV_pred	MutationTaster_pred	PROVEAN_pred	MutationAssessor_pred	SIFT_pred	CADD_phred	gnomAD_exome_ALL	gnomAD_exome_NFE
DCLK1	c.1243G>C,p.(E415Q)	FriuliVeneziaGiuli a_1	M	74 y.o.	moderately severe	het	B	D	N	N	D	32	NA	NA
SLC28A3	c.166C>T, p.(Q56X)	Sardinia_1	F	66 y.o.	moderately severe	hom	NA	A	NA	NA	NA	30	8,14E-06	NA
CEP104	c.2308G>T, p.(D770Y)	Sardinia_19	F	58 y.o.	severe	hom	D	D	D	M	D	34	4,06E-06	8,95E-06
PCDH20	c.784G>C,p.(E262Q)	Milan_1	F	53 y.o.	moderately severe	het	D	D	N	L	D	25,4	4,06E-06	8,95E-06
SLC44A2	c.1003C>T, p.(R335W)	Sardinia_25	F	65 y.o.	moderate	hom	D	D	D	M	D	34	NA	NA
STRN	c.1631A>T, p.(N544I)	Sardinia_26	M	56 y.o.	moderate	het	D	D	D	M	D	30	4,06E-06	8,96E-06
SIK3	c.3109A>G, p.(M1037V)	FriuliVeneziaGiuli a_2	F	82 y.o.	moderate	het	D	D	N	M	T	22,8	NA	NA

Table legend: Individual: DNA samples carrying the variant; Gender: M = male, F = female; Genotype: hom = homozygous, het = heterozygous; Polyphen-2_HDIV_pred: D Probably damaging (>=0.957), P: possibly damaging (0.453<=pp2_hdiv<=0.956), B: benign (pp2_hdiv<=0.452); MutationTaster_pred "A" ("disease_causing_automatic"); "D" ("disease_causing"); "N" ("polymorphism"); "P" ("polymorphism_automatic").

homozygous state in one individual from Sardinia (Table 1).

In another patient from Sardinia, a novel and likely pathogenic missense variants in ***CEP104*** (NM_014704), c.2308G>T, p.(D770Y), was identified at the homozygous state (Table 1). This gene encodes the Centrosomal Protein 104, required for ciliogenesis and for ciliary tip structural integrity (Satish Tammana et al., 2013).

A likely pathogenic ultra-rare missense variant in ***PCDH20*** (NM_022843), c.784G>C, p.(E262Q), was detected at the heterozygous state in a patient from Milan (Table 1). The encoded protein (Protocadherin 20) is a member of the protocadherin family and, although its specific function is undetermined, the cadherin-related neuronal receptor plays a role in the establishment and function of the specific cell-cell connections in the brain (Vuckovic et al., 2015).

Furthermore, we identified an ultra-rare homozygous missense allele in ***SLC44A2*** (NM_020428), c.1003C>T,p.(R335W) in one patient from Sardinia. The gene encodes the Solute Carrier Family 44 Member 2, a transmembrane glycoprotein expressed in many supporting cell types in the cochlea, implicated in hair cell survival and antibody-induced hearing loss (Nair et al., 2016). The variant is predicted as potentially pathogenic by several *in silico* tools (Table 1).

In another patient from Sardinia, a novel and likely pathogenic missense variant was detected in ***STRN*** (NM_003162) at the heterozygous state c.1631A>T,p.(N544I) (Table 1; Moqrich et al., 1998). The gene encodes Striatin, a calmodulin-binding protein that may act as scaffolding or signalling protein playing a role in dendritic Ca^{2+} signalling (Moqrich et al., 1998).

Finally, a new ***SIK3*** (NM_025164) likely pathogenic missense heterozygous variant c.3109A>G, p.(M1037V) was identified in one patient from FVG region (Table 1). The gene encodes the Salt-Inducible Kinase 3, a protein kinase belonging to the AMPK family (Charoenfuprasert et al., 2011).

To further evaluate the role of all the identified variants, in addition to check their frequency in public databases, we also tested their presence in healthy and elderly individuals. In particular, we used an internal database of 113 healthy controls (matched for sex and age), an additional database of 81 semi-supercentenarians, and did not find any of them in these cohorts.

2.1. Expression studies

To assess the mRNA transcript profile, we have performed qRT-PCR analysis in five mouse tissues at different developmental stages, namely heart, liver, brain, cochlea, lung, kidney (P0, P6, P12 and 2-month-old mice) and testis (2 month-old mice) (Fig. 1A.1-G.1). All the seven genes analyzed showed mRNA expression in mouse cochlea in all the developmental stage examined. Moreover to quantify the genes expression in the inner ear, we compared their expression with both *Myo7a* and *Myo6*, two genes required for hair cell differentiation, associated with hereditary deafness, and abundantly expressed in inner ear hair cells (Yan et al., 2011; Coffin et al., 2007). As shown in Fig S1(A.1-G.1), *Dclk1* and *Sik3* showed higher expression levels compared to both *Myo7a* and *Myo6*, *Slc44a2* and *Strn* has higher expression compared to *Myo7a*, while *Cep104*, *Pcdh20* and *Slc28a3* displayed a lower expression compared to both genes.

We studied all genes except the *Slc28a3*, due to its orthologous absence in Zebrafish, and *Sik3*, since its expression in the mouse cochlea was already available (Wolber et al., 2014). The expression of *Dclk1* in the mouse inner ear was also already tested, displaying a precise localization in the stria vascularis, a structure not present in the zebrafish inner ear (Girotto et al., 2014). For this reason, we decided to investigate the *Dclk1* expression also in the zebrafish model. As expected, all genes, except for *Dclk1*, are also expressed in the zebrafish inner ear (Fig. 1A.2–F.2).

2.2. Functional studies

To better understand the putative causative role of the genetic variants identified, we carried out *"in vitro"* (gene expression and protein translation analysis) and "*in silico*" (Molecular Dynamics simulation for ***DCLK1*** protein) experiments. The *in silico* study was limited to ***DCLK1***, for which a robust homology model of the kinase domain could be built. The absence of reliable structural templates for the proteins encoded by the other genes prevented their *in silico* modelling. Gene and protein expression studies were performed in HEK293 cells, transiently transfected with the cDNA of Wild-Type (WT) and the mutant Myc-tagged proteins. Among the seven genes/variants described above, four of them (*DCLK1, SLC28A3, CEP104, PCDH20*) showed an altered protein product while for the remaining three genes (*SLC44A2, STRN, SIK3*), we did not notice any apparent difference (Fig. 2) (suppl.Fig. S2).

As regards to ***DCLK1*** gene variant, we found no differences in mRNA levels but the mutant protein was expressed at a higher level (>70%) than the WT, after 48 h of transient transfection (Fig. 2A, B, C) (suppl.Fig. S1H). Considering the peculiar expression of this gene in the stria vascularis of the cochlea we further investigated the role of this variant through molecular dynamics (MD) simulation studies. The crystal structure of the human DCLK1 kinase domain was resolved at 1.7 Å resolution in complex with a non-hydrolyzable ADP analog and a small inhibitor and used as a template for building a homology model covering the whole 375–648 amino acid region corresponding to the kinase domain of DCLK1 (Pieper et al., 2009) (Fig. 3A). Interestingly, in the native structure the E415 forms an intermolecular salt bridge with K469, which is also electrostatically bound to E406 (Fig. 3 C). These electrostatic interactions contribute to the correct orientation of the two domains, namely the 2-layer sandwich and the phosphorylation kinase domain, whose interface determines the cleft that harbours the ADP (or ATP) moiety necessary for the catalytic activity.

In order to assess the effects of the p.(E415Q) substitution on the DCLK1 kinase domain we performed comparative 300 ns molecular dynamics simulations of both WT and E415Q DCLK1. Comparative MD simulations of WT and p.(E415Q) clearly show that the HHL-associated mutation deletes a stabilizing salt bridge with K469, which results in significant alterations of the pattern of local polar interactions (Fig. 3C). Indeed, a highly persistent salt bridge, occurring in 90.4% of the simulation time was lost. Although H-bonds were still present between Q415 and K469, their persistence was significantly reduced (78.3% vs. 21.7% of the simulation time, respectively).

The loss of the WT E415-K469 salt bridge also led to the weakening of another coulombic interaction occurring between E406 and K469, which existed in the 60% vs. 47.6% of the simulation time. We also observed that these two residues formed stabilizing H-bonds (46.7% persistence) in the WT form; the p.(E415Q) substitution reduced their persistence to 32.2% and led to the establishment of a novel, low persistence (6%) H-bond between Q415 and E406 in the ARHL-mutant. Despite the loss of several stabilizing local polar interactions, MD simulations suggest that the structure of the ARHL-associated variant does not dramatically change compared to that of the WT. The two variants indeed display a very similar RMSF profile indicative of a comparable protein flexibility (Fig. 3B). However, the mutation induces significantly higher flexibility in the 546–552 region of the kinase domain, while the flexibility of the already highly flexible regions 422–435 and 455–461 in the 2-layer sandwich domain decreases slightly.

Regarding ***SLC28A3***, a transient transfection of WT and mutated cDNA in HEK293 cells displayed an average level of mRNA (suppl.Fig. S1H), while the mutant allele induced the complete protein degradation (Fig. 2D,E). Finally, for ***CEP104*** and ***PCDH20*** genes, immunoblot analysis revealed a marked reduction of mutated proteins compared to the WTs 48 h after the transfection (Fig. 2F-M), despite an equally stable mRNA expression (suppl.Fig. S1H). In particular, **CEP104** and **PCDH20** protein levels were less than 70% and 60% compared to WT

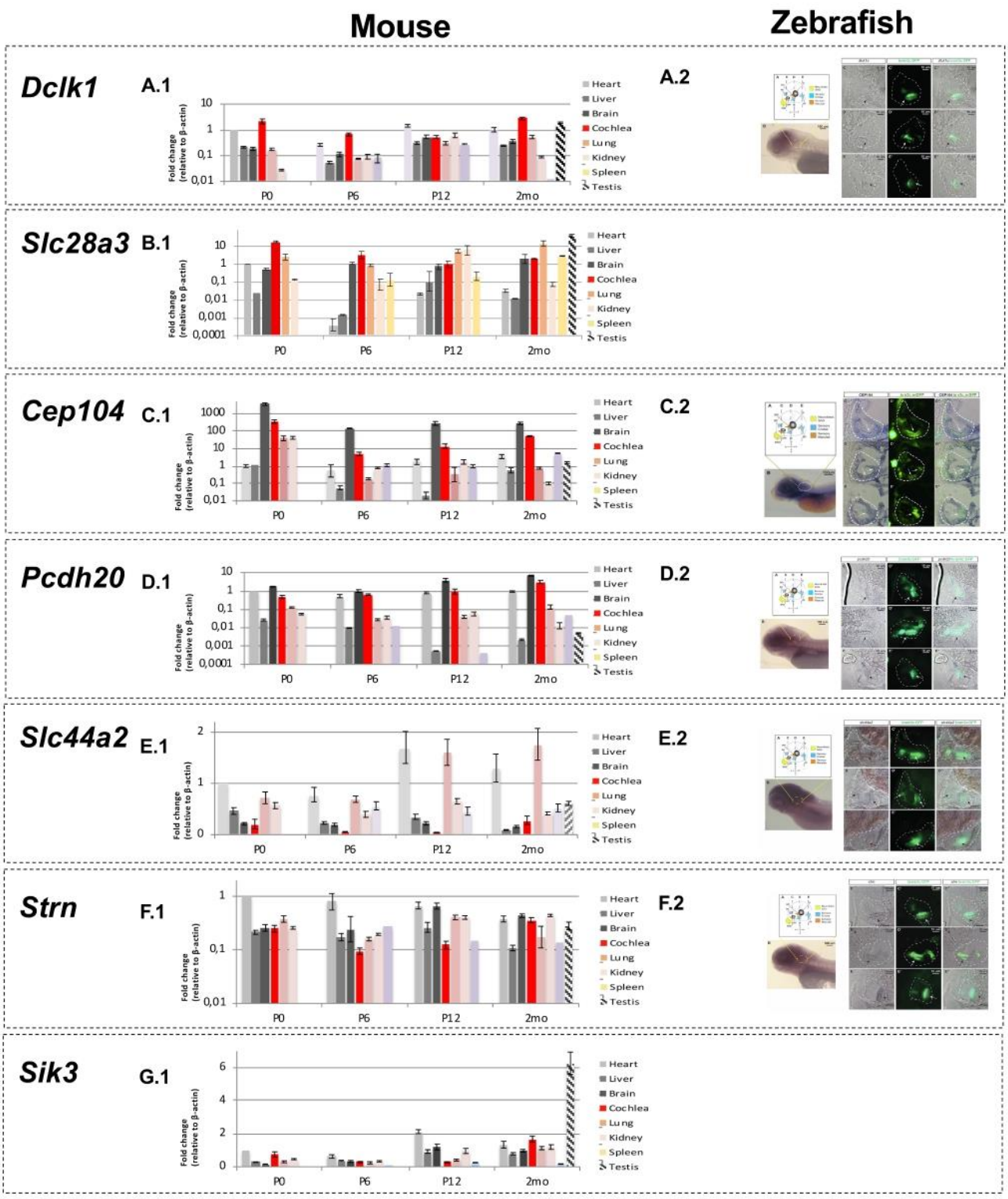

Fig. 1. Gene expression studies in mouse and zebrafish. The expression of all the seven genes have been analyzed by qRT-PCR in mouse tissues (i.e., heart, liver, brain, cochlea, lung, kidney, spleen, and testis) and whenever possbile in 5 dpf zebrafish larvae by whole-mount in situ hybridization as well. (A.1-G.1) The expression in mouse tissues is expressed as fold change compared to the levels of β-actin. (A.2-F.2) All the images of the gene expression in zebrafish larvae include: A) a schematic representation of 5 dpf inner ear cellular organization; the positions of the transversal views (C,D,E) are outlined by dotted lines; B) lateral view of anterior region of the 5 dpf larvae. Yellow circle delimit the inner ear location. C,D,E) Transversal view of the anterior, medial, and posterior regions of inner ear (outlined by a white dotted line). For each view, the specific gene expression by ISH, the brain3c:GFP, and the merged image, are present. (For interpretation of the references to colour in this figure legend, the reader is referred to the web version of this article.)

proteins (Fig. 2H,M). The stable mRNA expression and quantitative loss of the **CEP104** and **PCDH20** mutated protein in transfected cells, suggested that post-translational changes might occur in mutant proteins that could alter their stability. To identify which mechanism was involved in the degradation of the mutant proteins, we treated cells with proteasome inhibitors (MG132) or a lysosome inhibitor (Nh_4Cl), both of

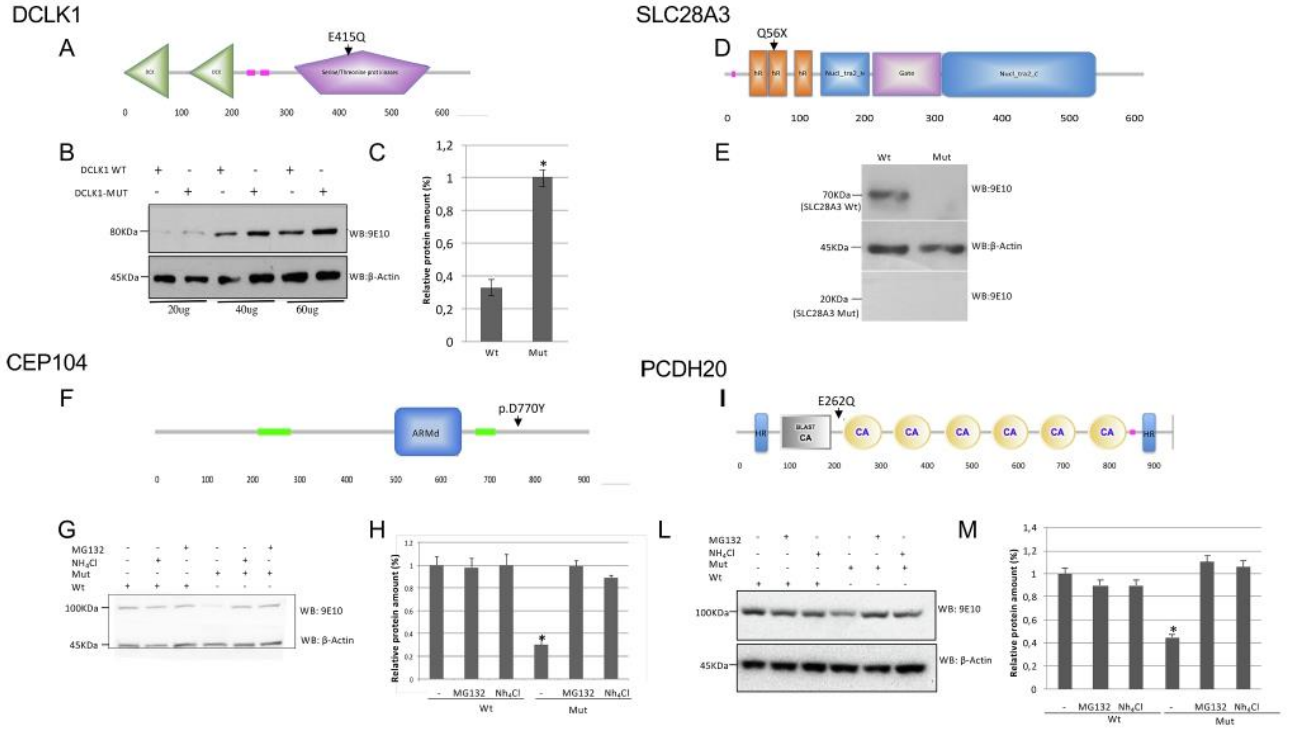

Fig. 2. In vitro protein expression studies. (A,D,F,I) showed the protein structures and the genetic variant position. (B,E,G,L) showed the western blot after transient transfection of WT and mutated cDNA. (C,H,M) are the graphic western blot quantifications, *P < 0.05.

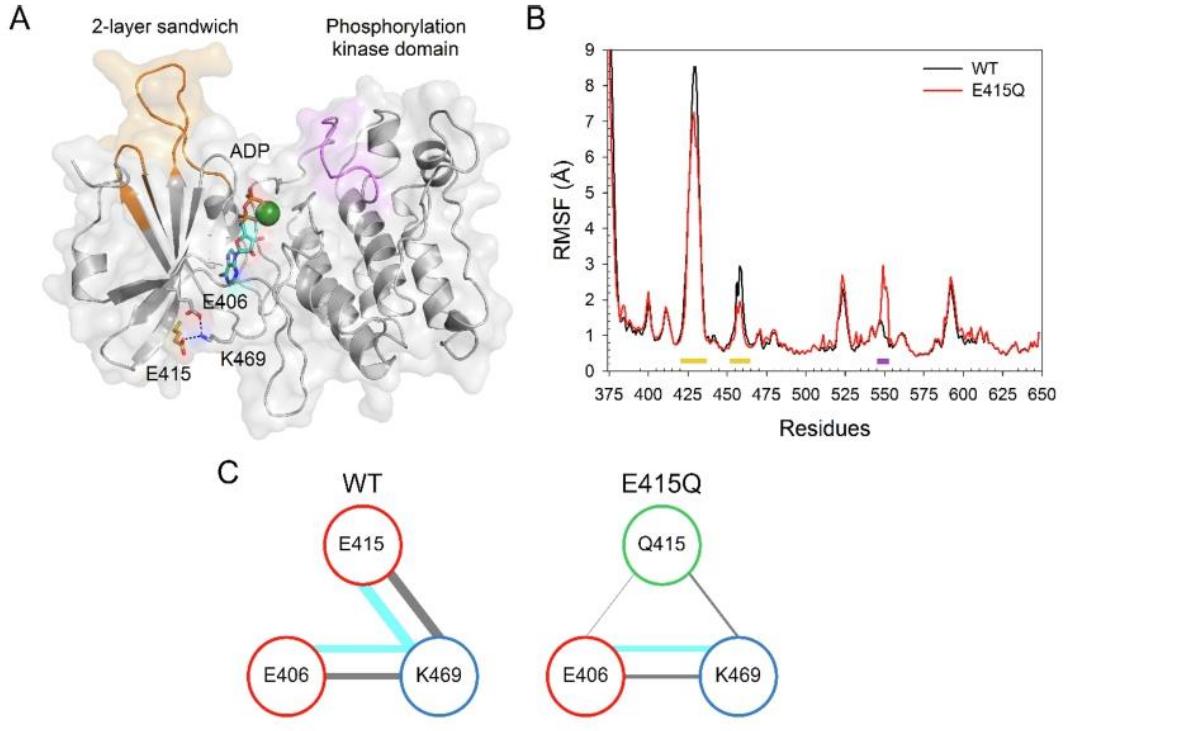

Fig. 3. A) Protein modelling. Three-dimensional structure of DCLK1 kinase domain is represented in grey cartoon and molecular surface, Mg^{2+} is shown as a green sphere, ADP is shown in cyan sticks, E406 and K469 are shown as grey sticks, HHL-associated residue E415 is shown in yellow sticks. Mutant region with higher flexibility with respect to WT is highlighted in purple, regions with lower flexibility are highlighted in orange. B) RMSF profiles along the 300 ns trajectories of WT (black) and E415Q (red) DCKL1. Colored bars represent the regions with differential flexibility according to panel A). C) Schematic representation of the interactions between residues 415, 406 and 469 of WT (left) and E415Q (right) DCLK1. Cyan lines represent salt bridges, grey lines represent H-bonds. Line width is proportional to the persistence of each interaction (see suppl. Table S2). (For interpretation of the references to colour in this figure legend, the reader is referred to the web version of this article.)

which restored normal protein levels (Fig. 2G, H, L, M).

In all the other cases (i.e., variants detected in ***SLC44A2***, ***STRN*** and ***SIK3*** genes), functional *in vitro* studies did not show any specific alteration in mRNA (suppl.Fig. S1H), or proteins expression (suppl.Fig. S2).

3. Discussion

Despite significant research efforts carried out so far, genetics risk factors involved in ARHL are still mainly unknown and only a few ARHL susceptibility genes have been detected. Using a combination of genetics (i.e., GWAS and targeted re-sequencing of candidate genes) and expression studies followed by functional analysis, we investigated the role of a series of genetic variants identified in seven genes (***DCLK1, SLC28A3, CEP104, PCDH20, SLC44A2, STRN,*** and ***SIK3)*** most likely associated to ARHL. Among them, the most promising candidates turned out to be ***DCLK1, SLC28A3***, ***CEP104*** and ***PCDH20*** showing a high expression in the inner ear and carrying variants with possible specific pathogenic significance in ARHL patients. The studies of ***DCLK1***, a gene recently described as strongly expressed in the stria vascularis, referred as a biomarker for several human cancers, involved in the epithelial-mesenchymal transition (EMT) and tumor progression (Gao et al., 2016; Chandrakesan et al., 2016) has recently reached valuable results. Functional studies of the ultra-rare genetic variant identified c.1243G>C; p.(E415Q) demonstrated a protein overexpression in transfected cells. According to the literature, this feature shows that an increased expression of ***DCLK1*** is linked to the tumor cells' proliferation, migration, invasion, and apoptosis through regulating endogenous microRNAs (Mohammadi et al., 2018). Therefore, it might be reasonable that the overexpression of this gene could be associated with an altered function of the encoded protein in aging diseases. We carried out MD simulations to better understand the role of the variant detected. The results suggest that, despite the absence of substantial structural changes of the ARHL-associated variant compared to that of the WT, the mutation induces significantly greater flexibility in the 546–552 region of the kinase domain, while slightly decreases it in the highly flexible regions 422–435 and 455–461 in the 2-layer sandwich domain. Thus, perturbation of remotely connected regions in DCLK1 tertiary structure suggests that the p.(E415Q) substitution exerts a long-range allosteric effect, which might affect the catalytic activity of the enzyme rather than the stability of its folding. This conclusion would be in line with the analysis performed by Patel et al. (2016), demonstrating the presence of a cluster of cancer-associated mutations in the same structural region affecting *DCLK1* catalytic activity.

Another appealing candidate is ***SLC28A3***, a gene recently identified by GWAS meta-analysis as significantly associated with auditory function in humans and hypothesized as having a specific role in the sensory epithelium of the utricle and cochlea (Vuckovic et al., 2015). The identification of a ***SLC28A3*** rare genetic variant in one ARHL individual coming from a remote area of the Sardinia island, combined with the functional *in vitro* studies showing a complete degradation of the protein variant, supports its pathogenetic role due to the haploinsufficiency mechanisms and make the ***SLC28A3*** gene an even stronger candidate for the late onset of ARHL.

Another ARHL candidate arising from our study is the ***CEP104*** gene. The knock-down of the protein in human retinal pigment cells results in severe defects in ciliogenesis with structural deformities at the ciliary tips (Srour et al., 2015). Expression and functional studies showed that the mutant allele detected in our ARHL patient enhances proteasomal and lysosomal protein degradation compared to the WT leading to a quantitative loss of the mutant ***CEP104***, which is, most likely, not sufficient to carry out its normal function. Interestingly, biallelic mutations (i.e., nonsense and splicing) in the ***CEP104*** gene have been described in patients affected by "Joubert syndrome" (OMIM * 616690), an autosomal-recessive disorder characterized by a distinctive mid-hindbrain and cerebellar malformation, oculomotor apraxia, irregular breathing, developmental delay, and ataxia (Srour et al., 2015). The case described in this paper carries a missense variant at the homozygous state and does not display any Joubert related clinical signs and symptoms; however, the literature data show that older cases of Joubert syndrome might develop a progressive, late-onset sensorineural HL, a phenotype overlapping with ARHL (Kroes et al., 2010). Finally, for ***PCDH20***, a member of the cadherin family, our findings demonstrate that the missense variant identified in one ARHL case is likely pathogenic leading to an instability of the protein structure and inducing a premature protein degradation through both the proteasome and the lysosome degradation pathways (Lv et al., 2015). Recently, ***PCDH20*** has been considered as a tumor-suppressor gene by antagonizing the Wnt/β-catenin, which is known to be necessary for hair-cell differentiation in the cochlea. Thus, one possibility is that the protein degradation, likely induced by mutated protein misfolding, would impair protein function leading to an alteration of the Wnt/β-caten in gene (Wolber et al., 2014). As for the remaining three genes, ***SLC44A2***, ***STRN*** and ***SIK3***, despite their clear expression in the inner ear, and the potential pathogenetic role of the variants identified in the ARHL patients, functional studies did not confirm the presence of any abnormality at mRNA level and protein expressions (O'Regan et al., 2000; Kommareddi et al., 2015; Charoenfuprasert et al., 2011; Zajic et al., 1991). Nevertheless, we cannot exclude that these variants might affect the protein localization, the targeting, proteins interaction or the transport. In this regard, we need further studies to see if they can, in any way, alter the function of proteins and thus lead to HL.

In conclusion, we have described the identification of a series of most likely pathogenic alleles in ***DCLK1***, ***SLC28A3***, ***CEP104***, ***PCDH20*** genes in ARHL patients coming from different Italian communities. We have detected none of these variants in our internal database of healthy controls, or in a database of centenarians. Although the number of semi-supercentenarians and controls is limited, they constitute a biological model of healthy ageing as they reached the last decades of life postponing or avoiding many age-related diseases. Further data on this population is required to replicate this result;however, it is interesting to note that none of these variants were detected in semi-supercentenarians, as well as in healthy controls, further supporting a possible role in the most common sensory decay of the aging process and in the related cognitive decline which, most likely, negatively affects life expectancy. Overall, these results highlight the difficulty in understanding the genetic architecture of ARHL a complex, highly heterogeneous and late-onset disease in which the variants here described might explain a small fraction of the total genetic variation. Nevertheless, the identification of some possible causative alleles contributes to the molecular dissection of the disease itself and might open new perspectives for the study of disease-specific molecular pathways.

4. Material and methods

All the experiments have been performed in accordance with relevant guidelines and regulations. The study was reviewed and approved by the Ethics Committee of Institute for Maternal and Child Health – IRCCS "Burlo Garofolo" (Italy) (2007 242/07) and informed consent was obtained from each participant. The protocol conformed to the tenets of the Declaration of Helsinki.

4.1. ARHL patients

We recruited, in this study, a total of 464 ARHL Italian patients coming from several inbred and outbred communities (Sardinia, Friuli Venezia Giulia-FVG, Carlantino and Milan cohorts). A complete audiological examination was performed on each patient to diagnose hearing loss and its clinical severity. Thresholds for six different frequencies (0.25, 0.5, 1, 2, 4 and 8 kHz) were measured (suppl. Table S1). We calculated three pure-tone averages (PTAs) of air-conduction thresholds: PTAL at low frequencies (0.25, 0.5, and 1 kHz), PTAM at

middle frequencies (0.5, 1, and 2 kHz) and PTAH at high frequencies (4 and 8 kHz). Patients were negative for the presence of any syndromic, vestibular signs, and conduction thresholds, excluding conductive hearing impairment.

4.2. Genetic analysis

We sequenced all the 464 ARHL patients using Ion Torrent PGM™ (Life-Technologies) with the targeted re-sequencing (TRS) panel described in Morgan et al. (2018) (REF) and analyzed the sequencing data according to the Ion Torrent Suite™ v3.6;; Single Nucleotide Variants (SNVs) and Insertions/Deletions (INDELs) were collected into a standardized VCF version 4.1 and filtered according to the following exclusion criteria: 1) SNVs/INDELs with QUAL < 20, 2) SNVs/INDELs called in off-target regions; 3) SNVs leading to synonymous amino acids substitutions not predicted to affect gene/protein function by any disease predictor tools (SIFT, Polyphen2, MutationTaster, LRT) (Schwarz et al., 2010; PROVEAN Home, 2016; Adzhubei et al., 2013) and not affecting splicing sites or highly conserved residues (PhyloP) (Pollard et al., 2010). Variants were then classified as ultra-rare (minor allele frequency (MAF < 0.001), rare (MAF < 0.01) or common (MAF > 0.01) based on the frequencies reported in public databases (i.e. NCBI dbSNP build150 (http://www.ncbi.nlm.nih.gov/SNP/), gnomAD (http://gnomad.broadinstitute.org/), NHLBI Exome Sequencing Project (ESP) Exome Variant Server) ('Exome Variant Server, NHLBI GO Exome Sequencing Project (ESP), Seattle, WA', n.d.). We assessed the variants effect on the protein function using several *in silico* "pathogenicity" predictor tools, such as Polyphen-2, MutationTaster, and Provean (Choi and Chan, 2015). The Human Gene Mutation Database (HGMD) (Stenson et al., 2009) and OMIM (Amberger et al., 2015) have been consulted to assess whether the identified SNVs were novel or already associated with a disease (Stenson et al., 2009; Amberger et al., 2015). Finally, we analyzed the variants that most likely affect protein function (i.e., rare and ultra-rare variants predicted as damaging by all in silico predictor tools) by Sanger sequencing and tested in controls.

4.3. Matched control samples

We have created an internal database with the whole genome sequencing data of 1071 healthy individuals (43% males, 57% females) from different Italian genetic isolates (INGI-Italian Network of Genetic Isolates), and, among these, we used 113 subjects as controls for ARHL (individuals aged >50 years old with PTA at the high frequencies (<25 dB).

4.4. Centenarians

The cohort consists of 81 healthy Italian semi-supercentenarians older than 104 years (average age 105.6 ± 1.6) recruited in North, Centre and South of the Italian peninsula. Semi-supercentenarians were born in a limited birth cohort range (1903–1909). We performed the extraction of genomic DNA from PBMCs using the AllPrep DNA/RNA/protein kit (QIAGEN, Hilden, Germany) and the DNA quantification, employing the Quant-iT dsDNA Broad-Range Assay Kit (Invitrogen Life Technologies, Carlsbad, CA, USA) or by Quant-iT PicoGreen dsDNA Assay Kit (Thermo Fisher Scientific) according to manufacturer protocols. The entire genome sequencing was carried out with Illumina technology and the TruSeq PCR-free library generation protocol. We reached an average depth of coverage of 90X in order to get a comprehensive and efficient analysis of variants. Genotypes of variant and non-variant sites have been called with Isaac Variant Caller (version 1.0.7). The WGS analysis was approved by the local Ethical Committee (S. Orsola Hospital – University of Bologna; Prot. n. 2006061707, amendment 08/11/2011; Fondazione IRCCS Cà Granda Ospedale Maggiore Policlinico, Prot. n. 2035, amendment 30/11/2011; University of Calabria 9/9/2004 amendment on 24/11/2011). Quality check followed the pipeline published (Anderson et al., 2010; Clarke et al., 2011).

4.5. Semi quantitative real time (sqRT-PCR)

We synthesized the cDNA starting from 0.5 μg of a mouse tissue RNA using the Transcriptor First Strand cDNA Synthesis kit (Roche, Indianapolis, USA) and subsequently used the aliquots (5 μL) of the RT products for PCR amplification. PCR reactions were optimized to 95 °C for 2 min, 30 amplification cycles at 95 °C for 10 sec, 60 °C for 15 s, 72 °C for 4 sec, and a final extension of 1 min at 72 °C using Kapa HiFi HotStart ReadyMix PCR kit (Kapa Biosystem, Cape town, South Africa). Amplified products were resolved on 2% agarose gels and visualized by ethidium bromide staining. The mRNA level transcripts in heart were arbitrarily chosen as a calibrator and standardized to one. The ß-actin expression was used as an endogenous control.

4.6. Western blot analysis

For protein analysis, HEK 293 cells were maintained using DMEM supplemented with 10% FBS, glutamine and penicillin-streptomycin (Invitrogen). Cells were lysed in IPLS buffer (50 mM Tris-HCL pH7.5, 120 mM NaCl, 0.5 mM EDTA and 0.5% Nonidet P-40) supplemented with proteases inhibitors (Roche, Indianapolis, IN, USA). After sonication and pre-clearing, protein lysate concentration was determined by Bradford Assay (Biorad). The proteins were resolved on 10% SDS-PAGE minigels and transferred to nitrocellulose membranes (GE Healthcare). Immunoblots were blocked in 5% BSA (Roche) in TBST (50 mM Tris-HCl, pH 7.4, 200 mM NaCl, and 0.1% Tween 20). Membranes were incubated with primary antibodies overnight and washed in Tris-buffered saline, 0.1% Tween-20. Secondary antibodies were diluted in blocking buffer and incubated with the membranes for 1 h at room temperature. Proteins were detected with the ECL detection kit (GE Health Care Bio-Sciences). Western blotting was performed with the following primary antibodies: polyclonal Myc antibody (Sigma, St. Louis, MO, USA), monoclonal Actin antibody (Sigma Sigma, St. Louis, MO, USA).

4.7. DNA cloning

The WT and human mutant genes of interest (*Slc44a2, Slc28a3, Cep104, Dclk1, Pcdh20, Sik3* and *Strn*) cDNAs were cloned into a pCMV6-Entry vector (by Origene, Rockville, MD), Myc tagged, respectively. Vectors were purified through the PureLink HiPure Plasmid Maxiprep kit (Invitrogen) for transfection and protein expression.

4.8. Cell culture and transient transfection

HEK293 cells were plated 5×10^5 cells per 6 cm plate, incubated overnight in DMEM with 10% FBS and 1% Pen/Strep. Cells were transfected using the standard Calcium Phosphate Transfection Method. Transfection protocol: 3 μg of plasmid DNA was mixed with 10 μL of 0.25 M $CaCl_2$, 75 μL H_2O, then 88 μL of HBS was added, and the mixture was incubated for 20′ at room temperature. Calcium phosphate-DNA solution (176 μL) was added dropwise to the plate of cells, and the mixture was swirled gently and incubated for 24 h at 35 °C under 2 to 4% CO_2). Cells were collected 48 h after transient transfection. One plate of cells, per each treatment, was incubated with Mg132 (9 uM, Sigma Aldrich) for 4 h at 35 to 37 °C under 5% CO2 and Nh_4Cl (10 mM, Sigma Aldrich).

4.9. Gene expression in zebrafish larvae

Gene expression in zebrafish larvae 5 days post fertilization (dpf) was performed in collaboration with ZeClinics (Barcelona, Spain).

Whole-mount *in situ* hybridization (ISH) was carried out in a Tg (brn3c:mGFP) line, which is a stable reporter line where a GFP tagged to the membrane is expressed under the control of the brn3c promoter (Xiao et al., 2005), thus specifically labeling a subset of retinal ganglion cells, hair cells of the inner ear and the lateral line (Di Donato et al., 2013). Specific riboprobes intended to recognize the mRNA of the genes of interest were designed (sequences available upon request). We amplified cDNAs by PCR from a custom zebrafish cDNAs library obtained by RT-PCR from an mRNA pool coming from 5 dpf zebrafish larvae. A T7 sequence linker in reverse primers was included to directly use the synthesized PCR products as templates to amplify the reverse digoxigenin-labeled riboprobe to be used for ISH.

Once dissected, embryos were fixed in 4% paraformaldehyde (PFA) overnight and then dehydrated with increasing concentrations of Methanol PBT for long-term storage. We then rehydrated, dechorionated, treated the embryos with proteinase K, incubated them with a hybridization mix containing the riboprobe, and with the antibody against digoxigenin Nitroblue Tetrazolium (NBT) was used with the alkaline phosphatase substrate 5-Bromo- 4- Chloro-3-Indolyl Phosphate (BCIP). These substrate systems produce an insoluble NBT di-formazan product colored from blue to purple and visually observable. In order to check gene expression in hair cells, marked with GFP through its activation by the Brn3c promoter, the secondary antibody against GFP was used. Stained embryos were processed for imaging through 2 different methods: 1. Whole embryos were imaged with a bright field stereoscope to determine the overall expression pattern. 2. Transversal sections were acquired through a cryostat (20 μm width) to determine precisely the mRNA location within the inner ear across 3 different anteroposterior positions. Gene expression pattern was compared with the position of hair cells, marked with GFP through its activation by the Brn3c promoter. Sections were imaged with Leica DM5 light/fluorescent microscope at 40x magnification.

4.10. Molecular dynamics (MD) protein simulation

MD simulations of DCLK1-ADP complex were performed using as a starting structure the A-monomer of the crystallographic dimer (Sondek et al., 1996). Since residues 590–595 were missing, the DCLK1 sequence was subjected to homology modeling using the online server ModWeb version r211 (Pieper et al., 2009) and 5JZJ_A as a template. The resulting model passed all quality checks performed by ModWeb, namely ModPipe.

Quality Score $\geq$ 1.1 (2.2), TSVMod NO35 $\geq$ 0.4 (0.98), GA341 $\geq$ 0.7 (1.0), E-value $<$ 0.0001 (0), zDOPE $<$ 0 (-1.27), therefore it was considered reliable. Finally, to restore the physiologically bound ADP, the final phosphate N atom of AMP-PN was converted to O.

In silico mutagenesis of E415Q was achieved by selecting the most probable rotamer proposed by the "mutate residue" function of Maestro (Schrodinger) software. MD simulations were run using GROMACS 2016.5 simulation package and CHARMM36m all-atom force field (Abraham et al., 2015; Huang et al., 2017; Marino et al., 2015).

The system size was 46,096 atoms for both WT DCLK1 and E415Q variant. System building, pre-production steps and energy minimization were performed as indicated in while parameters for the equilibration and production phases of the 300 ns trajectories (T = 310 K) were substantially the same as in Marino et al. (2015), Marino and Dell'Orco (2016).

The persistence of salt bridges and hydrogen bonds along the trajectories was calculated using PyInteraph software (Tiberti et al., 2014) as described in detail in and refers to the percentage of frames during which the given interaction is observed over the total number of frames. Such analysis has been shown to effectively identify allosteric properties in different protein systems undergoing thorough the MD simulations (Marino and Dell'Orco, 2016; Marino and Dell'Orco, 2019).

Root-Mean Square Fluctuation was calculated using the "gmx rmsf" function within GROMACS, which describes the time-averaged root-mean squared displacement of the coordinates of each amino acid concerning the reference structure, thus accounting for residue flexibility.

Declaration of Competing Interest

The authors declare that they have no known competing financial interests or personal relationships that could have appeared to influence the work reported in this paper.

Acknowledgments

We gratefully acknowledge: (1) the Technologic Center at the University of Verona in which Molecular Dynamics simulations were run. (2) ZeClinics company for their technical contribution in zebrafish models. (3) all the individuals who voluntarily participated in the study and Dr. Martina Bradaschia for the English revision of the manuscript.

Author contribution

MDS and AM: study design assessment, data production and analysis, and writing the manuscript. SB: *in vitro* data production; BM: raw data analysis and quality control; VM: protein modeling and molecular dynamics simulation; PG and CG: replication in semi-supercentenarians cohort raw data analysis and quality control. DDO: conceiving the experiments on protein modeling and molecular dynamics simulation; PG: support of conceiving the experiments and in writing the manuscript, GG: conceiving the experiments and writing the manuscript.

Funding

This research was supported by D70-RESRICGIROTTO and Beneficientia Stiftung to GG. The funders had no role in study design, data collection and analysis, decision to publish, or preparation of the manuscript.

Appendix A. Supplementary data

Supplementary data to this article can be found online at https://doi.org/10.1016/j.gene.2020.144561.

References

Abraham, M.J., Murtola, T., Schulz, R., Páll, S., Smith, J.C., Hess, B., Lindahl, E., 2015. GROMACS: High performance molecular simulations through multi-level parallelism from laptops to supercomputers. SoftwareX 1–2, 19–25. https://doi.org/10.1016/J.SOFTX.2015.06.001.

Adzhubei, I., Jordan, D.M., Sunyaev, S.R., 2013 Jan [cited 2015 Mar 4]. Predicting functional effect of human missense mutations using PolyPhen-2. Curr. Protoc. Hum. Genet. Chapter 7, Unit 7.20. Available from: http://www.pubmedcentral.nih.gov/articlerender.fcgi?artid=4480630&tool=pmcentrez&rendertype=abstract.

Amberger, J.S., Bocchini, C.A., Schiettecatte, F., Scott, A.F., Hamosh, A., 2015. OMIM.org: Online Mendelian Inheritance in Man (OMIM®), an online catalog of human genes and genetic disorders. Nucleic Acids Res. 43, D789–D798. https://doi.org/10.1093/nar/gku1205.

Anderson, C.A., Pettersson, F.H., Clarke, G.M., Cardon, L.R., Morris, A.P., Zondervan, K.T., 2010. Data quality control in genetic case-control association studies. Nat. Protoc. 5, 1564–1573. https://doi.org/10.1038/nprot.2010.116.

Bainbridge, K.E., Wallhagen, M.I., 2014. Hearing loss in an aging american population: extent, impact, and management. Annu. Rev. Public Health 35, 139–152. https://doi.org/10.1146/annurev-publhealth-032013-182510.

Chandrakesan, P., Panneerselvam, J., Qu, D., Weygant, N., May, R., Bronze, M., Houchen, C., 2016. Regulatory roles of Dclk1 in epithelial mesenchymal transition and cancer stem cells. J. Carcinog. Mutagen. 7. https://doi.org/10.4172/2157-2518.1000257.

Charoenfuprasert, S., Yang, Y.-Y., Lee, Y.-C., Chao, K.-C., Chu, P.-Y., Lai, C.-R., Hsu, K.-F., Chang, K.-C., Chen, Y.-C., Chen, L.-T., Chang, J.-Y., Leu, S.-J., Shih, N.-Y., 2011. Identification of salt-inducible kinase 3 as a novel tumor antigen associated with tumorigenesis of ovarian cancer. Oncogene 30, 3570–3584. https://doi.org/10.1038/onc.2011.77.

Choi, Y., Chan, A.P., 2015. PROVEAN web server: a tool to predict the functional effect of amino acid substitutions and indels. Bioinformatics 31, 2745–2747. https://doi.org/

10.1093/bioinformatics/btv195.
Clarke, G.M., Anderson, C.A., Pettersson, F.H., Cardon, L.R., Morris, A.P., Zondervan, K.T., 2011. Basic statistical analysis in genetic case-control studies. Nat. Protoc. 6, 121–133. https://doi.org/10.1038/nprot.2010.182.
Coffin, A.B., Dabdoub, A., Kelley, M.W., Popper, A.N., 2007. Myosin VI and VIIa distribution among inner ear epithelia in diverse fishes. Hear. Res. 224, 15–26. https://doi.org/10.1016/j.heares.2006.11.004.
Di Donato, V., Auer, T.O., Duroure, K., Del Bene, F., 2013. Characterization of the calcium binding protein family in zebrafish. PLoS ONE 8, e53299. https://doi.org/10.1371/journal.pone.0053299.
Errasti-Murugarren, E., Molina-Arcas, M., Casado, F.J., Pastor-Anglada, M., 2009. A splice variant of the SLC28A3 gene encodes a novel human concentrative nucleoside transporter-3 (hCNT3) protein localized in the endoplasmic reticulum. FASEB J. 23, 172–182. https://doi.org/10.1096/fj.08-113902.
Exome Variant Server, NHLBI GO Exome Sequencing Project (ESP), Seattle, WA [WWW Document], n.d.
Gao, T., Wang, M., Xu, L., Wen, T., Liu, J., An, G., 2016. DCLK1 is up-regulated and associated with metastasis and prognosis in colorectal cancer. J. Cancer Res. Clin. Oncol. 142, 2131–2140. https://doi.org/10.1007/s00432-016-2218-0.
Girotto, G., Vuckovic, D., Buniello, A., Lorente-Cánovas, B., Lewis, M., Gasparini, P., Steel, K.P., 2014. Expression and replication studies to identify new candidate genes involved in normal hearing function. PLoS ONE 9, e85352. https://doi.org/10.1371/journal.pone.0085352.
Huang, J., Rauscher, S., Nawrocki, G., Ran, T., Feig, M., de Groot, B.L., Grubmüller, H., MacKerell, A.D., 2017. CHARMM36m: an improved force field for folded and intrinsically disordered proteins. Nat. Methods 14, 71–73. https://doi.org/10.1038/nmeth.4067.
Keithley, E.M., 2019. Pathology and mechanisms of cochlear aging. J. Neurosci. Res. https://doi.org/10.1002/jnr.24439.
Kommareddi, P., Nair, T., Kakaraparthi, B.N., Galano, M.M., Miller, D., Laczkovich, I., Thomas, T., Lu, L., Rule, K., Kabara, L., Kanicki, A., Hughes, E.D., Jones, J.M., Hoenerhoff, M., Fisher, S.G., Altschuler, R.A., Dolan, D., Kohrman, D.C., Saunders, T.L., Carey, T.E., 2015. Hair cell loss, spiral ganglion degeneration, and progressive sensorineural hearing loss in mice with targeted deletion of Slc44a2/Ctl2. J. Assoc. Res. Otolaryngol. 16, 695–712. https://doi.org/10.1007/s10162-015-0547-3.
Kroes, H.Y., Van Zanten, B.G.A., De Ru, S.A., Boon, M., Mancini, G.M.S., Van der Knaap, M.S., Poll-The, B.T., Lindhout, D., 2010. Is hearing loss a feature of Joubert syndrome, a ciliopathy? Int. J. Pediatr. Otorhinolaryngol. 74, 1034–1038. https://doi.org/10.1016/j.ijporl.2010.05.034.
Lv, J., Zhu, P., Yang, Z., Li, M., Zhang, X., Cheng, J., Chen, X., Lu, F., 2015. PCDH20 functions as a tumour-suppressor gene through antagonizing the Wnt/β-catenin signalling pathway in hepatocellular carcinoma. J. Viral Hepat. 22, 201–211. https://doi.org/10.1111/jvh.12265.
Marino, V., Dell'Orco, D., 2019. Evolutionary-conserved allosteric properties of three neuronal calcium sensor proteins. Front. Mol. Neurosci. 12, 50. https://doi.org/10.3389/fnmol.2019.00050.
Marino, V., Dell'Orco, D., 2016. Allosteric communication pathways routed by Ca2+/Mg2+ exchange in GCAP1 selectively switch target regulation modes. Sci. Rep. 6, 34277. https://doi.org/10.1038/SREP34277.
Marino, Valerio, Sulmann, Stefan, Koch, Karl-Wilhelm, Dell'Orco, Daniele, 2015. Structural effects of Mg2+ on the regulatory states of three neuronal calcium sensors operating in vertebrate phototransduction. Biochim. Biophys. Acta (BBA) – Mol. Cell Res. 1853 (9), 2055–2065. https://doi.org/10.1016/j.bbamcr.2014.10.026.
Mohammadi, Y., Tavangar, S.M., Saidijam, M., Amini, R., Etemadi, K., Karimi Dermani, F., Najafi, R., 2018. DCLK1 plays an important role in colorectal cancer tumorgenesis through the regulation of miR-200c. Biomed. Pharmacother. 103, 301–307. https://doi.org/10.1016/j.biopha.2018.04.042.
Moqrich, A., Mattei, M.G., Bartoli, M., Rakitina, T., Baillat, G., Monneron, A., Castets, F., 1998. Cloning of human striatin cDNA (STRN), gene mapping to 2p22-p21, and preferential expression in brain. Genomics 51, 136–139. https://doi.org/10.1006/geno.1998.5342.
Morgan, A., Vuckovic, D., Krishnamoorthy, N., Rubinato, E., Ambrosetti, U., Castorina, P., Franzè, A., Vozzi, D., La Bianca, M., Cappellani, S., Di Stazio, M., Gasparini, P., Girotto, G., 2018. Next-generation sequencing identified SPATC1L as a possible candidate gene for both early-onset and age-related hearing loss. J. Hum. Genet Eur. https://doi.org/10.1038/s41431-018-0229-9 (830-17-EJHG).
Nair, T.S., Kommareddi, P.K., Galano, M.M., Miller, D.M., Kakaraparthi, B.N., Telian, S.A., Arts, H.A., El-Kashlan, H., Kilijanczyk, A., Lassig, A.A.D., Graham, M.P., Fisher, S.G., Stoll, S.W., Nair, R.P., Elder, J.T., Carey, T.E., 2016. SLC44A2 single nucleotide polymorphisms, isoforms, and expression: association with severity of Meniere's disease? Genomics 108, 201–208. https://doi.org/10.1016/j.ygeno.2016.11.002.
O'Regan, S., Traiffort, E., Ruat, M., Cha, N., Compaoré, D., Meunier, F.-M., 2000. An electric lobe suppressor for a yeast choline transport mutation belongs to a new family of transporter-like proteins. Proc. Natl. Acad. Sci. 97, 1835–1840. https://doi.org/10.1073/PNAS.030339697.
Patel, O., Dai, W., Mentzel, M., Griffin, M.D.W., Serindoux, J., Gay, Y., Fischer, S., Sterle, S., Kropp, A., Burns, C.J., Ernst, M., Buchert, M., Lucet, I.S., 2016. Biochemical and structural insights into doublecortin-like kinase domain 1. Structure 24, 1550–1561. https://doi.org/10.1016/j.str.2016.07.008.
Pieper, U., Eswar, N., Webb, B.M., Eramian, D., Kelly, L., Barkan, D.T., Carter, H., Mankoo, P., Karchin, R., Marti-Renom, M.A., Davis, F.P., Sali, A., 2009. MODBASE, a database of annotated comparative protein structure models and associated resources. Nucleic Acids Res. 37, D347–D354. https://doi.org/10.1093/nar/gkn791.
Pollard, K.S., Hubisz, M.J., Rosenbloom, K.R., Siepel, A., 2010 Jan [cited 2015 Nov 3]. Detection of nonneutral substitution rates on mammalian phylogenies. Genome Res. 20 (1), 110–121. Available from: http://www.pubmedcentral.nih.gov/articlerender.fcgi?artid=2798823&tool=pmcentrez&rendertype=abstract.
PROVEAN Home, [cited 2016 May 18]. Available from: http://provean.jcvi.org/index.php.
Salvi, R., Ding, D., Jiang, H., Chen, G.-D., Greco, A., Manohar, S., Sun, W., Ralli, M., 2018. Hidden age-related hearing loss and hearing disorders: current knowledge and future directions. Hear. Balanc. Commun. 1–9. https://doi.org/10.1080/21695717.2018.1442282.
Satish Tammana, T.V., Tammana, D., Diener, D.R., Rosenbaum, J., 2013. Centrosomal protein CEP104 (Chlamydomonas FAP256) moves to the ciliary tip during ciliary assembly. J. Cell Sci. 126, 5018–5029. https://doi.org/10.1242/jcs.133439.
Schwarz, J.M., Rödelsperger, C., Schuelke, M., Seelow, D., 2010 Aug [cited 2015 May 31]. MutationTaster evaluates disease-causing potential of sequence alterations. Nat. Methods 7 (8), 575–576. Available from: http://www.ncbi.nlm.nih.gov/pubmed/2067607514.
Sondek, J., Bohm, A., Lambright, D.G., Hamm, H.E., Sigler, P.B., 1996. Crystal structure of a G-protein beta gamma dimer at 2.1A resolution. Nature 379, 369–374. https://doi.org/10.1038/379369a0.
Srour, M., Hamdan, F.F., McKnight, D., Davis, E., Mandel, H., Schwartzentruber, J., Martin, B., Patry, L., Nassif, C., Dionne-Laporte, A., Ospina, L.H., Lemyre, E., Massicotte, C., Laframboise, R., Maranda, B., Labuda, D., Décarie, J.-C., Rypens, F., Goldsher, D., Fallet-Bianco, C., Soucy, J.-F., Laberge, A.-M., Maftei, C., Boycott, K., Brais, B., Boucher, R.-M., Rouleau, G.A., Katsanis, N., Majewski, J., Elpeleg, O., Kukolich, M.K., Shalev, S., Michaud, J.L., 2015. Joubert Syndrome in French Canadians and Identification of Mutations in CEP104. Am. J. Hum. Genet. 97, 744–753. https://doi.org/10.1016/J.AJHG.2015.09.009.
Stenson, P.D., Mort, M., Ball, E.V., Howells, K., Phillips, A.D., Thomas, N.S., Cooper, D.N., 2009. The human gene mutation database: 2008 update. Genome Med. 1, 13. https://doi.org/10.1186/gm13.
The evolving doublecortin (DCX) superfamily. - PubMed - NCBI [WWW Document], n.d. URL https://www.ncbi.nlm.nih.gov/pubmed/16869982 (accessed 10.9.19).
Tiberti, M., Invernizzi, G., Lambrughi, M., Inbar, Y., Schreiber, G., Papaleo, E., 2014. PyInteraph: a framework for the analysis of interaction networks in structural ensembles of proteins. J. Chem. Inf. Model. 54, 1537–1551. https://doi.org/10.1021/ci400639r.
Tu, N.C., Friedman, R.A., 2018. Age-related hearing loss: Unraveling the pieces. Laryngoscope Investig. Otolaryngol. https://doi.org/10.1002/lio2.134.
Van Laer, L., Huyghe, J.R., Hannula, S., Van Eyken, E., Stephan, D.A., Mäki-Torkko, E., Aikio, P., Fransen, E., Lysholm-Bernacchi, A., Sorri, M., Huentelman, M.J., Van Camp, G., 2010. A genome-wide association study for age-related hearing impairment in the Saami. Eur. J. Hum. Genet. 18, 685–693. https://doi.org/10.1038/ejhg.2009.234.
Vuckovic, D., Dawson, S., Scheffer, D.I., Rantanen, T., Morgan, A., Di Stazio, M., Vozzi, D., Nutile, T., Concas, M.P., Biino, G., Nolan, L., Bahl, A., Loukola, A., Viljanen, A., Davis, A., Ciullo, M., Corey, D.P., Pirastu, M., Gasparini, P., Girotto, G., 2015. Genome-wide association analysis on normal hearing function identifies PCDH20 and SLC28A3 as candidates for hearing function and loss. Hum. Mol. Genet. 24, 5655–5664. https://doi.org/10.1093/hmg/ddv279.
Wolber, Lisa E., Girotto, G., Buniello, A., Vuckovic, D., Pirastu, N., Lorente-Cánovas, B., Rudan, I., Hayward, C., Polasek, O., Ciullo, M., Mangino, M., Steves, C., Concas, M.P., Cocca, M., Spector, T.D., Gasparini, P., Steel, K.P., Williams, F.M.K., 2014. Salt-inducible kinase 3, SIK3, is a new gene associated with hearing. Hum. Mol. Genet. 23, 6407–6418. https://doi.org/10.1093/hmg/ddu346.
Xiao, T., Roeser, T., Staub, W., Baier, H., 2005. A GFP-based genetic screen reveals mutations that disrupt the architecture of the zebrafish retinotectal projection. Development 132, 2955–2967. https://doi.org/10.1242/dev.01861.
Yan, D., Kamiya, K., Ouyang, X.M., Liu, X.Z., 2011. Analysis of subcellular localization of Myo7a, Pcdh15 and Sans in Ush1c knockout mice. Int. J. Exp. Pathol. 92, 66–71. https://doi.org/10.1111/j.1365-2613.2010.00751.x.
Zajic, G., Nair, T.S., Ptok, M., Van Waes, C., Altschuler, R.A., Schacht, J., Carey, T.E., 1991. Monoclonal antibodies to inner ear antigens: I. Antigens expressed by supporting cells of the guinea pig cochlea. Hear. Res. 52, 59–71.

4 DISCUSSION

Deafness has a significant impact on life quality affecting, for example, educational attainment, communication and life quality[71].
Prompt recognition and accurate genetic diagnosis are crucial to optimize outcomes and treatment of both congenital and late onset HL[71,72].
This thesis demonstrates how the application of a multi-step strategy together with a multi-disciplinary team and collaborations has proved to be a powerful approach for the molecular diagnosis of HL, achieving the identification of novel genes involved in NSHHL and ARHL.

NSHHL

Regarding the NSHHL study, we have highlighted the importance of a combined strategy: TRS and WES analysis, together with functional studies for the identification of the *USP48* gene as a new candidate associated with NSHHL. In particular, the *in-vitro* functional studies allowed the characterization of variants affecting the USP48 function and allowed us to prove the expression of this gene in auditory and vestibular structures in human embryo inner ear. The engineering of *usp48* Knock-down zebrafish model further confirms the involvement of this gene in the auditory function and specifically in the statoacoustic neurons of zebrafish.
In the last year, this type of strategy has led to the identification of several novel genes. For example, Morgan et al., from our Italian group, has described PLS1[32] and SLC12A2[73] as new candidate genes involved in autosomal dominant NSHHL in humans, furthermore Barbara Vona and colleagues have identified *CLRN2* as a new deafness gene in an extended consanguineous family with pre-lingual autosomal recessive HL[74]. *NCOA3* has been reported as a new candidate gene to explain autosomal dominant progressive HL by Rodrigo Salazar da Silva and colleagues[75]; while Brownstein et al., described *ATOH1* as a new HL gene in the Israeli Jewish population, potentially due to its crucial role for the development and differentiation of inner ear hair cells[72].

Despite these recent discoveries, the aetiology of hereditary deafness is clinically and genetically heterogeneous and it is still not entirely well understood.
For example, many genes have been described to be associated with both the autosomal recessive and the dominant condition.

Furthermore, variable penetrance of this trait has been reported for different genes, widening the range of phenotypes from normal hearing to profound deafness[76] between individuals carrying the same variants. In particular, we faced this phenomenon in our Italian family affected by NSHHL that presented a healthy individual carrying the causative variant. Incomplete penetrance can make challenging the interpretation of the family clinical history and the identification of causative variants.

This phenotypic variation in “Mendelian” disorders might be due to the genetic interaction of several genes[47]. Thus, we should consider that multiple genetic variants could contribute to a different degree of the phenotype and moreover some variants could also present a protective role.

Moreover, it is becoming more evident that monogenic forms of deafness are quite rare[77]. This suggests that we are too focused on the identification of the “one and only” causative variant, without considering the potential contribution of other elements.

These data, again, support the idea that, even in the monogenic forms of deafness, other factors could contribute to the final phenotype[78].

We should consider, for instance, the (i) polygenic inheritance, (contribution of variants in different genes of even in the same gene) and (ii) oligogenic inheritance (when the monogenic trait is predominantly influenced by one gene but mutations in a small number of other genes may interact and modulate the manifestation of the phenotype)[77].

As consequence, the traditional distinction between Mendelian and complex disorders might be blurred[47] or might be an over-simplification. Thus, the analysis of mendelian traits, such as deafness, should carefully consider the involvement of more than one variant or genes in the development of the phenotype.

The traditional tools for investigating complex relationships between genes can be useful in the identification of the polygenic or oligogenic basis of a genetic trait and for modelling these disorders using Mendelian principles[47].

ARHL

So far, different GWAS on ARHL trait have been published[37,39,51,52,79,80]. These studies proved to be essential for the identification of novel genes involved in several complex traits and diseases such as hearing function and ARHL. For example, Girotto et al., thanks to the establishment of the G-EAR Consortium identified several genes identified in normal hearing function and ARHL[51]. Moreover, Hoffmann T.J. et al. identified a candidate gene for ARHL in *ISG20*, and they also hypothesized the involvement of *TRIOBP*, *EYA4* and *ILDR1*, genes known to be related to other forms of deafness[79]. A more recent investigation in 2019[35] analyzed ARHL as a quantitative trait identifying a list of five novel associated loci and strengthened the possible involvement of *ILDR1* in ARHL. Together with our results, the combination of GWAS data and TRS approach proved to be a powerful tool in the study of genetic bases of ARHL.

In fact, the use of GWAS data and TRS allowed us to identify rare and ultra-rare variants in seven new genes most likely involved in ARHL. In particular, expression studies in mice and zebrafish and the *in-vitro* analysis led to the identification of four most promising candidates: *DCLK1*, *SLC28A3*, *CEP104* and *PCDH20* highly expressed in the inner ear and showing variants that can predispose the development of ARHL.

Although many candidate genes have been associated with ARHL by GWAS, there was a lack of significant genome-wide findings and a poor replication of them across these studies[33]. The reason could be an over-estimated heritability of ARHL or the presence of thousands of rare variants of small effect in the population that could contribute together to ARHL risk, which would be really difficult to detect only with GWAS[48].

However, the are many explanations related to why common ARHL risk variants may not have been detected in these studies. The power of GWA studies relies on two main factors[81,82]: (i) a good phenotyping measure, between patients and controls, that requires trained audiologist and (ii) a very large cohort involving sample sizes that is highly expensive and requires a significant amount of time. A compromise often has to be made between the quality of the hearing data collected and the sample size, causing a lack of replication between individual GWAS[33]. Therefore, there is a great need for larger genetic studies, also introducing the use of whole-exome or whole-genome sequencing that present greater power to detect the relatively subtle effects of more rare variants[33].

In addition, given these difficulties of studying presbycusis in human cohorts, researchers started to use animal models. Despite no model organism displays all aspects of human

presbycusis, the mouse is the predominant model for studying the mammalian auditory function and has become a robust and reliable model for ageing research[83]. It is possible to strictly control intrinsic and extrinsic factors, e.g., genetic background, diet, health status and environment. Supplementing human studies with mouse model analysis could be useful to validate ARHL GWAS hits and also provide insights into the genetic mechanism underlying ARHL[33].

5 FUTURE PERSPECTIVES

The results of this work demonstrate how the unceasing improvement of sequencing technologies can lead to the identification of novel deafness genes, although we still fail to provide a diagnosis in many cases: something is still missing.
One of the major players is represented by the power of the sequencing technologies. TRS presents several limitations, for example causative genes may not be included in the panel and variants can lie in regions with low coverage or in intronic regions.
The application of WES analyses has allowed the identification of more than 20 new NSHHL genes in the last decade (https://hereditaryhearingloss.org/), however it also presents some limitations: for example, the phenotype may be caused by structural variants or deep intronic variants, not detectable neither with TRS or WES.
To overcome these limits, Whole Genome Sequencing (WGS) may represent the most suitable alternative in the future. This technology encompasses both coding and noncoding regions, including the 98% of the genome not captured by WES[84].
It is now well understood that non-coding variants can lead to disease and intronic regions can have crucial roles[84]. WES technology has already helped clinicians to identify rare birth defects, diagnose and treat rare diseases[85] advancing the personalized medicine.
It also presents several limitations as costs, quality issues, not standardized protocols[41].
Additionally, variations in non-coding regions are less well understood than variation in the coding region because the current knowledge is not sufficient for their interpretation[84].
All these biases make more difficult the prediction of which variants might be relevant to a trait of interest in whole genome datasets[84].
However, considering the falling cost of sequencing [71], it is foreseeable that the use of WGS could become a standard of care for individuals, in our case applied to samples with severe level of hearing loss at birth and for identify rare variants in genes that can led to ARHL susceptibility.

At the same time, other elements could be improved to better understand the deafness phenotypes and avoid errors or incompatibly in comparing different studies, for example: (i) standardize the examination protocols for auditory ability in mendelian and complex deafness traits; (ii) encourage the collaboration between clinicians and researchers for a better comprehension of the phenotypical data; (iii) consider the involvement of more variants and genes also in mendelian deafness cases, not only for complex deafness traits; (iii) engineering different animal models e.g., zebrafish, to understand the molecular

mechanisms involved in auditory ability and (vi) the development of novel therapies exploiting gene editing approach to correct potential causative variants, that could represent novel medical approaches.

In conclusions, there is the necessity of the genetic community to introduce comprehensive and fast clinical genomic testing allowing early diagnosis and facilitating optimum clinical care[71]. Rapid genetic screening at birth may prevent specific forms of HL completely, such as for individuals carrying mitochondrial mutations which can led to HL development after treatment with aminoglycoside antibiotics.
Furthermore, the identification of genetics risk factors for both Hereditary HL and ARHL, and the elaboration of appropriate interventions will be a worthwhile goal for the development of preventive strategies and improve the quality of life for deaf people[52]. These approaches will be hopefully developed as technologies improve, costs decrease and different treatment options will become available[71].

The results showed in this thesis provide a significant contribution to understand the genetic bases of NSHHL and underlying the complexity of ARHL. This study could have an important impact in the future development of preventive strategies, diagnosis and screenings of HL patients, and in the progress of new personalized therapeutic approaches.

6 REFERENCES

1. Hawkins JE. Human Ear. *Natl Saf News*. 2018;117(5):51-58.
2. Anthwal N, Thompson H. The development of the mammalian outer and middle ear. *J Anat*. 2016;228(2):217-232. doi:10.1111/joa.12344
3. Standring S. *Gray's Anathomy: The Anatomical Basis of Clinical Practice*. 40th ed. (Borley NR (ed.)., ed.).; 2008.
4. Konishi T, Hamrick PE, Walsh PJ. Ion transport in Guinea pig cochlea: I. Potassium and sodium transport. *Acta Otolaryngol*. 1978;86(1-6):22-34. doi:10.3109/00016487809124717
5. Hensen V. Zur Morphologie der Schnecke des Menschen und der Saugertiere. *Z Wiss Zool*. 1863;13:481-512.
6. Van De Water TR. Historical Aspects of Inner Ear Anatomy and Biology that Underlie the Design of Hearing and Balance Prosthetic Devices. *Anat Rec*. 2012;295(11):1741-1759. doi:https://doi.org/10.1002/ar.22598
7. Dayaratne MWN, Vlajkovic SM, Lipski J, Thorne PR. Kölliker's organ and the development of spontaneous activity in the auditory system: Implications for hearing dysfunction. *Biomed Res Int*. 2014;2014. doi:10.1155/2014/367939
8. Betlejewski S. Nauka a życie – historia markiza Alfonso Cortiego. *Otolaryngol Pol*. 2008;62(3):344-347. doi:https://doi.org/10.1016/S0030-6657(08)70268-3
9. Hackney CM, Furness DN. The composition and role of cross links in mechanoelectrical transduction in vertebrate sensory hair cells. *J Cell Sci*. 2013;126(8):1721-1731. doi:10.1242/jcs.106120
10. Corns LF, Johnson SL, Roberts T, et al. Mechanotransduction is required for establishing and maintaining mature inner hair cells and regulating efferent innervation. *Nat Commun*. 2018;9(1). doi:10.1038/s41467-018-06307-w
11. Ó Maoiléidigh D, Ricci AJ. A Bundle of Mechanisms: Inner-Ear Hair-Cell Mechanotransduction. *Trends Neurosci*. 2019;42(3):221-236. doi:10.1016/j.tins.2018.12.006
12. Eton & Lepore. Making connections in the inner ear: recent insights into the development of spiral ganglion neurons and their connectivity with sensory hair cells. *Bone*. 2008;23(1):1-7. doi:10.1016/j.semcdb.2013.04.003.Making
13. Shearer AE, Hildebrand MS, Smith RJ. Hereditary Hearing Loss and Deafness Overview. *GeneReviews*®. 2017:1-27.

http://www.ncbi.nlm.nih.gov/pubmed/20301607.

14. Yamasoba T, Lin FR, Someya S, Kashio A, Sakamoto T, Kondo K. Current concepts in age-related hearing loss: Epidemiology and mechanistic pathways. *Hear Res*. 2013;303:30-38. doi:10.1016/j.heares.2013.01.021
15. Koffler T, Ushakov K, Avraham KB. Genetics of Hearing Loss: Syndromic. *Otolaryngol Clin North Am*. 2015;48(6):1041-1061. doi:10.1016/j.otc.2015.07.007
16. Sheffield AM, Smith RJH. The epidemiology of deafness. *Cold Spring Harb Perspect Med*. 2019;9(9):1-16. doi:10.1101/cshperspect.a033258
17. Shibata SB, Shearer AE SR. Genetic sensorineural hearing loss. In Cummings otolaryngology head and neck surgery. *Elsevier*. 2015;305(4):413-414.
18. Chang KW. Genetics of Hearing Loss-Nonsyndromic. *Otolaryngol Clin North Am*. 2015;48(6):1063-1072. doi:10.1016/j.otc.2015.06.005
19. Carpena NT, Lee MY. Genetic Hearing Loss and Gene Therapy. *Genomics Inform*. 2018;16(4):e20. doi:10.5808/gi.2018.16.4.e20
20. Sloan-Heggen CM, Bierer AO, Shearer AE, et al. Comprehensive genetic testing in the clinical evaluation of 1119 patients with hearing loss. *Hum Genet*. 2016;135(4):441-450. doi:10.1007/s00439-016-1648-8
21. Verpy E, Weil D, Leibovici M, et al. Stereocilin-deficient mice reveal the origin of cochlear waveform distortions. *Nature*. 2008;456(7219):255-258. doi:10.1038/nature07380
22. Taku Ito, Julie Muskett, Parna Chattaraj, Byung Yoon Choi, Kyu Yup Lee, Christopher K Zalewski, Kelly A King, Xiangming Li, Philine Wangemann, Thomas Shawker, Carmen C Brewer, Seth L Alper and AJG. SLC26A4 mutation testing for hearing loss associated with enlargement of the vestibular aqueduct. *World J Otorhinolaryngol*. 2013;176(1):139-148. doi:10.5319/wjo.v3.i2.26.SLC26A4
23. Yamamoto N, Mutai H, Namba K, et al. Prevalence of TECTA mutation in patients with mid-frequency sensorineural hearing loss. *Orphanet J Rare Dis*. 2017;12(1):1-11. doi:10.1186/s13023-017-0708-z
24. Chaib H, Lina-granade G, Guilford P, et al. A gene responsible for a dominant form of neurosensory non-syndromic deafness maps to the NSRD1 recessive deafness gene interval. *Hum Mol Genet*. 1994;3(12):2219-2222. doi:10.1093/hmg/3.12.2219
25. Morgan A, Lenarduzzi S, Cappellani S, et al. Genomic studies in a large cohort of hearing impaired italian patients revealed several new alleles, a rare case of uniparental disomy (Upd) and the importance to search for copy number variations.

Front Genet. 2018;9(December). doi:10.3389/fgene.2018.00681

26. Pusch M. Myotonia caused by mutations in the muscle chloride channel gene CLCN1. *Hum Mutat*. 2002;19(4):423-434. doi:https://doi.org/10.1002/humu.10063
27. Roman-Sanchez R, Wensel TG, Wilson JH. Nonsense mutations in the rhodopsin gene that give rise to mild phenotypes trigger mRNA degradation in human cells by nonsense-mediated decay. *Exp Eye Res*. 2016;145:444-449. doi:https://doi.org/10.1016/j.exer.2015.09.013
28. Jung J, Choi HB, Koh YI, et al. Whole-exome sequencing identifies two novel mutations in KCNQ4 in individuals with nonsyndromic hearing loss. *Sci Rep*. 2018;8(1):1-11. doi:10.1038/s41598-018-34876-9
29. Takeda K, Inoue H, Tanizawa Y, et al. WFS1 (Wolfram syndrome 1) gene product: Predominant subcellular localization to endoplasmic reticulum in cultured cells and neuronal expression in rat brain. *Hum Mol Genet*. 2001;10(5):477-484. doi:10.1093/hmg/10.5.477
30. X.Z. Liu, S. Angeli, X.M. Ouyang, W. Liu, , X.M. Ke, Y.H. Liu, S.X. Liu, L.L. Du XW, Deng, H. Yuan and DY. Audiological and genetic features of the mtDNA mutations. 2008;344(6188):1173-1178. doi:10.1126/science.1249098.Sleep
31. Azaiez H, Booth KT, Ephraim SS, et al. Genomic Landscape and Mutational Signatures of Deafness-Associated Genes. *Am J Hum Genet*. 2018;103(4):484-497. doi:10.1016/j.ajhg.2018.08.006
32. Morgan A, Koboldt DC, Barrie ES, et al. Mutations in PLS1, encoding fimbrin, cause autosomal dominant nonsyndromic hearing loss. *Hum Mutat*. 2019;40(12):2286-2295. doi:10.1002/humu.23891
33. Bowl MR, Dawson SJ. Age-related hearing loss. *Cold Spring Harb Perspect Med*. 2019;9(8). doi:10.1101/cshperspect.a033217
34. Slade K, Plack CJ, Nuttall HE. The Effects of Age-Related Hearing Loss on the Brain and Cognitive Function. *Trends Neurosci*. 2020;43(10):810-821. doi:10.1016/j.tins.2020.07.005
35. Nagtegaal AP, Broer L, Zilhao NR, et al. Genome-wide association meta-analysis identifies five novel loci for age-related hearing impairment. *Sci Rep*. 2019;9(1):15192. doi:10.1038/s41598-019-51630-x
36. Roth TN. Aging of the auditory system. *Handb Clin Neurol*. 2015;129:357-373. doi:10.1016/B978-0-444-62630-1.00020-2
37. Friedman RA, Van Laer L, Huentelman MJ, et al. GRM7 variants confer

susceptibility to age-related hearing impairment. *Hum Mol Genet*. 2009;18(4):785-796. doi:10.1093/hmg/ddn402

38. Girotto G, Pirastu N, Sorice R, et al. Hearing function and thresholds: A genome-wide association study in European isolated populations identifies new loci and pathways. *J Med Genet*. 2011;48(6):369-374. doi:10.1136/jmg.2010.088310
39. Wolber LE, Girotto G, Buniello A, et al. Salt-inducible kinase 3, SIK3, is a new gene associated with hearing. *Hum Mol Genet*. 2014;23(23):6407-6418. doi:10.1093/hmg/ddu346
40. Vuckovic D, Dawson S, Scheffer DI, et al. Genome-wide association analysis on normal hearing function identifies PCDH20 and SLC28A3 as candidates for hearing function and loss. *Hum Mol Genet*. 2015;24(19):5655-5664. doi:10.1093/hmg/ddv279
41. Gao X, Dai P. Impact of next-generation sequencing on molecular diagnosis of inherited non-syndromic hearing loss. *J Otol*. 2014;9(3):122-125. doi:10.1016/j.joto.2014.11.003
42. Wong LJC. *Next Generation Sequencing Based Clinical Molecular Diagnosis of Human Genetic Disorders*.; 2017. doi:10.1007/978-3-319-56418-0
43. Málaga DR, Brusius-Facchin AC, Siebert M, et al. Sensitivity, advantages, limitations, and clinical utility of targeted next-generation sequencing panels for the diagnosis of selected lysosomal storage disorders. *Genet Mol Biol*. 2019;42(1):197-206. doi:10.1590/1678-4685-gmb-2018-0092
44. Teer JK, Mullikin JC. Exome sequencing: The sweet spot before whole genomes. *Hum Mol Genet*. 2010;19(R2):145-151. doi:10.1093/hmg/ddq333
45. Ng SB, Turner EH, Robertson PD, et al. Targeted capture and massively parallel sequencing of 12 human exomes. *Nature*. 2009;461(7261):272-276. doi:10.1038/nature08250
46. Juan C Celedón, MD, DrPHGary M Hunninghake, MD M. Principles of complex trait genetics. *UpToDate*. 2020.
47. Badano JL, Katsanis N. Beyond Mendel: an evolving view of human genetic disease transmission. *Nat Rev Genet*. 2002;3(10):779-789. doi:10.1038/nrg910
48. Fransen E, Bonneux S, Corneveaux JJ, et al. Genome-wide association analysis demonstrates the highly polygenic character of age-related hearing impairment. *Eur J Hum Genet*. 2015;23(1):110-115. doi:10.1038/ejhg.2014.56
49. Yang C-H, Schrepfer T, Schacht J. Age-related hearing impairment and the triad of

acquired hearing loss . *Front Cell Neurosci* . 2015;9:276. https://www.frontiersin.org/article/10.3389/fncel.2015.00276.

50. Visscher PM, Wray NR, Zhang Q, et al. 10 Years of GWAS Discovery: Biology, Function, and Translation. *Am J Hum Genet*. 2017;101(1):5-22. doi:10.1016/j.ajhg.2017.06.005
51. Girotto G, Pirastu N, Sorice R, et al. Hearing function and thresholds: a genome-wide association study in European isolated populations identifies new loci and pathways. *J Med Genet*. 2011;48(6):369 LP - 374. doi:10.1136/jmg.2010.088310
52. Vuckovic D, Dawson S, Scheffer DI, et al. Genome-wide association analysis on normal hearing function identifies *PCDH20* and *SLC28A3* as candidates for hearing function and loss. *Hum Mol Genet*. 2015;24(19):5655-5664. doi:10.1093/hmg/ddv279
53. Huyghe JR, Van Laer L, Hendrickx JJ, et al. Genome-wide SNP-Based Linkage Scan Identifies a Locus on 8q24 for an Age-Related Hearing Impairment Trait. *Am J Hum Genet*. 2008;83(3):401-407. doi:10.1016/j.ajhg.2008.08.002
54. Konings A, Van Laer L, Van Camp G. Genetic studies on noise-induced hearing loss: A review. *Ear Hear*. 2009;30(2):151-159. doi:10.1097/AUD.0b013e3181987080
55. Van Eyken E, Van Camp G, Van Laer L. The complexity of age-related hearing impairment: Contributing environmental and genetic factors. *Audiol Neurotol*. 2007;12(6):345-358. doi:10.1159/000106478
56. Spence R, Gerlach G, Lawrence C, Smith C. The behaviour and ecology of the zebrafish, Danio rerio. *Biol Rev*. 2008;83(1):13-34. doi:10.1111/j.1469-185X.2007.00030.x
57. Lieschke GJ, Currie PD. Animal models of human disease: zebrafish swim into view. *Nat Rev Genet*. 2007;8(5):353-367. doi:10.1038/nrg2091
58. Stewart AM, Kalueff A V. The behavioral effects of acute Δ9-tetrahydrocannabinol and heroin (diacetylmorphine) exposure in adult zebrafish. *Brain Res*. 2014;1543:109-119. doi:10.1016/j.brainres.2013.11.002
59. Varshney GK, Pei W, Burgess SM. Using zebrafish to study human deafness and hearing regeneration. *Monogr Hum Genet*. 2016;20(1):110-131. doi:10.1159/000444569
60. Jatllon O, Aury JM, Brunet F, et al. Genome duplication in the teleost fish Tetraodon nigroviridis reveals the early vertebrate proto-karyotype. *Nature*. 2004;431(7011):946-957. doi:10.1038/nature03025

61. Bhandiwad AA, Zeddies DG, Raible DW, Rubel EW, Sisneros JA. Auditory sensitivity of larval zebrafish (Danio rerio) measured using a behavioral prepulse inhibition assay. *J Exp Biol*. 2013;216(18):3504-3513. doi:10.1242/jeb.087635
62. Liu J, Zhou Y, Qi X, et al. CRISPR/Cas9 in zebrafish: an efficient combination for human genetic diseases modeling. *Hum Genet*. 2017;136(1):1-12. doi:10.1007/s00439-016-1739-6
63. Vona B, Doll J, Hofrichter MAH, Haaf T, Varshney GK. Small fish, big prospects: using zebrafish to unravel the mechanisms of hereditary hearing loss. *Hear Res*. 2020;(xxxx):107906. doi:10.1016/j.heares.2020.107906
64. Zeddies DG, Fay RR. Development of the acoustically evoked behavioral response in zebrafish to pure tones. *J Exp Biol*. 2005;208(7):1363-1372. doi:10.1242/jeb.01534
65. POPPER, ARTHUR N, ALLISON COFFIN, MATTHEW KELLEY, GEOFFREY A. MANLEY A. Evolution of the Vertebrate Auditory System. *Book*. 2004;22:55.
66. Schwarzer S, Asokan N, Bludau O, et al. Erratum: Neurogenesis in the inner ear: The zebrafish statoacoustic ganglion provides new neurons from a Neurod/ Nestin-positive progenitor pool well into adulthood (Development (2020) 147 (dev176750) DOI: 10.1242/dev.176750). *Dev*. 2020;147(9). doi:10.1242/dev.191775
67. Nicolson T. The genetics of hearing and balance in zebrafish. *Annu Rev Genet*. 2005;39:9-22. doi:10.1146/annurev.genet.39.073003.105049
68. Litvak MK. Response of shoaling fish to the threat of aerial predation. *Environ Biol Fishes*. 1993;36(2):183-192. doi:10.1007/BF00002798
69. Riley BB, Moorman SJ. Development of utricular otoliths, but not saccular otoliths, is necessary for vestibular function and survival in zebrafish. *J Neurobiol*. 2000;43(4):329-337. doi:10.1002/1097-4695(20000615)43:4<329::aid-neu2>3.0.co;2-h
70. Busch-Nentwich E, Söllner C, Roehl H, Nicolson T. The deafness gene dfna5 is crucial for ugdh expression and HA production in the developing ear in zebrafish. *Development*. 2004;131(4):943 LP - 951. doi:10.1242/dev.00961
71. McDermott JH, Molina-Ramírez LP, Bruce IA, et al. Diagnosing and Preventing Hearing Loss in the Genomic Age. *Trends Hear*. 2019;23:1-8. doi:10.1177/2331216519878983
72. Brownstein Z, Gulsuner S, Walsh T, et al. Spectrum of genes for inherited hearing

loss in the Israeli Jewish population, including the novel human deafness gene ATOH1 *bioRxiv*. January 2020:2020.06.11.144790. doi:10.1101/2020.06.11.144790

73. Morgan A, Pelliccione G, Ambrosetti U, Dell'Orco D, Girotto G. SLC12A2: a new gene associated with autosomal dominant Non-Syndromic hearing loss in humans. *Hear Balanc Commun*. 2020;18(2):149-151. doi:10.1080/21695717.2020.1726670
74. Vona B, Mazaheri N, Lin S-J, et al. Biallelic mutation of CLRN2 causes non-syndromic hearing loss in humans. *bioRxiv*. January 2020:2020.07.29.222828. doi:10.1101/2020.07.29.222828
75. da Silva RS, Dantas VLG, Alves LU, et al. NCOA3 identified as a new candidate to explain autosomal dominant progressive hearing loss. *bioRxiv*. January 2020:2020.06.07.138909. doi:10.1101/2020.06.07.138909
76. Zhong LX, Kun S, Jing Q, Jing C, Denise Y. Non-Syndromic Hearing Loss and High-Throughput Strategies to Decipher Its Genetic Heterogeneity. *J Otol*. 2013;8(1):6-24. doi:https://doi.org/10.1016/S1672-2930(13)50002-X
77. Robinson JF, Katsanis N. Oligogenic Disease BT - Vogel and Motulsky's Human Genetics. In: Speicher MR, Motulsky AG, Antonarakis SE, eds. Berlin, Heidelberg: Springer Berlin Heidelberg; 2010:243-262. doi:10.1007/978-3-540-37654-5_8
78. Peng W, Zhong Y, Zhao X, Yuan J. Low penetrance of hearing loss in two Chinese families carrying the mitochondrial tRNASer(UCN) mutations. *Mol Med Rep*. 2020;22(1):77-86. doi:10.3892/mmr.2020.11100
79. Hoffmann TJ, Keats BJ, Yoshikawa N, Schaefer C, Risch N, Lustig LR. A Large Genome-Wide Association Study of Age-Related Hearing Impairment Using Electronic Health Records. *PLOS Genet*. 2016;12(10):e1006371. https://doi.org/10.1371/journal.pgen.1006371.
80. Nolan LS, Maier H, Hermans-Borgmeyer I, et al. Estrogen-related receptor gamma and hearing function: evidence of a role in humans and mice. *Neurobiol Aging*. 2013;34(8):2077.e1-2077.e9. doi:https://doi.org/10.1016/j.neurobiolaging.2013.02.009
81. Manolio TA, Collins FS, Cox NJ, et al. Finding the missing heritability of complex diseases. *Nature*. 2009;461(7265):747-753. doi:10.1038/nature08494
82. Ku CS, Loy EY, Pawitan Y, Chia KS. The pursuit of genome-wide association studies: where are we now? *J Hum Genet*. 2010;55(4):195-206. doi:10.1038/jhg.2010.19

83. Vanhooren V, Libert C. The mouse as a model organism in aging research: usefulness, pitfalls and possibilities. *Ageing Res Rev*. 2013;12(1):8-21. doi:10.1016/j.arr.2012.03.010
84. White PM. Perspectives on Human Hearing Loss , Cochlear Regeneration , and the Potential for Hearing Restoration Therapies. *brain Sci*. 2020.
85. Saunders CJ, Miller NA, Soden SE, et al. Rapid whole-genome sequencing for genetic disease diagnosis in neonatal intensive care units. *Sci Transl Med*. 2012;4(154). doi:10.1126/scitranslmed.3004041